STUDIES ON MANGANESE, IRON AND COBALT CHEMISTRY WITH DIAZINE AND DIOXIME LIGANDS

A THESIS

SUBMITTED FOR THE DEGREE OF

DOCTOR OF PHILOSOPHY

By

SUBRAMANYA GUPTA SREERAMA

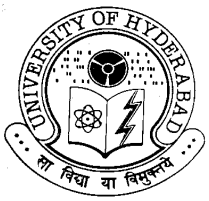

SCHOOL OF CHEMISTRY
UNIVERSITY OF HYDERABAD
HYDERABAD 500 046
INDIA

JULY 2005

Ankitham

Amma
Naanna

STATEMENT

I hereby declare that the matter embodied in this thesis entitled "***Studies on Manganese, Iron and Cobalt Chemistry with Diazine and Dioxime Ligands"*** is the result of the investigations carried out by me in the School of Chemistry, University of Hyderabad, under the supervision of **Prof. Samudranil Pal**.

In keeping the general practice of reporting scientific observations, due acknowledgement has been made wherever the work is described is based on findings of other investigators. Any omission, which might have occurred by oversight or error is regretted.

July 2005 **Subramanya Gupta Sreerama**

PROF. SAMUDRANIL PAL
SCHOOL OF CHEMISTRY
UNIVERSITY OF HYDERABAD
HYDERABAD-500 046, INDIA

Phone: +91-40-23134756
(office)
Fax: +91-40-23012460
Email: spsc@uohyd.ernet.in

July, 2005

CERTIFICATE

Certified that the work embodied in the thesis entitled "***Studies on Manganese, Iron and Cobalt Chemistry with Diazine and Dioxime Ligands"*** has been carried out by **Mr. Subramanya Gupta Sreerama** under my supervision and the same has not been submitted elsewhere for any degree.

Prof. Samudranil Pal
(Thesis supervisor)

Dean
School of Chemistry
University of Hyderabad

ACKNOWLEDGEMENT

I express my deep sense of gratitude and profound respect to my research supervisor **Prof. Samudranil Pal** for his invaluable guidance, support and constant encouragement. I have been able to learn a great deal from him and consider my association with him to be a rewarding experience. He has been always approachable, helpful and extremely patient throughout my research career. I am quite lucky to get such a person as my supervisor. These words are not adequate to express all about him. To me he is my friend, philosopher and guide.

It is my pleasure to thank Prof. M. Periasamy, Dean, School of Chemistry and former Deans, for their co-operation on various occasions. I am extremely thankful to all faculty members of this school for their kind help and encouragement in various stages of my research work.

I thank DST and CSIR, New Delhi for the financial assistance.

I express my sincere thanks to Prof. A. R. Chakravarty (IISC, Bangalore) for providing the variable temperature magnetic data.

I am thankful to Prof. A. Varada Reddy, Prof. G. V. Subbaraju and all my M. Sc. faculty at Sri Venkateshwara University, Tirupathi.

I wish to thank my friendly and cooperative labmates Dr. N. R. Sangeetha, Dr. Satyanarayan Pal, M. Vamsee Krishna, Abhik Mukhopadhyay, Sunirban Das, Raji Raveendran and Anindita Sarkar for creating cheerful work atmosphere.

I am grateful to thank my AA-IMAX gang—Dr. Venu, Basavoju, Balu, Reddaiah, Pavan, Malla, L. S. Reddy, Ravikanth, Vasulu and Jaggu.

I gratefully acknowledge my Doora Dharshan club members—Suresh, Shyam, Satish, Narsi, Perumal and Chandu. My stay on this campus has been pleasant with the

association of all the scholars at the School of Chemistry. I am thankful to my friends Bandaru, Sampath, Thallapally, Senthil, Sairam, Srivardhan, Kommana, Narayana, Pradeep, Phani, Tin, Mariappan, Ramprasad, Mahipal, Eshwar, Harish, Devendar, Rajesh, Anbu, Bhuvan, K.V. Rao, Raju, Shiviah, Narahari, Kishore, Yadaiah, Vankatesh, Padmanabhan, Aparna, Tejender, Aravind, Sridhar, Santhosh, Venu Srinu, Phani, Satish, Nagaraj, Madhu, Binoy, Archan, Subhas, Manab, Prashant and Bipul.

I would like to thank my SVU friends Poorna, Suresh, Sreekanth, Bhargavi, Balchandra, Triveni–Rajesh, Sreenu, Madhu, Konda, Ramki, Radhika and Sireesha for their cheerful company.

I also thank Mr. V. M. Shetty and Raghavaiah, all the staff of the school, COSIST and CIL have been extremely helpful.

My special thanks are due to Sri. S. P. Shivaiah and Smt. Venkatasubbamma for their encouragement, affection and moral support.

Without **my beloved parents** relentless support and blessings I would not have reached to this stage of my life. I owe everthing to them. The blessings and wishes of my sister (Vasavi), brother-in-law (Anand), brothers (Suresh and Ganesh) and sister-in-laws (Indu and Lavanya) have made me what I am. I am grateful to my twin brother S. N. Gupta for his love and support. Last but certainly not the least, all the children (Vaishu, Likki, Nithya and Vedanth) of our family deserve a word of thanks for their smiles.

S Gupta Sreerama

CONTENTS

Chapter1

Introduction

1.1. Abstract

In this chapter, the importance of diazine and oxime/dioxime ligands has been briefly discussed. The aim of present investigation in the background of known metal complexes with these ligands has been stated.

1.2. Overview

Modern coordination chemistry started with the groundbreaking work of Alfred Werner in the 19th century. Basic knowledge of the three-dimensional arrangement of ligands coordinated to the metal ions was provided at that time[1]. From the beginning, coordination chemists have been fascinated by the ability of organic molecules those sequester metal ions, and impart unusual properties like, colorimetric, electrochemical, magnetic and catalytic.[2] As a result extension of this simple coordination chemistry towards more complex and widely spread fields such as polymers, oligomers, dendrimers, catalysis, organometallics etc. has occurred.

In this respect, the transition metal complexes with N and O donor polydentate Schiff bases were studied extensively due to their important role in the development of coordination chemistry. Among these N,O donor polydentate Schiff bases, molecules having diazine (=N–N=) and oxime (–C=N–OH) back bone have drawn immense attention in the recent years due to their versatile coordination chemistry with novel features. The research field dealing with

diazine (open-chain) and oxime metal complexes is very broad due in part to their potential interest for a number of interdisciplinary areas that includes bioinorganic, supramolecular, magnetochemistry and catalysis.[3,4] The most interesting feature of this class of ligands, containing high oxidation state promoting (L $\rightarrow$ M donating) σ - basic phenolate-O or deprotonated amide–O or alkoxide functionalities as different terminals on diazine (=N–N=)[5a-c] moiety and deprotonated =N-O^{-}, group in dioxime (C=N-OH)[5d-e] moiety is to produce higher-valent metal complexes. The higher valent (> ca. +3) Mn, Fe and Co complexes are of considerable interest in the area of bioinorganic chemistry, because of important roles played by these metal ions in the functions of several metalloenzymes. Oxygen evolving center in photosystem II (tetravalent manganese); heme-monooxygenases, -peroxidases (tetra and pentavalent iron) vitamin B_{12} -cynocobalamine (trivalent cobalt) are few examples of these types of metalloenzymes.[6]

In addition, these polydentate ligands that can serve as molecular bridges between metal centers. As they contain delocalized π–electron[7] system, they can also mediate strong magnetic spin coupling between paramagnetic centers.[8] Thus they can be provided a base for the understanding of new molecular magnets. Due to such possibilities intensive efforts in terms of design and synthesis of new bridging systems have been devoted.

The diazine ligands contain rotationally flexible N-N single bond and produce several μ(N–N) bridged complexes readily. These complexes are subjected to a number of studies related to magnetic and structural features (from molecular to supramolecular level). Similarly in oxime containing ligands, the terminal =NO^{-} moiety acts as a bridging unit to bring the two metal ions into

close proximity and provides an easily communicating intramolecular pathway for spin exchange interactions. Such polyfunctional diazine and dioxime ligands have been shown to form various mono-, homo- and hetero- dinuclear, tri and polynuclear metal complexes depending upon the reaction conditions.

Due to their unique properties and wide range of applications there is a continuous quest for novel complexes derived with diazine and dioxime based Schiff bases.

1.3. Some aspects of the diazine chemistry

Azines/diazines represent a well-known class of organic compounds, which exhibits rich coordination chemistry that has emerged over last three decades. These ligands were derived by the condensation two mole equivalents of an aldehyde or a ketone with one mole equivalent of hydrazine and there is a possibility to obtain symmetrical and unsymmetrical systems by using two identical or different carbonyl compounds. Even though the diazine moiety has been found in some conjugated aromatic heterocyclic polyfunctional systems like pyrazole, triazole, pyridazine and pthalazines, but they are rigidly fixed. On the other hand, open chain diazine (dipyridyl etc.) systems are much more flexible, and provide several possible mono and dinucleating coordination modes.[9] Such open chain systems appealing due to various applications of them and their complexes in number of areas. These include molecular electronics, salicylaldazine shows a strongly luminescent and thermochromic properties[10] in the solid state; analytical, the syringaldazine has been used for determination of chlorine in water by colorimetry;[11] NLO active materials, 4-bromo-4'-methoxyacetophenone azine[12] and some macrocylic bis(azines)[13] show strong

second harmonic generation. Some ferroelectric liquid crystals containing *ortho*-palladated azines were also reported.[14] Due to its unique coordination modes the diazine class of ligands have been found to form monometallic, homo/hetero di to poly-metallic complexes, with interesting properties in the fields of metallo-supramolecular and magnetochemistry.[15a] On the other hand such diazine based amide-containing hydrazones and its derivatives display wide range of bioactivities. These have found extensive applications in pharmacology.[15b]

In the following section, we have described few types of dinucleating open chain diazine ligands and their complexes with a general discussion on their synthesis, structure, properties and applications.

1.3.1. Types of ligands and their modes of coordination

The flexible diazine ligands provide very interesting topological arrangements due to the presence of terminal main donor groups as pyridyl, pyrazyl, salicyl, etc., and additional donor groups as OH, SH, NH_2, etc. A number of open chain diazine ligands with such fragments have been reported. We have restricted our discussion to:

1) Dinucleating hydrazides having picolinylidene or salicylidene chelating groups with NH_2 or OH as additional donor groups.

2) Aroyl or acyl hydrazones, which contain deprotonable amide functionality.

The pictorial representations of such polydentate hydrazides and hydrazones are shown below.

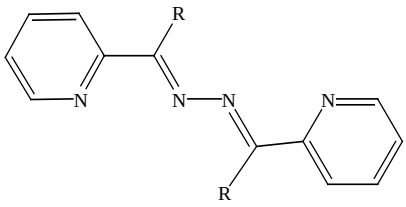

L^1: R = H, L^2: R = Me

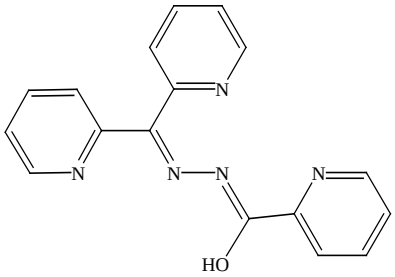

L^3

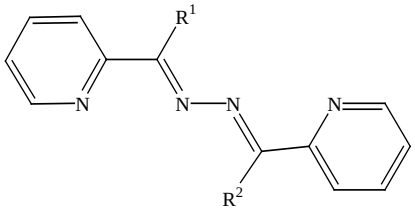

L^4: $R^1 = R^2 = NH_2$, L^5: $R^1 = NH_2$ $R^2 = H$

L^6: $R^1 = NH_2$, $R^2 = CH_3$

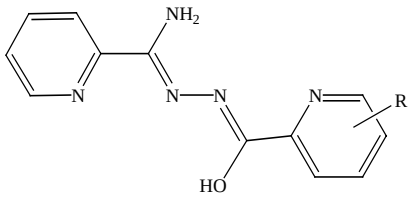

L^7: R = H, L^8: R = 3-OH

L^9: R = 6-OH, L^{10}: R = 6-Me

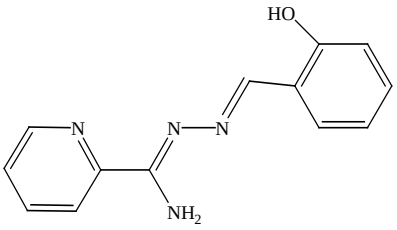

L^{11}

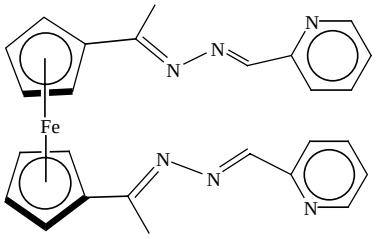

(a)

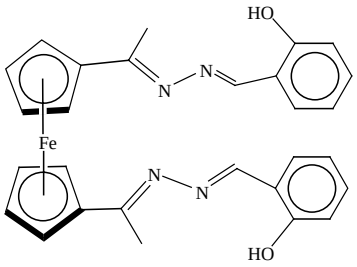

(b)

L^{12}

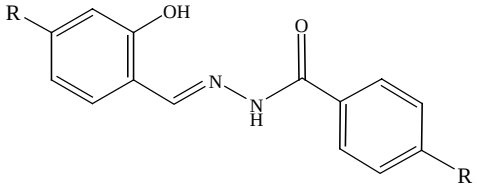

L^{13}: R = H, CH_3, OH, OCH_3, $N(CH_3)_2$ NH_2 Cl, Br, NO_2

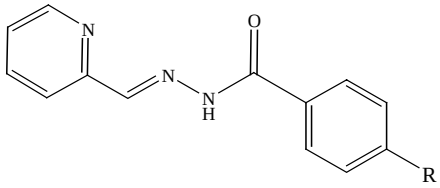

L^{14}: R = H, CH_3, OH, OCH_3, $N(CH_3)_2$, NH_2, Cl, NO_2

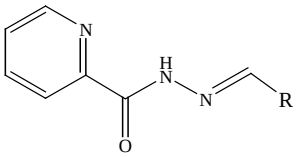

L^{15}

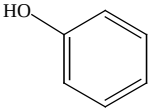

L^{16}

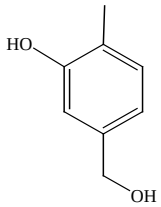

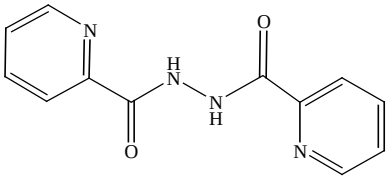

L^{17}

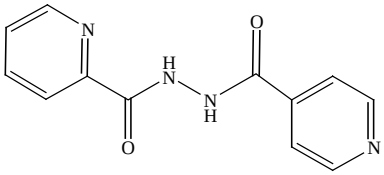

L^{18}

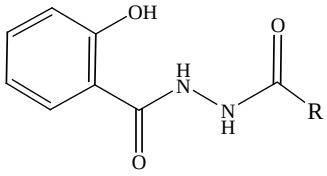

L^{19}: R = H, CH_3, Ph, NH_2, C_5H_8O, $C_6H_5C_4H_5O$

For these types of hydrazides Thompson and coworkers have proposed possible coordination modes, through a series of topological operations.[16a] Depending upon the donor groups and the assembled metal ions, the coordination modes of the ligands will vary with the changes at azine moiety by two types of angles, namely the torsion angle (α) about the N–N single bond and the bending angle at two N toms (β, β').

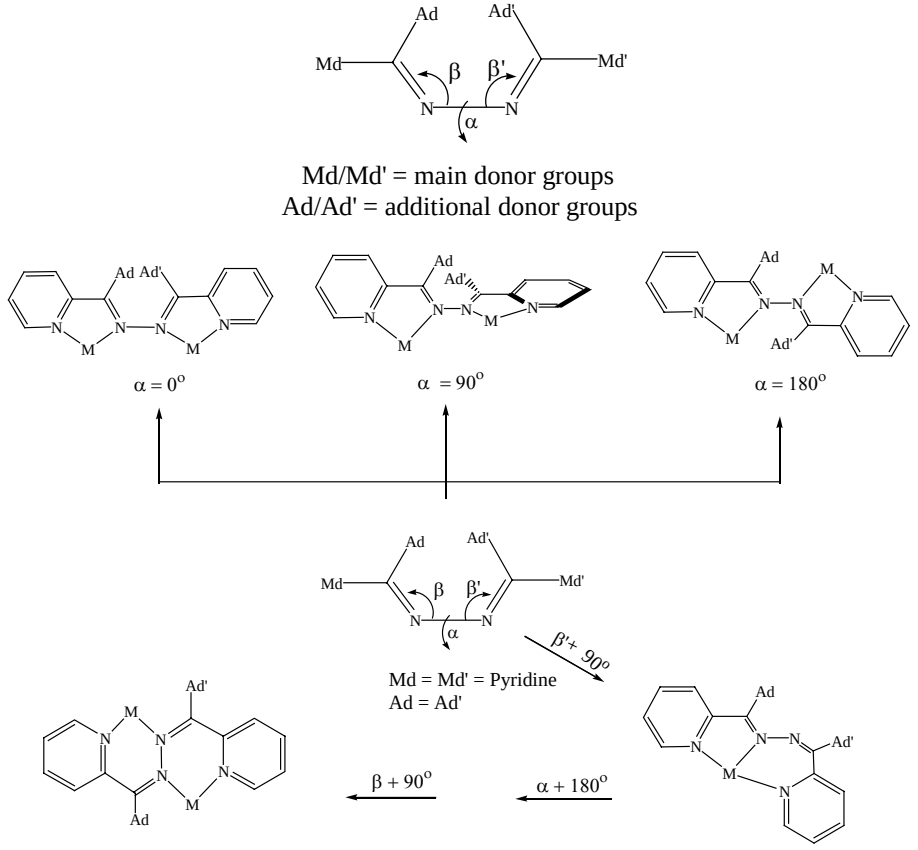

Figure 1.1

The simple N,N´-bis(pi/colinilydene)hydrazine ligand have show at least five possible coordination modes due to the changes in the α and β planes (Figure 1.1).[9a] Most of the remaining hydrazine systems adopt a typical dinucleating mode *via* bridging N–N single bond due to terminal chelating sites (Figure 1.2).[16b] In all these dinucleating modes the N–N fragments are found to be in *cis*, *trans* or in between manner, depending upon the terminal and additional-donor groups and the ancillary ligands coordinated to the metal ions. The ligand having an alkoxide group as an additional coordinating site, adopts two types of binding modes.[16c] The dominating mode provides alkoxy bridge in addition to the N–N bridge between the metal ions. This was demonstrated by a number of polynuclear complexes. The minor is a non-bridging mode (Figure 1.2).[16d]

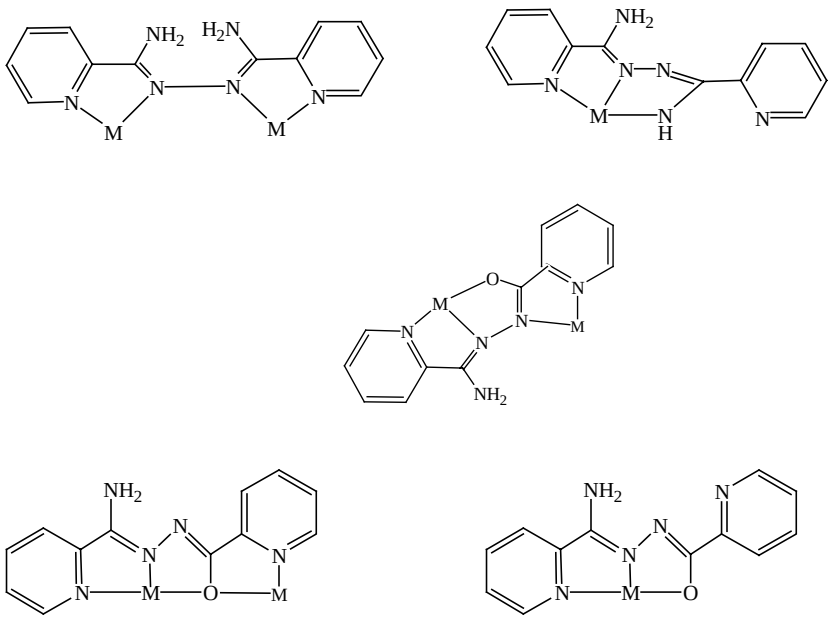

Figure 1.2

1.3.2. A brief survey on diazine based metal complexes

Self-assembly of molecules *via* metal–ligand interactions leads various supramolecular architectures such as helicates, grids, cylinders and boxes.[17,18,19] Due to the arrangement of donor sites and high flexibility, these polydentate hydrazides can coordinate in a variety of ways leading to such diverse molecular structures. The studies on such species have attracted great attention due to their potential applications in magnetism, molecular selection, ion exchange, catalysis, medicine, electrical conductivity and enantioselectivity.[20]

Due to such a wide range of applications a large literature is now available in this area, out of which, some recent and interesting examples are briefly presented.

1.3.2.1. Helicates and twisted complexes and their magnetic properties

With obvious parallels to the structure of DNA, metal complexes that spontaneously adopt helical structures have a long held fascination.[19] Helicates based on imine ligands or particularly diazine ligands are synthetically versatile and inexpensive.[21] Studies on the helicates formation have elucidated many supramolecular coordination chemistry principles. Flexibility of the polydentate ligand and how it is partitioned into distinct metal binding sites, are the two crucial factors to be considered for the fabrication of helicates. In many cases, ligands have been constructed as a polyfunctional system, which contain bis bidentate or terdentate domains. These bis chelating ligands are separated by a spacer or connected directly, to bind two metal ions separately rather than chelating to a single metal ion (essential for helication).[22]

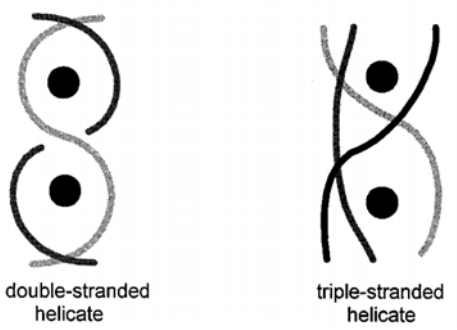

Figure 1.3

The coordination chemistry of the simplest Schiff bases L^1 and L^2 was reported by Stratton and Bush[23a-c] in 1950's. Based on the magnetic studies they have concluded the dinuclear structures of the $[M_2L^1{}_3]^{4+}$ cations (M = Fe(II) Co(II) and Ni(II)). Subsequent variable temperature magnetic studies of $[Ni_2L^1{}_3]^{4+}$ (by Blake)[23d] and $[M_2L^2{}_3]^{4+}$ (M = Fe(II) Co(II) and Ni(II) by Stratton)[23e] supported the dinuclear nature and spiral structures of this class of complexes. Although none of the structures were confirmed by X-ray crystallographic studies, but these studies are of particular historic importance to the field of metallo-supramolecular chemistry and in particular to helicate formation.

The X-ray structure of one of these complexes was first reported by Sheldrick.[24] In the dicobalt(II) $[Co_2(L^2)_3]ZnCl_4{\cdot}[ZnCl_3(H_2O)]_2{\cdot}4H_2O$, the distorted octahedral Co(II) centers are bridged by three ligand molecules in a twisted manner with an average (Co–N–N–Co) angle 44° (Figure 1.4). Recently Hannon and coworkers have also reported the similar triple helicate X-ray structures of hexafluorophospahte salts of Stratton and Busch's original iron(II) complex with L^1 and Zn(II) complex with L^2 (Figure 1.4).[25] Further, the Schiff

base L^2 with $AgClO_4$ (in 1:1 mole ratio) produced double helical complex cation[26] $[Ag_2L^2{}_2](ClO_4)_2$. However, in presence of $NaClO_4$ the triple-helical $[Ag_2L^2{}_3]^{+2}$ structure was generated, with crystallographic C_3 symmetry passing through the Ag(I) ions.

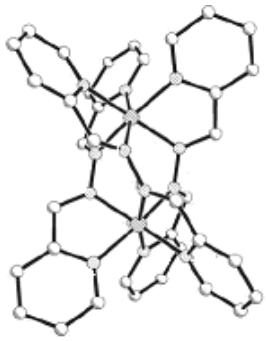

Figure 1.4

Thompson *et al*. have reported a systematic study on structural and magnetic properties[2] of the first row transition metal complexes with open chain diazine ligands like amidrazones, hydrazones, dihydrazones etc. They have reported a series of dicopper(II) systems by using the mono ligand L^4 and various co-ligands (Cl^-, Br^- and NO_3^-).[17a] In these complexes two copper(II) centers are bridged by a single N–N bond. In $[Cu_2L^4(NO_3)_2(H_2O)_6]\cdot(NO_3)_2$ (Figure 1.5a), the two metal centers are in distorted octahedral coordination geometry, with an 100.2° dihedral angle between the magnetic planes. This compound exhibits antiferromagnetic spin exchange. In contrast, the complex $[Cu_2L^4Br_4]\cdot H_2O$ (Figure 1.5b) with the same ligand has a much smaller rotational angle between the metal magnetic planes (75.08°) and exhibits significant intramolecular ferromagnetic spin coupling.

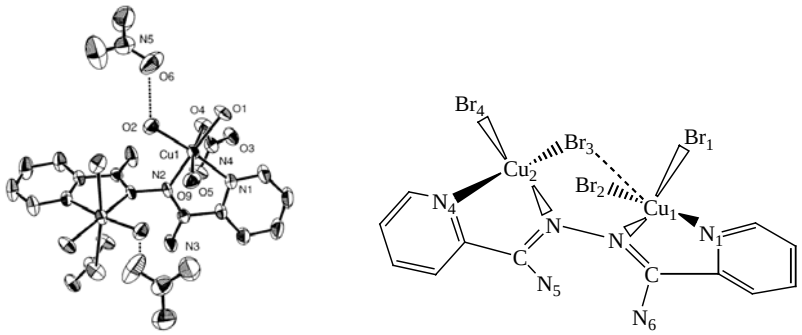

(a) (b)

Figure 1.5

An expanded study related to the extent and type of metal ion spin-exchange as a function of twist of the copper magnetic planes about N–N single bond, shows a linear correlation between the exchange integral and rotational angles.[17c] This observations was supported by the extended Hückel calculations. The orthogonality between the nitrogen p-orbitals and copper magnetic (e.g.- d_{x2-y2}) orbitals, is attained at ~70°. Below this angle ferromagnetic coupling and above this angle antiferromagnetic coupling occur.[27a] They have also studied few more dinuclear triple helicate structures of general formula $[M_2L_3]$ [M = Mn(II), Fe(II), Fe(III), Co(II) and Ni(II)] with L^4. In each complex, the hexa-coordinated metal centers are bridged by three N–N single bonds as shown in Figure 1.6. In this series, the dimanganese(II) complex shows a weak ferromagnetic spin exchange, which is consistent with the average twist angle (67.8°) of the three ligands. However, an isostructural Ni(II) complex does not show any such spin exchange.[27b]

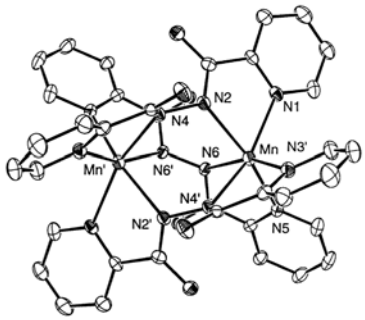

Figure 1.6

Cationic $[M_2L^3_3]^+$ triple helicates were produced by the reaction of L^3 with Cu(II) and Zn(II) salts. Similarly Meng and coworkers generated ferrocene containing double helical[28] (Cu_2L_2[12b]) copper(II) complex with L[12b] and mononuclear Ag(I) and Cu(II) complexes with L[12a].

1.3.2.2. Supramolecular species

(a) Self-assembled Grids and Clusters

Self-assembly strategies for the formation of metal ion containing advanced materials with predetermined topological architectures are limited. Significant success has been achieved by using polytopic hydrazides with contiguous coordinating packets separated by pyridazine, pyrimidine, phenoxide, and alkoxide bridging fragments,[29a] that allow the metal ions in a roughly linear fashion. Essentially self-assembled rectangular tetranuclear [2x2] grids, square [3x3] nine metal grids, and high-nuclearity [4x4] grids have been produced in high yield.[29]

Mathews *et al*. reported self assembled [2x2] square tetranuclear homometallic[29b,30a] M(II) (M = Mn, Co, Ni, Cu, Zn) and heterometallic[30b]

($Co^{II}_2Fe^{III}_2$, and $Fe^{III}Cu^{II}_3$) grid complexes (Figure 1.7) with the hydrazides like L^7. In these square tetranuclear homometallic clusters, the antiferromagnetic spin coupling within the structure is dominated for the Mn(II), Co(II) and Ni(II) systems, due to large M–O–M bridge angles.

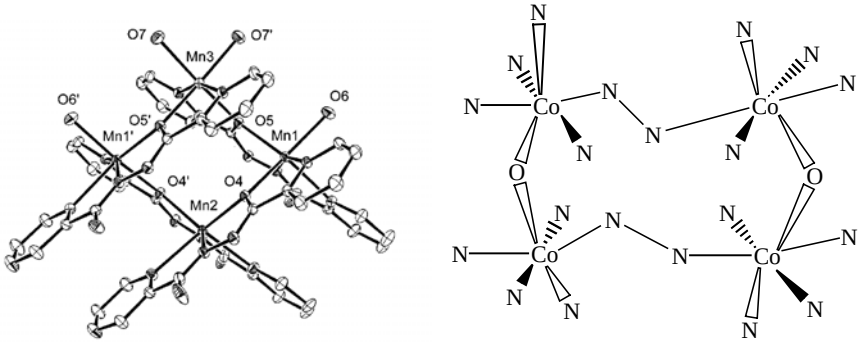

Figure 1.7

However in the case of Cu(II), the strictly orthogonal bridging arrangement between the adjacent copper magnetic orbitals and the close proximity of the Cu centers lead to intramolecular ferromagnetic spin exchange.

By a controlled self assembly process the L^7 ligand yields, homoleptic pentanuclear trigonal-bipyramidal M(II) (M = Mn, Co, and Zn)[31] clusters (Figure 1.8). In both the Mn(II) and Co(II) complexes an antiferromagnetic interaction is operative between the metal centers.

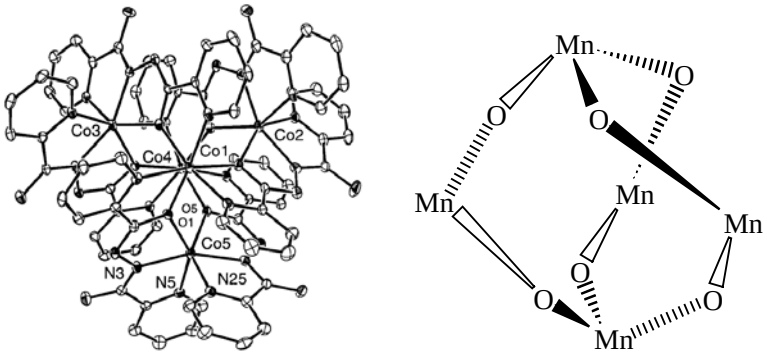

Figure 1.8

In addition to the spiral $[M_2L^3_3]^+$ complexes, the L^3 ligand has also provided a trinuclear species $[Cu_3(L^3)_2(H_2O)_2](ClO_4)_4{\cdot}2H_2O$ (Figure 1.9),[32] which exhibits moderately strong antiferromagnetic exchange as a result of super exchange *via* N–N bridges.

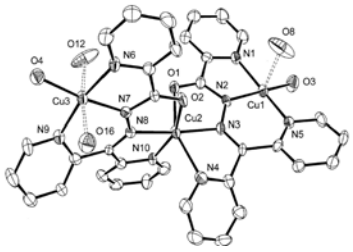

Figure 1.9

(b) Metallacrown compounds

The new class of polynuclear clusters that are analogous to crown ethers with respect to both structure and function are described as metallacrown

compounds (Figure 1.10).[33] The studies on crown ethers and metallacrowns, fall in the new branch of chemistry known as "host–guest" or supramolecular chemistry.[34a] Self-assembly is one of the most efficient method[34b-c] for the synthesis of such variety of supramolecular species. Before these species, most of the studies were focused on organic host molecules. Inorganic metallacrown cluster can also mimic the macrocyclic organic host molecules.[34d] The interest in metallacrown system is not only from their high symmetry and aesthetic molecular frameworks, but also from the potential applications as chemically modified electrodes, anion-selective separation agents, liquid crystal precursors and magnetic materials.[33]

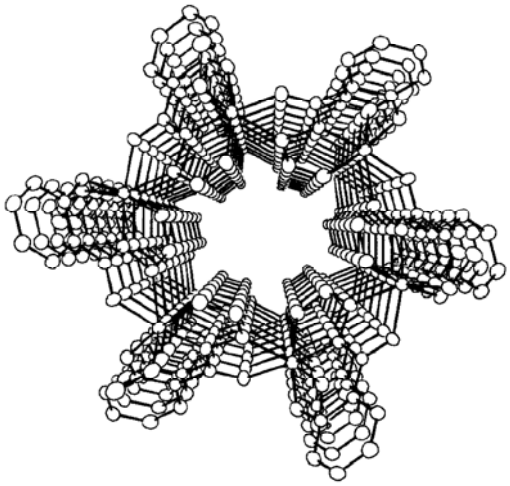

Figure 1.10

In 1989 Pecoraro and coworkers reported[33a] the first metallacrown compound and described a synthetic strategy by using a metal salt and a bifunctional hydroxamic acid. Latter a rich variety of structural types, *e.g.* [9]metallacrown-3, [12]metallacrown-4, [15]metallacrown-5 and [18]metallacrowns-6 were reported with a $[M–N–O]_n$ repeat unit.[33b,c,35] However Lah and coworkers have described Mn(III) [18]metallacrown-6 complexes with a triply deprotonated diazine[36a,b] based hydrazides L^{13}. In each complex, the ligands bridge the metal ions using the hydrazide N–N group with $[M–N–N]_n$ repeat unit[36] as shown in Figure 1.11. After that several metallacrowns like

Fe(III)/Co(III)[18]metallacrown-6 and Mn(III)/Fe(III)[30]metallacrown-10 compounds[36c,d] have been synthesized using L^{13} ligand system.

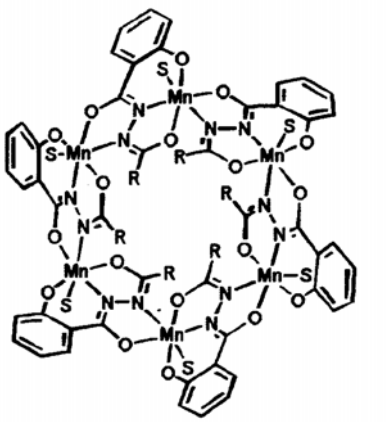

R = CH_3, CH_2CH_3, $(CH_2)_4CH_3$ and $(CH_2)_{10}CH_3$, S = Solvent

Figure 1.11

1.3.2.3. Pharmacologically versatile metal–hydrazone complexes

Hydrazones and their transition metal complexes are known to provide useful models for elucidation of the mechanism of enzyme inhibition. Due to the chemistry and pharmacological applications hydrazones have been extensively investigated.[37a-g] The biological properties of hydrazones are often related to metal ion coordination. The lipophilicity, which controls the rate of entry into the cell, was less to the metal complexes rather than free ligand.[37h] Moreover some side effects may decrease upon complexation. In some cases the complex can exhibit bioactivities, where the free ligands dose not show any such activity. The mechanism of action can involve binding to a metal ion *in vivo* or the metal

complex may be a vehicle for activation of the ligand as the cytotoxic agent. In addition, coordination may lead to significant reduction of drug-resistance.[37i] These hydrazones are good chelating agents by coordinating the metal ions through the phenolic or acylic or alkoxy or amide oxygen and pyridyl or imine nitrogen atoms.

Several research groups reported bioactive copper(II) complexes with salicylaldehyde bezoylhydrazones (L^{13}), which were shown as potent inhibitors of DNA synthesis and cell growth.[38] The analogues have been also investigated as potential oral iron chelating drugs. Recently Kurup *et al*. synthesized [CuL^{13}(bipy)] (R = OH) complex (Figure 1.12a) and studied their bioactivity against Gram-positive *Bacillicus sp. a*nd Gram negative *V. cholerae*.[39a] Similarly the hydrazones in combination with cholesterol[39b] have also shown promising antimicrobial activity against the *C. abicans and S. Aureus*.

A pioneering work of Richardson in synthesis and studies (*in vitro* and *in vivo*) of orally effective high Fe chelating hydrazones in place of DFO therapy are came into light recently. [40] DFO (desferrioxamine) is a Fe chelator that has been extensively used for the treatment of Fe overload disease (e.g. *thalassemia*). He has successfully screened several aroylhydrazones, like L^{15}, L^{16} and salicylaldehyde isonicotinoyl hydrazones etc. having greater activity than DFO as anti-malarial agents against chloroquine-resistance and -sensitive parasite. In further investigations on anti malarial hydrazones, Bernhardt *et al*. has reported the results on pyridoxal isonicotinoyl hydrazones (L^{17}) and its analogues (L^{18}) having clinically useful Fe chelator properties (Figure 1.12b).[41] Moreover these chelators have shown low toxicity (*in vitro*) in cultured cells and they are simple and economical to prepare. They have also prepared Mn(II), Co(II), and Cu(II)

bis-complexes with these hydrazones and studied them systematically. The recent reports on the antibacterial and antifungal active bis acylhydrazones (L^{19}) (R = CH_3) and their complexes with some first row transition metal salts, revealed good activity against *Gram positive* bacteria.

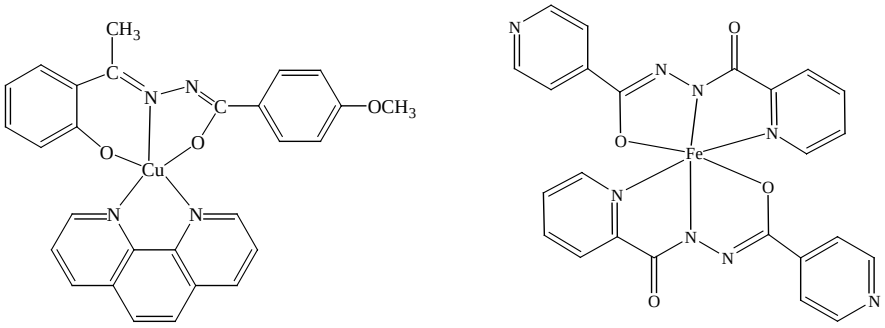

(a) (b)

Figure 1.12

Apart from the bioactive complexes, hydrazones have been used to prepare NLO active[42] materials like penta coordinated Cu(II) and tetra coordinated square-planar Cu(II) and Pd(II) complexes (Figure 1.13) by using hydrazine-based donor-acceptor L^{13} type Schiff bases and their derivatives.

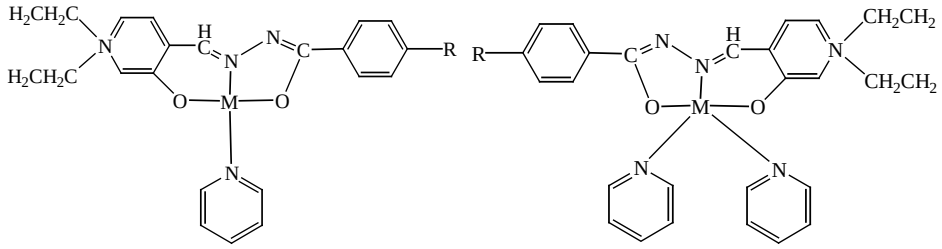

Figure 1.13

Over the past decade, a wide variety of mono and dinuclear transition metal (V, Mn, Fe, Ni, Cu, and Ru) complexes (Figure 1.14) with amide containing aroyl hydrazones (L^{14}) have been reported from our laboratory.[43] We have also isolated some square-planar Ni(II) and Cu(II) complexes with L^{19} (R = acac) and ruthenium(III) bis-complex by using L^{19} (R = CH_3) Schiff bases. In all the cases, the ligands coordinate the metal ion *via* deprotonated amide-O, imine-N and pyridine-N/phenolate-O/alkoxy-O atoms.

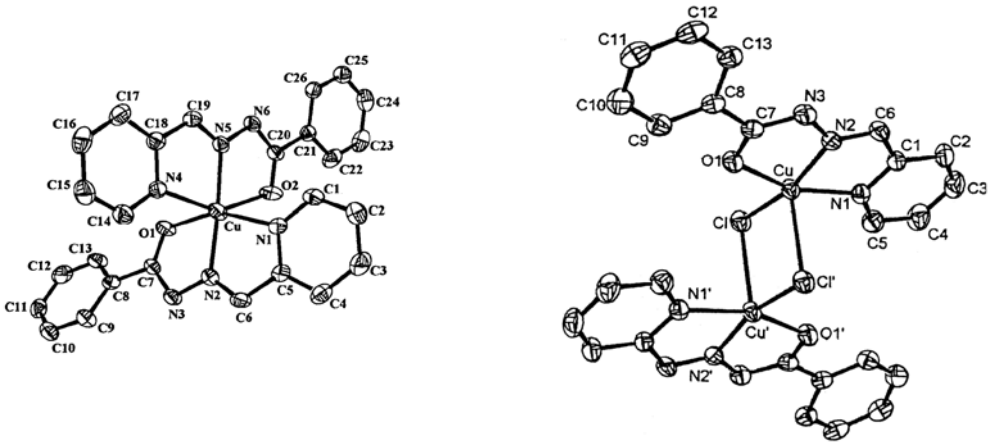

Figure 1.14

1.4. A short note on oximes and their metal complexes

Chemistry of oxime/oximate metal complexes have been investigated actively since 1890, when Schugaeff first introduced dimethylglyoxime as a reagent for nickel. Later Chugaev recognized its five-memberd chelating character[44]. These oxime ligands have played an important role for the continuing progress in the coordination chemistry. A vast amount of fascinating oxime

chemistry has been accumulated from various research works on structure, stability and reactivity of transition metal complexes. Extensive applications of these complexes have been found for their unusual electronic properties and as biochemical models. A. Chakravorty's excellent treatises and reviews in 1974 and 1980 described the synthesis and electron transfer studies of higher valent complexes with $L^7$and L^8 oxime containing ligands.[45a,b] After that, few more review articles have been published on synthesis and reactivity of oxime/oximate complexes.[45c-f]

Both diazine and dioxime ligand systems are known to act as molecular bridges between metal centers in polynuclear metal complexes. Additionally deprotonated oximes have been demonstrated to stabilize the metal centers in high oxidation states through strong L $\rightarrow$ M σ donation.[5d,e] In such higher-valent polynuclear (both homo- and hetero- nuclear) metal-oximates, the (=N–O^-) oxime function acts as a bridging[46] unit to yield several varieties of compounds. Such complexes are specially interesting with respect to new molecule based magnetic materials and bioinspired and /or biomimic materials. Dimethylglyoxime has been widely used for preparation of linear homo- and heterometallic oligonuclear complexes. Similarly oximes containing additional nitrogen, phenolate oxygen or thioether donors, such as those Schiff bases formed by condensation of diamines with diacetyl monooxime, 2,6-diacylphenol dioximes and the dioxime of 4,7-dithiadecane-2,9-dione, have also found applications in the preparation of various polynuclear complexes.[47] To date, several varieties of oxime-ligands are known for synthesizing high nuclearity clusters. A few of them are shown below.

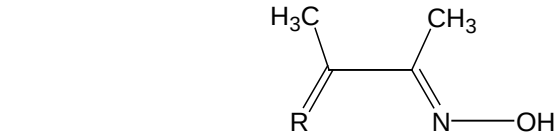

R =

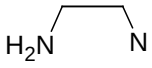

L^1

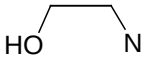

L^2

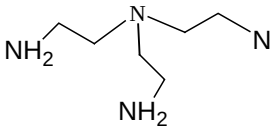

L^3

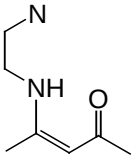

L^4

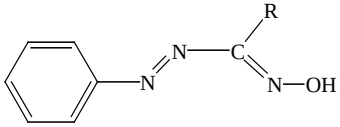

L^5

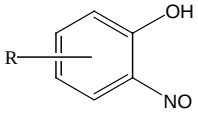

L^6

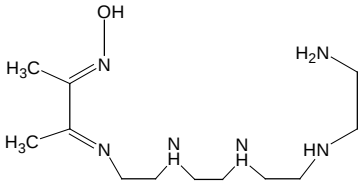

L^7

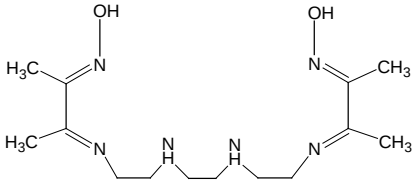

L^8

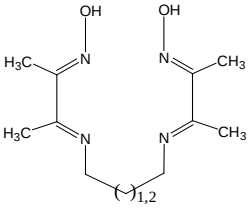

L^9

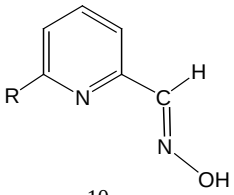

L^{10}

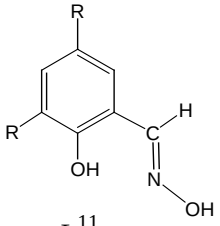

L^{11}

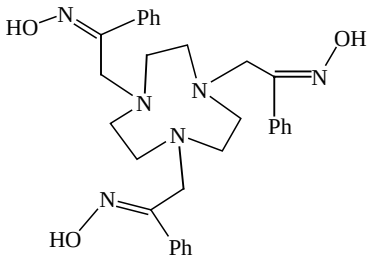

L^{12}

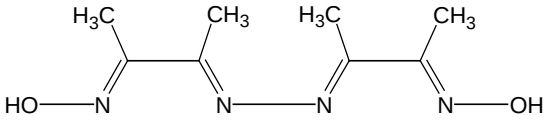

L^{13}

Okawa *et al.* reported the linear trinulcear Cu(II) complexes bridged by dimethylglyoximates showing very strong antiferromagnetic interactions between the copper centers. Later, a related butterfly shaped trinuclear copper(II) complex (Figure 1.15a) and the homo (Cu, Cu and Ni, Ni) and hetero (Cu, Ni) dinuclear complexes with L^9 have been reported.[48] A. Chakravorty and coworkers synthesized and studied various homo- and hetero- metallic dinuclear and linear trinuclear complexes (Figure 1.15c) containing oximate bridges with arylazo oximes and nitroso phenols.[49] Later Chauduri *et al*. reported some similar oximato (=N–O^-) bridged homo- and hetero- dinuclear ($M^{II}M^{II}$ and $Cu^{II}M^{III}$) transition metal complexes (Figure 1.16a.).[50] These complexes exhibit weak to strong antiferromagnetic and also ferromagnetic coupling between the metal centers. A number of asymmetric dinuclear $[Cr^{III}\mu(O–N)_3M^{II}]$ transition metal complexes $[LCr^{III}\mu(PyA)_3M^{II}]^{2+/3+}$ M = Fe, Ni, Cu, Zn and Co(III) (Figure 1.16b) have been produced by using pyridine-2-aldoxime (L^{10}).[51a] Earlier to these dimetallic complexes, a triangular μ_3-oxo bridged copper(II) complex with this same ligand L^{10} (Figure 1.15b) has been reported.[51b] In this triangular complex, each copper center is in square-pryramidal geometry with sulfate–O group in the

axial position. The magnetic moment of the compound reveals strong antiferromagnetic interaction.

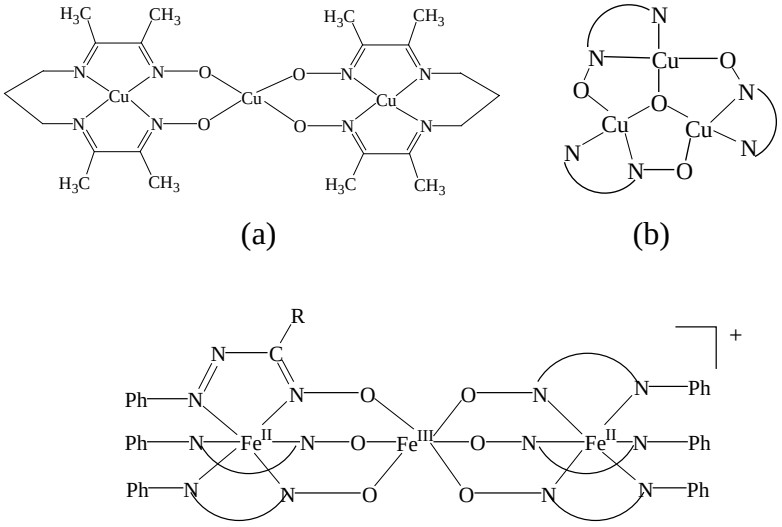

Figure 1.15

The hexanuclear M^{III} complexes containing $[M^{III}_6(\mu_3\text{-}O)_2]$ (M = V, Cr, Mn and Fe) structural core by using salicylaldoxime (L^{11}) ligand systems have been reported (Figure 1.17a).[51c] These complexes having the general formula $[M^{III}_6(\mu_3\text{-}O)_2(L^{11})_6(\mu_2OOCR)_2(OH)_2(RCN)_2]$, $RCOO^-$ = pivalate, benzylate, benzoate or propionate, and RCN = acetonitrile, propionitrile or butyronitrile, have been structurally characterized and found to be isotypic.

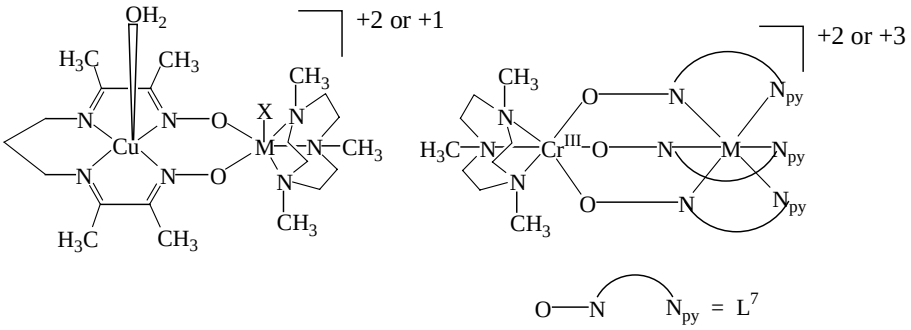

(a) (b)

Figure 1.16

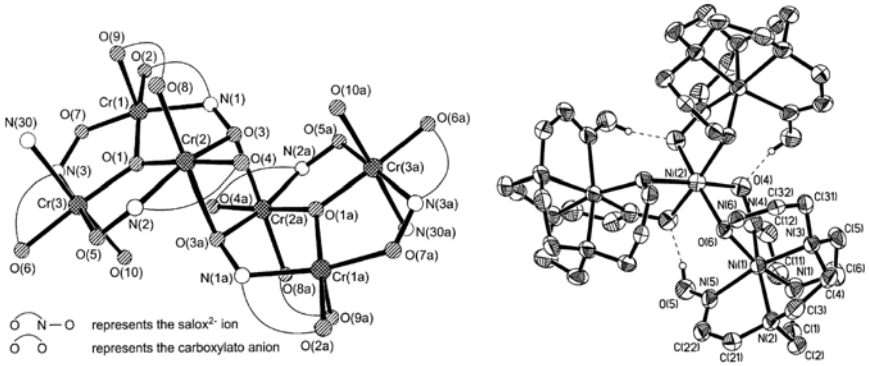

(a) (b)

Figure 1.17

A significant number of metallacrown and inverse metallacrown[33,35] compounds synthesized using salicylhydroxamic acid and its analogous ligand systems, with an additional (–C=O ↔ =C–O$^-$) bridging O$^-$ atom in compared to the L[11] ligands. There is an enormous growth of pendent-arm derivatives of azamacrocylclic ligands. Pavlishchuk *et al*. synthesized the 1,4,7–

(acetophenoneoxime)-1,4,7-triazacyclononane ligand (L^{12}), a new member of the *N*-functionalised TACN series[51d] derived by the combination of azamacrocycle and strong ligand field oxime group. Polynuclear Mn, Co and Ni complexes (Figure 1.17b) with high-spin ground states, having ferro and antiferromagnetic spin-exchange interactions between the metal centers have been synthesized with this ligand.

1.5. About the present investigation

In the previous sections we have discussed briefly about the different types of diazine and oxime/dioxime ligands and their coordination modes. A brief survey of the known first row transition metal complexes of these ligands with unique properties is outlined.

In the present investigation, we have used two diazine compounds (**1** and **2**), aroylhydrazones of 2-pyridinecarboxaldehyde (**3**) and a dioxime compound (**4**) to explore the chemistry of the Mn, Fe and Co.

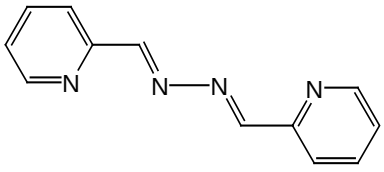

L

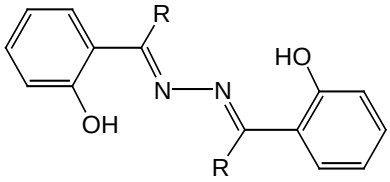

H_2L (R = H, Me)

1 **2**

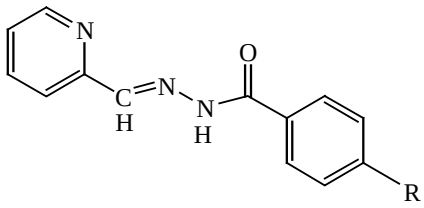

HL (R = H, Cl, OMe, Me, NMe_2, NO_2)

3

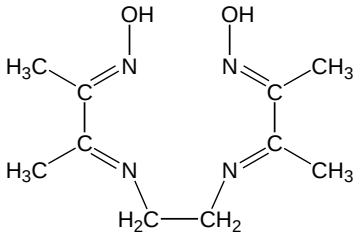

H_2bamen

4

The diazine compounds (**1** and **2**) have been selected with the aim of synthesizing dinuclear helical species. New higher-valent and polynuclear complexes have been targeted with the aroylhydrazones (**3**) and the dioxime (**4**) compounds. In the following chapters we have described our observations in the above efforts. With special reference to (i) synthesis and characterization, (ii) structure and bonding and (iii) chemical, spectroscopic and electrochemical properties.

1.6. References

1. A. Werner, *Z. Anorg. Chem.*, **1893**, *3*, 267.
2. L. K. Thompson, *Coord. Chem. Rev.*, **2002**, *233*, 193.
3. (a) A. Tsafack, J. Golenser, J. Libman, A. Shanzer, Z. I. Cabantchik, *Mol. Pharmacol.*, **1995,** *47*, 403. (b) A. Tsafack, M. Loyevsky, P. Ponka, Z. I. Cabantchik, *J. Lab. Clin. Med.*, **1996**, *127*, 574. (c) See for example: R. H. Holm, E. I. Solomon, Guest Editors, *Chem. Rev.*, **1996**, 7.

4. (a) C. B. Aakeroy, A. M. Beatty, D. S. Leinen, *J. Am. Chem. Soc.*, **1998**, *120*, 7383. (b) Z. Xu, L. K. Thompson, V. A. Milway, L. Zhao, T. Kelly, D. O. Miller *Inorg. Chem.*, **2003**, *42*, 2950. (c) F. Birkelbach, U. Florke, H. J. Haupt, C. Butzlaff, A. X. Trautwein, K. Wieghardt, P. Chauduri, *Inorg. Chem.*, **1998**, *37*, 2000.
5. (a) N. R. Sangeetha, S. Pal, *Bull. Chem. Soc. Jpn.*, **2000**, *73*, 357. (b) M. Mikuriya, D. Jie, Y. Kakuta, T. Tokii, *Bull. Chem. Soc. Jpn.*, **1993**, *66*, 1132. (c) S. N. Pal, S. Pal *E. J. Inorg. Chem.*, **2003**, 4244. (d) J. G. Mahanty, A. Chakravorty, *Inorg. Chem.*, **1977**, *16*, 1561. (e) A. Hussein, Y. Sulfab, M. Nasreldin, *Inorg. Chem.*, **1989**, *28*, 157.
6. (a) M. J. Clague, N. L. Keder, A. Butter, *Inorg. Chem.*, **1993**, *32*, 4754. (b) R. J. Debus, *Biochim. Biophys. Acta.* **1992**, *269*, 1102. (c) G. T. Groves, Y. Watanabe, *J. Am. Chem. Soc.*, **1988**, *110*, 8443. (d) G. Waldo, S. Yu, J. E. P. Hahn, *J. Am. Chem. Soc.*, **1992**, *114*, 5869. (e) A. E. Przybylz, J. Robbinson, N. Menon, H. D. Pecr, Jr., *FEMS Microbiol. Rev.*, **1992**, *88*, 109.
7. D. K. Dey, A. Lycka, S. Mitra, G. M. Rosair, *J. Org. met. Chem.*, **2004**, *689*, 88.
8. C. N. Verani, E. Rentschelr, T. Weyhermüller, E. Bill, P. Chaudhuri, *J. Chem. Soc., Dalton Trans.*, **2000**, 4263.
9. (a) C. J. Ó Connor, R. J. Romananch, D. M. Robertson, E. E. Eduok, F. R. Fronczek, *Inorg. Chem.*, **1983**, *22*, 449. (b) J. Saroja, V. Manivannan, P. Chakraborty, S. Pal, *Inorg. Chem.*, **1995**, *34*, 3099. (c) Z. Xu, *Ph.D. Thesis*, Memorial University of Newfoundland, **1998**.
10. X. Xu, X. You, Z. Sun, X.Wang, H. Liu, *Acta Crystallogr., Sect. C*, **1994**, *50*, 1169.
11. R. Bauer, C. O. Rupe, *Anal. Chem.*, **1971**, *43*, 421.
12. G. S. Chen, J. K. Wilbur, C. L. Barnes, R. Glaser, *J. Chem. Soc., Perkin Trans. 2*, **1995**, 2311.

13. (a) V. L. Goedken, Y. Park, S. M. Peng, J. M. Norris, *J. Am. Chem. Soc.*, **1974**, *96*, 7693. (b) C. Thilgen, F. Vögtle, *Chem. Ber.*, **1991**, *124*, 671. (c) T. W. Bell, A. T. Papoulis, *Angew. Chem., Int. Ed. Engl.*, **1992**, *31*, 749.
14. P. Espinet, J. Etxebarria, M. Marcos, J. Pérez, A. Remon, J. L. Serrano, *Angew. Chem., Int. Ed. Engl.*, **1989**, *28*, 1065.
15. (a) J. D Ranford, J. J. Vittal, Yu. M. Wang, *Inorg. Chem.*, **1998**, *37*, 1226. (b) J. R. Merchant, D. S. Clothia, *J. Med. Chem.*, **1970**, *13*, 335.
16. (a) Z. Xu, L. K. Thompson, Edt. A. P. B. Lever, *Comprehensive coordination chemistry*, **2004** *Vol. 1*, 63. (b) Z. Xu, L. K. Thompson, D. O. Miller, *Inorg. Chem.*, **1997**, *36*, 3985. (c) L. Zhao, C. J. Metthews L. K. Thompson. *J. Chem. Soc., Chem. Com.*, **2001**, 1170. (d) Z. Xu, L. K. Thompson, D. O. Miller, J. A. K. Howard, A. E. Goeta, *Inorg. Chem.*, **1998**, *37*, 3620.
17. J. -M. Lehn, *Supramolecular Chemistry – Concepts and Perspectives*, **1995,** VCH, Weinheim.
18. (a) M. Elhabiri, R. Scopelliti, J. C. G. Bunzli, C. Piguet, *J. Chem. Soc., Chem. Commun.*, **1998**, 2347. (b) G. Rapenne, B. T. Patterson, J. P. Sauvage, F. R. Keene, *J. Chem. Soc., Chem. Commun.*, **1999**, 1853. (c) C.Y. Duan, Z. H. Liu, X. Z. You, F. Xue, T. C. W. Mak, *J. Chem. Soc., Chem. Commun.*, **1997**, 381. (d) G. S. Hannan, D. Volkmer, U. S. Schubert, J. -M. Lehn, G. Baum, D. Fenske, *Angew. Chem., Int. Ed. Engl.*, **1997**, *36*, 1842. (e) D. M. Bassani, J. -M. Lehn, K. Fromm, D. Fenske, *Angew. Chem., Int. Ed.*, **1998**, *37*, 236.
19. (a) C. Piguet, G. Bernardinelli, G. Hopfgartner, *Chem. Rev.*, **1997**, *97*, 2005. (b) M. Albrecht, *J. Inclusion Phenom., Macrocyclic Chem.*, **2000,** *36*, 127. (c) A. F. Williams, *Pure Appl. Chem.*, **1996**, *68*, 1285. (d) M. Fujita, *Acc. Chem. Res.*, **1999**, *32*, 53. (e) B. Olenyuk, A. Fechtenkotter, P. J. Stang, *J. Chem. Soc., Dalton Trans.*, **1998**, 1707. (f) K. N. Raymond, *Acc. Chem.*

Res., **1999**, *32*, 975. (g) E. C. Constable, *Prog. Inorg. Chem.*, **1994**, *42*, 67. (h) C. D. Buchecker, G. Rapenne, J. P. Sauvage, *Coord. Chem. Rev.*, **1999**, *186*, 167.

20. (a) S. I. Stupp, P. V. Braun, *Science*, **1997**, *277*, 1242. (b) D. Philp, J. F. Stoddart, *Angew. Chem., Int. Ed. Engl.*, **1996**, *35*,1154. (c) Z. Guo, P. J. Sadler, *Angew. Chem., Int. Ed. Engl.*, **1999**, *38*, 1512. (d) P. D. Smith, D. A. Slizys, G. N. George, C. G. Young, *J. Am.Chem. Soc.*, **2000**, *122*, 2946.
21. M. J. Hannon, C. L. Painting, J. Hamblin, A. Jackson, W. Errington, *Chem. Commun.*, **1997**, 1807.
22. (a) C. R. Rice, C. J. Baylies, H. J. Clayton, J. C. Jeffery, R. L. Paul, M. D. Ward, *Inorg. Chim. Acta*, **2003,** *351*, 207. (b) J. Hamblin, L. J. Childs, N. W. Alcock, M. J. Hannon, *J. Chem. Soc., Dalton Trans.*, **2002**, 164.
23. (a) W. J. Stratton, D. H. Busch, *J. Am. Chem. Soc.*, **1958**, *80*, 1286. (b) W. J. Stratton, D. H. Busch, *J. Am. Chem. Soc.*, **1958**, *80*, 3191. (c) W. J. Stratton, D. H. Busch, *J. Am. Chem. Soc.*, **1960**, *82*, 4834. (d) P.W. Ball, A. B. Blake, *J. Chem. Soc., A.* **1969**, 1415. (e) W. J. Stratton, *Inorg. Chem.*, **1970**, *3*, 517.
24. P. D. Boyd, G. M. Sheldric, *J. Chem. Soc., Dalton Trans.*, 1**974**, 1097.
25. J. Hamblin, A. Jackson, N. W. Alcock, M. J. Hannon, *J. Chem. Soc., Dalton Trans.*, **2002**, 1635.
26. G. Dong, P. K. Liang, D. C. Ying, Z. Y. Gang, M. Q. Jin, *Chemistry Letters*, **2002**, 1014.
27. (a) L. K. Thompson, Z. Xu, A. E. Goeta, J. A. K. Howard, H. J. Clase, D. O. Miller, *Inorg. Chem.*, **1998**, *37*, 3217. (b) Z. Xu, L. K. Thompson, C. J. Metthews, D. O. Miller, A. E. Goeta, C. Wilson, J. A. K. Howard, M. Ohaba, H. Okawa, *J. Chem. Soc., Dalton Trans.*, **2000**, 69.
28. F. C. Jie, D. C. Ying, M. Hong, H. Cheng, M. Q. Jin, L. Y. Jang, M. Y. Hua, W. Z. Ming, *Organometallics*, **2001,** *20*, 2525.

29. (a) L. Zhao, V. Niel, L. K. Thompson, Z. Xu, V. A. Milway, R. G. Harvey, D. O. Miller, C. Wilson, M. Leech, J. A. K. Howard, d S. L. Heath, *J. Chem. Soc., Dalton Trans.,* **2004**, 1446. (b) C. J. Matthews, K. Avery, Z. Xu, L. K. Thompson, L. Zhao, D. O. Miller, K. Biradha, K. Poirier, M. J. Zaworotko, C. Wilson, A. E. Goeta, J. A. K. Howard, *Inorg. Chem.,* **1999**, *38*, 5276. (c) L. Zhao, C. J. Matthews, L. K. Thompson, S. L. Heath, *J. Chem. Soc., Chem. Commun.,* **2000**, 265. (d) O. Waldmann, L. Zhao, L. K. Thompson, *Phys. Rev. Lett.,* **2002**, *88*, 66401.18 (e) O. Waldmann, R. Koch, S. Schromm, P. Müller, L. Zhao, L. K. Thompson, *Chem. Phys. Lett.*, **2000**, *332*, 73. (f) L. K. Thompson, L. Zhao, Z. Xu, D. O. Miller, W. M. Reiff, *Inorg. Chem.*, **2003**, *42*, 128. (g) L. Zhao, Z. Xu, L. K. Thompson, S. L. Heath, D. O. Miller, M. Ohba, *Angew. Chem., Int. Ed.*, **2000**, *39*, 3114.

30. (a) L. K. Thompson, C. J. Matthews, L. Zhao, Z. Xu, D. O. Miller, C. Wilson, M. A. Leech, J. A. K. Howard, S. L. Heath, A. G. Whittaker, R. E. P. Winpenny, *J. Solid State Chem.*, **2001**, *159*, 308. (b) Z. Xu, L. K. Thompson, C. J. Matthews, D. O. Miller, A. E. Goeta, J. A. K. Howard, *Inorg. Chem.*, **2001**, *40*, 2446.

31. (a) C. J. Matthews, Z. Xu, S. K. Mandal, L. K. Thompson, K. Biradha, K. Poirier, M.J. Zaworotko, *J. Chem. Soc. Chem. Commun.*, **1999**, 347. (b) *Inorg. Chem.*, **2001**, *40*, 4448.

32. L. Zhao, L.K. Thompson, Z. Xu, D.O. Miller, D.R. Stirling, *J. Chem. Soc. Dalton Trans.,* **2001,** 1706.

33. (a) M. S. Lah, V. L. Pecoraro, *J. Am. Chem. Soc.*, **1989**, *111*, 7258. (b) V. L. Pecoraro, A. J. Stemmler, B. R. Gibney, J. J. Bodwin, H. Wang, J. W. Kampf, A. Barwinski, *Progress in Inorganic Chemistry*, **1997,** *45* 83, (Ed. K. D. Karlin), Wiley, New York (c) M. S. Lah, V. L. Pecoraro, *Comments Inorg. Chem.*, **1990**, *11*, 59.

34. (a) D. J. Cram, J. M. Cram, *Container Molecules and Their Guests*, **1994,** The Royal Society of Chemistry, Cambridge, UK. (b) M. Berger, F. P. Schmidtchen, *J. Am. Chem. Soc.*, **1996,** *118*, 8947. (c) J. M. Rivera, T. Martin, J. Rebek Jr., *Science*, **1998**, *279*, 1021. (d) R. W. Saalfrank, B. Demleitner, in *Perspectives in Supramolecular Chemistry*, **1999,** *5*, 1., (Ed. J. P. Sauvage), Wiley-VCH, Weinheim.

35. (a) B. Kurzak, E. Farkas, T. Glowiak, H. Kozlowski, *J. Chem. Soc., Dalton Trans.*, **1991**, 163. (b) B. R. Gibney, A. J. Stemmler, S. Pilotek, J. W. Kampf, V. L. Pecoraro, *Inorg. Chem.*, **1993**, *32*, 6008. (c) B. R. Gibney, D. P. Kessissoglou, J. W. Kampf, V. L. Pecoraro, *Inorg. Chem.*, **1994**, *33*, 4840. (d) A. J. Stemmler, J. W. Kampf, V. L. Pecoraro, *Inorg. Chem.*, **1995**, *34*, 2271. (e) B. R. Gibney, H. Wang, J. W. Kampf, V. L. Pecoraro, *Inorg. Chem.*, **1996**, *35*, 6184. (f) J. A. Halfen, J. J. Bodwin, V. L. Pecoraro, *Inorg. Chem.*, **1998**, *37*, 5416.

36. (a) B. Kwak, H. Rhee, S. Park, M. S. Lah, *Inorg. Chem.*, **1998,** *37*, 3599 (b) B. Kwak, H. Rhee, M. S. Lah, *Polyhedron*, **2000**, *19*, 1985 (c) S. X. Liu, S. Lin, B. Z. Lin, C. C. Lin, J. Q. Huang, *Angew. Chem., Int. Ed.*, **2001**, *40*, 1084. (d) S. Lin, S. X. Liu, J. Q. Huang, C. C. Lin, *J. Chem. Soc., Dalton Trans.*, **2002**, 1595.

37. (a) Z. H. Chohan, *Synth. React. Inorg. Met. Org. Chem.*, **2001**, *31*, (1), 1. (b) D. V. Reyk, S.. Sarel, N. Hunt, *Biochem. Pharmacol.*, **2000**, *60*. (4), 581. (c) N. Nawar, M. A. Khattab, N. M. Hosny, *Synth. React. Inorg. Met. Org. Chem.*, **1999**, *28* (8), 1365. (d) D. Negoiu, M. Calinescu, A. Emandi, E. Badau, *Russ. J. Coord. Chem.*, **1999**, 25 (1), 36. (e) S. Ersan, S. Nacak, R. Berkem, *Farmaco*, **1998**, *53* (12), 773. (f) A. Gürsoy, N. Terzioglu, G. Ö tük, *J. Med. Chem.*, **1997**, *32*, 753. (g) R. C. Sharma, J. Ambwani, V. K. Varshney, *J. Indian Chem. Soc.*, **1992**, *69*, 770. (h) N. Farrell, *Coord. Chem.*

Rev., **2002**, *1*, 232. (i) D. X. West, S. B. Padhye, P. B. Sonawane, In *Structure and Bonding*, **1991**, Vol. *76*, 1, Springer-Verlag: New York.

38. (a) D. K. Johnson, T. B. Murphy, N. J. Rose, W. H. Goodwin, L. Pickart, *Inorg. Chim. Acta*. **1982**, *67*, 159. (b) L. Pickart, W. H. Goodwin, W. Burgua, T. B. Murphy, D. K. Johnson, *Biochem. Pharmacol*., **1983**, *32*, 3868.
39. P. B. Sreeja, M. R. P. Kurupa, A. Kishore, C. Jasmin, *Polyhedron*, **2004,** *23*, 575. (b) L. Céline, J. M. Brunel, N. Vidal, M. Herbomez, Y. Letourneux, *Eur. J. Med. Chem.*, **2004,** *39*, 1067, references there in.
40. (a) D. R. Richardson, E. H. Tran, P. Ponka, *Blood*, **1995**, *86*, 4295. (b) D. R. Richardson, P. Ponka *J. Lab. Clin. Med.*, **1998**, *132*, 351. (c) D. R. Richardson, *Exp. Opin. Invest. Drugs*, **1999,** *8*, 2141. (d) D. B. Lovejoy, D. R. Richardson, *Blood*, **2002**, *100*, 666. (e) T. Chaston, D. Lovejoy, R. N. Watts, D. R. Richardson, *Clin. Cancer Res.*, **2003**, *9*, 402.
41. (a) C. M. Armstrong, P. V. Bernhardt, P. Chin, D. R. Richardson, *Eur. J. Inorg. Chem.*, **2003**, 1145. (b) P. V. Bernhardt, P. Chin, D. R. Richardson, *J. Chem. Soc., Dalton Trans.*, **2004**, 3342. (c) P. V. Bernhardt, P. Chin, D. R. Richardson, *J. Biol. Inorg. Chem.*, **2001**, *6*, 801, and references there in.
42. F. Cariati, U. Caruso, R. Centore, W. Marcolli, A. De Maria, B. Panunzi, A. Roviello, A. Tuzi, *Inorg. Chem.*, **2002**, 41, 6597.
43. (a) N. R. Sangeetha, S. N. Pal, S. Pal, *Polyhedron*, **2000**, *19*, 1593. (b) S. N. Pal and S. Pal, *J. Chem. Soc., Dalton Trans.*, **2002**, 2102. (c) A. Mukhopadhyay, S. Pal, *Polyhedron*, **2004**, *23*, 1997. (d) N. R. Sangeetha, K. Baradi, R. Gupta, C. K. Pal, V. Manivanna, S. Pal, *Polyhedro*n, **1999**, *18*, 1425. (e) N. R. Sangeetha, C. K. Pal, P. Ghosh, S. Pal, *J. Chem. Soc., Dalton Trans.*, **1996**, 3293. (f) A. Choudhury, B. Geetha, N. R. Sangeetha, V. Kavitha, V. Susila, S. Pal, *J. Coord. Chem.*, **1999**, *48*, 87. (g) G V.

Karunakar, N. R. Sangeetha, V. Susila, S. Pal, *J. Coord. Chem.*, **2000**, *50*, 51.

44. (a) L. Tschugaeff, *Chem. Ber.*, **1890,** *23*, 1. (b) L. A. Chugaev, *Zh. Russ. Physicochem. Soc.*, **1909**, *41*, 184.
45. (a) A. Chakravorty, *Coord. Chem. Rev.*, **1974**, *13*, 1. (b) K. Nag, A. Chakravorty, *Coord. Chem. Rev.*, **1980**, *33*, 87. (c) P. Chaudhuri, *Coord. Chem. Rev*., **2003**, *243*, 143. (d) M. E. Keeney, K. O. Asare, K. A. Woode, *Coord. Chem. Rev*., **1984**, *59*, 141. (e) V. Y. Kukushkin, A. J. L. Pombeiro, *Coord. Chem. Rev*., **1999,** *181*, 147. (f) P. Chaudhuri, *Proc. Indian Acad. Sci. Chem. Sci.*, **1999**, *111*, 397.
46. (a) S. Chattopadhyay, P. Basu, S. Pal, A. Chakravorty, *J. Chem. Soc., Dalton Trans.*, **1990,** 3829. (b) J. P. Costes, F. Dahan, A. Dupuis, J. P. Laurent, *J. Chem. Soc,. Dalton Trans.*, **1998**, 1307.
47. (a) S. Zhan, C. Hu, X. Chen, Q. Meng, C. Lu, G. Wang, P. Zheng, *Polyhedron*, **1999**, *18*, 2035. (b) R. Ruiz, F. Löret, M. Julve, M. Carmen Muñoz, C. Bois, *Inorg. Chim. Acta*, **1994**, *219*, 179. (c) D. Black, A. J. Blake, K. P. Dancey, A. Harrison, M. McPartlin, S. Parsons, P. A. Tasker, G. Whittaker, M. Schröder, *J. Chem. Soc., Dalton Trans.*, **1998**, 3953.
48. (a) D. Luneau, H. Oshio, H. Okawa, S. Kida, *J. Chem. Soc., Dalton Trans.*, 1990, 2283. (b) D. Luneau, H. Oshio, H. Okawa, M. Koikawa, S. Kida, *Bull. Chem. Soc. Jpn.*, **1990**, *63*, 2212.
49. (a) S. Pal, D. Bandyopadhyay, D. Datta, A. Chakravorty, *J. Chem. Soc., Dalton Trans.*, **1985**, 159. (b) S. Pal, T. Melton, R. N. Mukherjee, A. R. Chakravarty, M. Tomas, L. R. Falvello, A. Chakravorty, *Inorg. Chem.*, **1985**, *24*, 1250. (c) S. Pal, R. N. Mukherjee, M. Tomas, L. R. Falvello, A. Chakravorty, *Inorg. Chem.*, **1986**, *25*, 200. (d) S. Pal, A. Chakravorty, *Inorg. Chem.*, **1987**, *26*, 4331. (e) P. Basu, S. Pal, A. Chakravorty, *J. Chem. Soc., Chem. Commun.*, **1989**, 977. (f) P. Basu, S. B. Choudhury, S. Pal, A.

Chakravorty, *Inorg. Chem.*, **1989**, *28*, 2680. (g) P. Basu, S. Pal, A. Chakravorty, *J. Chem. Soc., Dalton Trans.*, **1990**, 9. (h) S. Chattopadhyay, P. Basu, D. Ray, S. Pal, A. Chakravorty, *Proc. Indian Acad. Sci., Chem. Sci.*, **1990**, *102*, 195. (i) S. Chattopadhyay, P. Basu, S. Pal, A. Chakravorty, *J. Chem. Soc., Dalton Trans.*, **1990**, 3829. (j) P. Basu, S. Pal, A. Chakravorty, *J. Chem. Soc., Dalton Trans.*, **1991**, 3217.

50. (a) P. Chaudhuri, M. Winter, P. Fleischhauer, W. Haase, U. Flo¨rke, H. J. Haupt, *J. Chem. Soc., Chem. Commun.*, **1993**, 566. (b) P. Chaudhuri, M. Winter, P. Fleischhauer, W. Haase, U. Flo¨rke, H. J. Haupt, *Inorg. Chim. Acta*. **1993,** *212*, 241. (c) D. Burdinski, E. Bill, F. Birkelbach, K. Wieghardt, P. Chaudhuri, *Inorg. Chem.*, **2001**, *40*, 1160. (d) P. Chaudhuri, M. Hess, E. Rentschler, T. Weyhermüller, U. Flörke, *New J. Chem,*. **1998**, 553. (e) C. N. Verani, E. Bothe, D. Burdinski, T. Weyhermüller, U. Flo¨rke, P. Chaudhuri, *Eur. J. Inorg. Chem.*, **2001**, 2161. (f) F. Birkelbach, M. Winter, U. Flörke, H. J. Haupt, C. Butzlaff, M. Lengen, E. Bill, A. X Trautwein, K. Wieghardt, P. Chaudhuri, *Inorg. Chem.*, **1994**, *33*, 3990.
51. (a) S. Ross, T. Weyhermüller, E. Bill, K. Wieghardt, P. Chaudhuri, *Inorg. Chem.*, **2001**, *40*, 6656. (b) R. Beckket, B. F. Hoskins, *J. Chem. Soc., Dalton Trans.*, **1972**, 291. (c) D. Burdinski, F. Birkelbach, T. Weyhermüller, U. Flörke, H. J. Haupt, M. Lengen, A. X. Trautwein, E. Bill, K. Wieghardt, P. Chaudhuri, *Inorg. Chem.*, **1998,** *37*, 1009. (d) V. Pavlishchu, F. Birkelbach, T. Weyhermüller, K. Wieghardt, P. Chaudhuri, *Inorg. Chem.*, **2002**, *41*, 4405.

Chapter 2

Trigonal Prismatic and Octahedral Mn(II) Complexes derived from N,N′bis-(picolinylidene)hydrazine[§]

2.1. Abstract

Synthesis, structure and properties of two manganese(II) complexes, $[MnL_2Cl_2]\cdot 0.125H_2O$ and $[MnL^1(H_2O)]I_2\cdot 4H_2O$ have been described. The reaction of tetradentate ligand (L) N,N'-bis(picolinylidene)hydrazine with $MnCl_2\cdot 4H_2O$ produced $[MnL_2Cl_2]\cdot 0.125H_2O$ a hexa-coordinated octahedral complex. Here L acts as bidentate ligand and the metal center is in N_4Cl_2 coordination sphere. The complex, $[MnL^1(H_2O)]I_2\cdot 4H_2O$, having trigonal prismatic N_5O coordination sphere, has been isolated by the reaction of L with N-(picolinylidene)hydrazine in presence of Mn^{2+}. The pentadentate N_5 donor ligand, bis(picolinylidenehydrazyl)(2-pyridyl)methane (L^1), is formed by the addition of N-(picolinylidene)hydrazine to one of the metal activated azomethine fragment of the tetradentate diazine ligand N,N'-bis(picolinylidene)hydrazine (L). Analytical, spectroscopic and magnetic techniques have been used for the characterization of these complexes. Structures of the complexes were determined by X-ray crystallography. EPR spectral features of the complexes are typical for mononuclear high–spin d^5 manganese(II) systems. In the solid state, the $[MnL_2Cl_2]\cdot 0.125H_2O$ molecules forms a chain like arrangements *via* C–H···N interactions, this infinite chains were further connected by neighbouring water–O atoms *via* very weak C–H···O interactions leading to a two dimensional network.

[§] A part of this work has been published in *Inorg. Chem. Commun*., **2001**, *4*, 656–660.

On the other hand, in $[MnL^1(H_2O)]I_2{\cdot}4H_2O$ the water and iodide ions forms two different types of hydrogen bonded infinite helices. Further interaction between these two (H_2O-I) helices leads to a one-dimensional water-iodide tapes. The complex cations were linked to these water-iodide tapes *via* O–H···O and N–H···O interactions and a two dimensional array is formed.

2.2. Introduction

The dinuclear $[M_2L_3]^{4+}$ (M = Fe, Co, Ni) complexes, with N,N'–bis(picolinylidene)hydrazine Schiff base, were first reported by Stratton and Bush.[1] The X-ray structure of a dicobalt(II) complex with the Schiff base derived from 2-acetylpyridine and hydrazine was the first confirmation of the triple helicate motif in this type of complexes.[2] Later several 3d transition metal complexes[3] (except manganese) have been reported with this Schiff base and its derivatives. In such dinuclear complexes the N–N single bond acts as the bridging unit and wraps around two metal ions in a helical fashion. However, in our attempts to prepare such helical complexes by using N,N′–bis(picolinylidene)hydrazine (L) with manganese, we have isolated a mononuclear octahedral and a mononuclear trigonal prismatic manganese(II) complexes. Due to the involvement of manganese in various biological systems there has been immense interest in the coordination chemistry of manganese complexes.[4,5,6] As a result; a vast literature on manganese complexes is now available. In most of the structurally characterized complexes, the hexa-

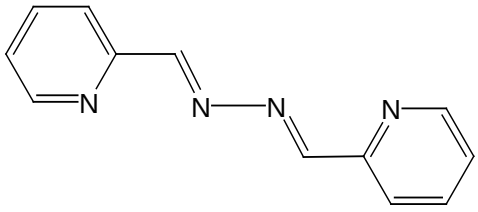

Figure 2.1. Ligand L

coordinated metal center is in octahedral coordination sphere. Another possibility for the hexa-coordinated system is trigonal prismatic coordination geometry. However, the hexa-coordinated metal complexes with trigonal prismatic coordination geometry around the metal center are not very common. The octahedral arrangement of the coordinating atoms is considered energetically more favored than the trigonal prismatic arrangement due to ligand-field stabilization and intermolecular repulsion of the coordinating atoms. The classic examples of trigonal prismatic complexes are metal tris(dithiolenes). In these complexes, the ligand constraints, overall charge of the complex, bonding between the coordinating atoms and π-bonding are the important parameters for stabilization of the trigonal prismatic geometry.[7,8] Recently several hexa-coordinated trigonal prismatic complexes of d^0 metal ions with monodentate ligands are reported.[9,10] The preference for trigonal prismatic geometry over octahedral geometry is attributed to the absence of steric and π-bonding effects of these monodentate ligands.[10,11] Another approach is the use of a rigid hexadentate ligand in which the coordinating atoms are so disposed that they create a trigonal prismatic pocket to accommodate the metal centre. Examples of such N_6 donor ligands are *cis*-1,3,5-tris(2-pyridinealdimino)cyclohexane,[12] tris(2-aldoximo-6-pyridyl)phosphine,[13,14] *cis*-1,3,5-tris(2-pyridylmethylamino)cyclohexane[15] and tris(3-(2-pyridyl)pyrazolyl)-hydroborate.[16]

Herein, we describe the synthesis and characterization of the octahedral manganese(II) complex $[MnL_2Cl_2]$ with the parent ligand N,N'-bis (picolinylidene)hydrazine (L) and a trigonal prismatic manganese(II) complex, $[MnL^1(H_2O)]^{2+}$, with a rigid but N_5 donor ligand, bis(picolinylidenehydrazyl)(2-pyridyl)methane (L^1) formed by metal activated transformation of L.

2.3. Experimental section

2.3.1. Materials

The ligand N,N'-bis(picolinylidene)hydrazine was prepared in high yield by condensation of two mole equivalents of 2-pyridinecarboxaldehyde with one mole equivalent of hydrazine hydrate by following reported procedure.[2a] All other chemicals and solvents were of analytical grade available commercially and were used as received.

2.3.2. Physical measurements

Elemental (C, H, N) analysis data were obtained with a Perkin-Elmer Model 240C elemental analyzer. Methanol solutions of the complexes were used to record the electronic spectra on a Shimadzu 3101-PC UV/vis/NIR spectrophotometer. Infrared spectra were collected by using KBr pellets on a Jasco-5300 FT-IR spectrophotometer. EPR spectra were recorded on a Jeol JES-FA200. The magnetic susceptibility at 298 K was measured on a PAR vibrating-sample magnetometer fitted with a Walker Scientific L75FBAL magnet. A diamagnetic corrections (-247 x 10^{-6} for **1** and -359 x 10^{-6} cgsu for **2**) calculated from Pascal's constants,[17] were used to obtain the molar paramagnetic susceptibilities. Solution electrical conductivity was measured with a Digisun DI-909 conductivity meter.

2.3.3. Synthesis of Manganese (II) complexes

$[MnL_2CL_2]\cdot 0.125H_2O$ (1)

To a hot yellow methanol solution (20 ml) of N,N'-bis(picolinylidene)hydrazine (443 mg 2.10 mmol) (L) another methanolic solution (20 ml) of $MnCl_2\cdot 4H_2O$ (208 mg 1.05 mmol) was added drop wise. The mixture was then refluxed for 16 h continuously. The reddish brown reaction mixture was evaporated to 1/3rd of the original volume and the remaining solution was kept for slow evaporation. After few days a brownish-orange crystalline solid was obtained. Yield 280 mg (48.6 %).

Selected IR bands (cm^{-1}): 3447(br,w), 1628(s), 1590(s), 1564(m), 1467(s), 1439(s), 1302(s), 1257(m), 1219(m), 1156(m), 1010(s), 1038(m), 869(s), 771(s), 696(s), 619(s), 536(s), 495(s), 466(s).

$[MnL^1(H_2O)]I_2\cdot 4H_2O$ (2)

A methanol solution (15 mL) of $MnCl_2\cdot 4H_2O$ (448 mg, 2.26 mmol) was added to a clear methanol solution (20 mL) of N-(picolinylidene)hydrazine (274 mg, 2.26 mmol) and N,N'-bis(picolinylidene)hydrazine (475 mg, 2.26 mmol). The mixture was refluxed for 24 h. The volume of the resulting light brown solution was reduced to 15 mL on a rotary evaporator. To this solution an aqueous solution (10 mL) of KI (1 g) was added and the mixture was kept at –5 ^oC. After 5-7 days brown crystals deposited, were collected by filtration, washed with ice-cold water and dried in air. Yield, 495 mg (30%).

Selected IR bands (cm^{-1}): 3435(br,s), 1603(s), 1549(m), 1476(s), 1437(s), 1377(w), 1304(m), 1236(m), 1132(s), 1099(s), 1038(m), 876(m), 775(s), 637(m), 596(m), 414(m).

2.3.4. X–ray crystallography

Single crystals of both $[MnL_2Cl_2)]\cdot 0.125H_2O$ (**1**) and $[MnL^1(H_2O)]I_2\cdot 4\ H_2O$ **(2)** were collected as crystalline product obtained directly from the reaction mixtures. The data were collected on an Enraf-Nonius Mach-3 single crystal diffractometer using graphite monochromated Mo$K\alpha$ radiation (λ = 0.71073 Å) by ω-scan method at 298 K. Unit cell parameters were determined by least-squares fit of 25 reflections. Intensities of 3 check reflections were measured after every 1.5 h during the data collection to monitor the crystal stability. No decay was observed in either case. Empirical absorption correction was[18] applied to both data sets based on the Ψ-scans of 6 reflections in each case. These reflections have 2θ in the range 2.5–25° and χ within 81-88° for $[MnL_2Cl_2)]\cdot 0.125H_2O$ and 2θ in the range 8–28° and χ within 82–89° for $[MnL^1(H_2O)]I_2\cdot 4H_2O$. The structures were solved by direct method and refined on F^2 by full-matrix least-squares procedures. The asymmetric unit of $[MnL_2Cl_2)]\cdot 0.125H_2O$ contains a molecule of the complex with $1/8^{th}$ of a water molecule sitting at the corner of the unit cell and that of $[MnL^1(H_2O)]I_2\cdot 4\ H_2O$ contains a complex cation, two iodide anions and four H_2O molecules. All non-hydrogen atoms were refined using anisotropic thermal parameters. Hydrogen atoms of the water molecules and secondary amine fragments were found in a difference map. The other hydrogen atoms were placed geometrically by using a riding model. All the hydrogen atoms were included in the structure factor

calculation at idealized positions, but not refined. Calculations were done using the programs of WinGX[19] for data reduction and absorption correction and SHELX-97 programs[20] for structure solution and refinement. ORTEX6a package[21a] and Platon[21b] programs were used for molecular graphics. Significant crystal data are summarized in Table 2.1. The atomic coordinates and equivalent isotropic displacement parameters for the $[MnL_2Cl_2)]\cdot 0.125H_2O$ and $[MnL^1(H_2O)]I_2\cdot 4\ H_2O$ have been listed in Tables 2.2 and 2.3, respectively.

Table 2.1. Crystallographic data for $[MnL_2CL_2]\cdot 0.125H_2O$ (**1**) and $[MnL^1(H_2O)]I_2\cdot 4H_2O$ (**2**)

Complex	**1**	**2**
Chemical formula	$MnC_{24}H_{20.50}N_8Cl_2O_{0.06}$	$MnC_{18}H_{27}N_5O_5I_2$
Crystal size, mm	0.42 x 0.40 x 0.31	0.48 x 0.40 x 0.24
Formula weight	549.150	730.21
Space group	Triclinic, $P\bar{1}$	Monoclinic, $P2_1/n$
a, Å	8.964(3)	14.698(4)
b, Å	11.4399(12)	9.9680(14)
c, Å	13.772(2)	18.920(2)
α, deg.	85.630(11	90.00
β, deg.	72.244(20)	101.647
γ, deg.	74.858(14)	90.00
V, Å^3	1298.4(5)	2714.9(9)
Z	2	4
ρ_{calcd}, g cm^{-3}	1.4018	1.768
μ mm^{-1}	0.734	2.80
Reflections collected/unique	4498/4498	5070/4762
Reflections $I > 2\sigma(I)$	3143	3232
Parameters	322	298
$R1$,[a] w$R2$[b] [$(I > 2\sigma(I)$]	0.0436, 0.1109	0.0406, 0.0890
$R1$,[a] w$R2$ [b] (all data)	0.0770, 0.1264	0.0744, 0.1010
Goodness-of-fit[c]	1.049	1.049
Largest peak, hole [e Å^{-3}]	0.954 and -0.230	1.182 and –0.884

[a] $R1 = \sum||F_o| - |F_c||/\sum|F_o|$. [b] $wR2 = \{\sum[(F_o^2 - F_c^2)^2]/\sum[w(F_o^2)^2]\}^{1/2}$.

[c] $GOF = \{\sum[w(F_o^2 - F_c^2)^2]/(n - p)\}^{1/2}$ where 'n' is the number of reflections and 'p' is the number of parameters refined.

Table 2.2. Atomic coordinates (x 10^4) and equivalent isotropic displacement parameters ($Å^2$ x 10^3) for $[MnL_2CL_2]\cdot 0.125H_2O$

Atom	x	y	z	U(eq)
Mn	1934(1)	2914(1)	7100(1)	37(1)
Cl(1)	3600(1)	3785(1)	7787(1)	55(1)
Cl(2)	2754(1)	782(1)	7403(1)	60(1)
O(1)	0	0	0	74(5)
N(1)	-335(3)	3361(2)	8428(2)	39(1)
N(2)	-267(3)	2653(2)	6601(2)	37(1)
N(3)	-289(3)	2294(2)	5653(2)	40(1)
N(4)	2608(4)	79(3)	3936(3)	55(1)
N(5)	3505(3)	2964(2)	5462(2)	40(1)
N(6)	1030(3)	4822(2)	6359(2)	41(1)
N(7)	-386(3)	5723(2)	6750(2)	46(1)
N(8)	-2074(5)	7153(3)	9151(3)	66(1)
C(1)	-386(5)	3627(3)	9360(3)	50(1)
C(2)	-1794(5)	3894(4)	10158(3)	60(1)
C(3)	-3203(5)	3871(4)	9991(3)	62(1)
C(4)	-3202(4)	3593(3)	9036(3)	54(1)
C(5)	-1747(4)	3335(3)	8270(3)	40(1)
C(6)	-1645(4)	2994(3)	7248(3)	39(1)
C(7)	923(4)	1439(3)	5257(3)	40(1)
C(8)	1200(4)	907(3)	4267(3)	41(1)
C(9)	68(4)	1241(3)	3735(3)	46(1)
C(10)	433(5)	696(4)	2800(3)	56(1)
C(11)	1878(5)	-132(4)	2447(3)	60(1)
C(12)	2916(5)	-426(4)	3024(3)	62(1)
C(13)	4738(4)	2068(3)	5012(3)	53(1)
C(14)	5837(5)	2177(4)	4084(3)	63(1)
C(15)	5675(5)	3283(5)	3608(3)	67(1)
C(16)	4391(5)	4235(4)	4057(3)	59(1)
C(17)	3303(4)	4048(3)	4974(3)	43(1)
C(18)	1886(4)	4988(3)	5465(3)	46(1)
C(19)	-591(4)	6048(3)	7647(3)	45(1)
C(20)	-2045(4)	6921(3)	8211(3)	45(1)

C(21)	-3299(5)	7455(3)	7812(3)	52(1)
C(22)	-4645(5)	8261(4)	8404(4)	64(1)
C(23)	-4682(5)	8506(4)	9365(4)	68(1)
C(24)	-3392(6)	7946(4)	9723(3)	76(1)

Table 2.3. Atomic coordinates (x 10^4) and equivalent isotropic displacement parameters ($Å^2$ x 10^3) for $[MnL^1(H_2O)]I_2 \cdot 4H_2O$

Atom	x	y	z	U(eq)
Mn	2637(1)	9697(1)	249(1)	38(1)
I(1)	7070(1)	12657(1)	3043(1)	72(1)
I(2)	1468(1)	8474(1)	2311(1)	(1)
O(1)	3077(3)	9524(4)	1380(2)	56(1)
O(2)	4765(3)	8962(5)	2090(2)	78(1)
O(3)	-78(4)	8737(6)	-2586(3)	109(2)
O(4)	-94(4)	5751(6)	1769(3)	107(2)
O(5)	6196(4)	15200(6)	1771(4)	124(2)
N(1)	2540(3)	7432(4)	135(2)	44(1)
N(2)	2947(3)	8498(5)	-1254(2)	55(1)
N(3)	3258(3)	9436(5)	-750(2)	41(1)
N(4)	3813(3)	11178(4)	302(2)	44(1)
N(5)	1304(3)	8610(5)	-1187(3)	54(1)
N(6)	1367(3)	9529(5)	-657(2)	42(1)
N(7)	1571(3)	11211(5)	450(3)	46(1)
C(1)	2119(4)	7793(6)	-1179(3)	51(2)
C(2)	2315(4)	6885(6)	-522(3)	44(1)
C(3)	2268(4)	5514(6)	-623(4)	65(2)
C(4)	2456(5)	4679(7)	-37(5)	76(2)
C(5)	2694(5)	5239(7)	633(4)	72(2)
C(6)	2722(4)	6599(6)	697(3)	55(2)
C(7)	3850(4)	10315(6)	-858(3)	46(1)
C(8)	4179(4)	11277(5)	-291(3)	44(1)
C(9)	4830(4)	12246(6)	-361(4)	57(2)
C(10)	5118(4)	13114(7)	203(4)	70(2)
C(11)	4773(5)	12992(7)	825(4)	71(2)
C(12)	4121(4)	12019(6)	847(4)	58(2)

C(13)	763(4)	10457(6)	-698(3)	52(2)
C(14)	840(4)	11384(6)	-92(3)	50(2)
C(15)	181(4)	12380(7)	-79(4)	65(2)
C(16)	277(5)	13186(7)	514(5)	73(2)
C(17)	1007(5)	12993(7)	1076(4)	67(2)
C(18)	1638(4)	11990(6)	1021(3)	56(2)

2.4. Results and discussion

2.4.1. Synthesis of $[MnL_2Cl_2]\cdot 0.125H_2O$ (1) and $[MnL^1(H_2O)]I_2\cdot 4H_2O$ (2)

Initially we have tried to synthesize a dinuclear helical manganese(II) complex by reacting three mole equivalents of ligand L with two mole equivalents of $MnCl_2\cdot 4H_2O$. However, an orange-brown mononuclear manganese(II) complex of formula $[MnL_2Cl_2]\cdot 0.125H_2O$ was obtained. The structure of the complex was determined by X-ray crystallography, only one of the two picolinyldene fragments of each L coordinates the metal ions in $[MnL_2Cl_2]\cdot 0.125H_2O$. The remaining two *cis* sites are satisfied by the two chloride ions. Thus the metal ion is in distorted octahedral N_4Cl_2 coordination sphere. This octahedral complex can be synthesized in good yields by reacting $MnCl_2\cdot 4H_2O$ and N,N'-bis(picolinylidene)hydrazine (L) in 1:2 mole ratio in boiling methanol. Elemental analysis data (Table 2.4) of the complex was consistent with the formula $[MnL_2Cl_2]\cdot 0.125H_2O$. As expected, the complex was non conducting in methanol solution. The room temperature magnetic moment of the complex in solid state (5.98 μ_B) conform to S = 5/2 spin state.

In our next attempt for dinuclear helical complexes, we reacted the ligand L with $Mn(ClO_4)_2\cdot 6H_2O$ in 3:2 mole ratio in methanol to avoid the chloride coordination as observed in $[MnL_2Cl_2]$. However, we could not isolate the

desired dinuclear helical complex. Interestingly in this reaction, a mononuclear trigonal prismatic manganese(II) complex having the formula $[MnL^1(H_2O)]^{2+}$ (L^1 bis(picolinylidenehydrazyl)(2-pyridyl)methane) was produced. Possibly the free acid present in $Mn(ClO_4)_2 \cdot 6H_2O$ causes the hydrolysis of L and produces same amount of N-(picolinylidene)hydrazine. Nucleophilic attack on the activated carbon atom of the metal coordinated imine function in L by N-(picolinylidene)hydrazine (see section 2.4.2) is the most likely origin for the formulation of the N_5 donor L^1. To verify this hypothesis we have reacted one mole equivalent each of $MnCl_2 \cdot 4H_2O$, N,N'-bis(picolinylidene)hydrazine, and N-(picolinylidene)hydrazine in boiling methanol (Scheme 2.1). In this reaction, the cationic complex, $[MnL^1(H_2O)]^{2+}$, where L^1 is bis(picolinylidenehydrazyl)(2-pyridyl)methane was isolated in solid state as iodide salt with four water molecules in the crystal lattice. The elemental analysis data (Table 2.4) are satisfactory with the formula $[MnL^1(H_2O)]I_2 \cdot 4H_2O$. The complex behaves as 1:2 electrolyte in methanol solution. The molar conductivity value is 182 Ω^{-1} cm^2 mol^{-1}.[22] The room temperature (298 K) magnetic moment (5.98 μ_B) is consistent with an S = 5/2 spin state.

Table 2.4 Elemental analysis data[a]

Complex	C%	H%	N%
1	52.03 (52.49)	3.61(3.75)	19.75(20.40)
2	29.33(29.61)	3.58(3.73)	13.34(13.43)

[a] Calculated values are in parentheses

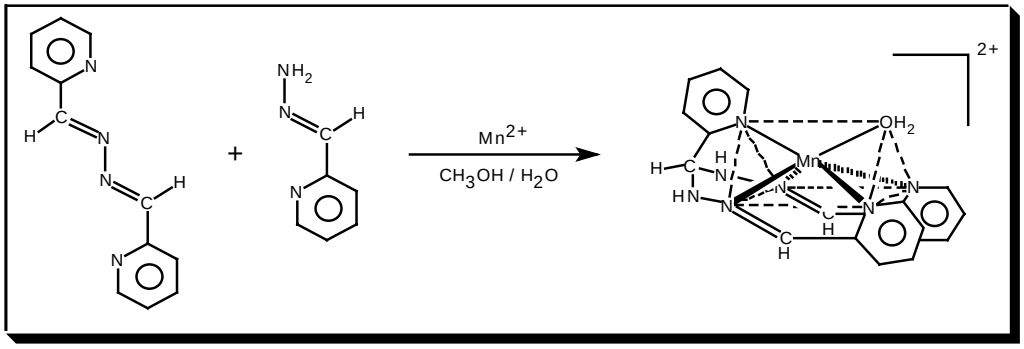

Scheme 2.1. Synthetic procedure.

2.4.2. Mechanism for the formation of L^1

The formation of the ligand L^1 and the complex can be rationalized as follows. In the first step, Mn^{2+} is coordinated to one of the two 2-pyridinealdimine moieties of the N,N′-bis(picolinylidene)hydrazine (L) and forms a five-membered chelate ring. Due to this metal coordination the azomethine fragment becomes more polarized and a nucleophilic attack at the polarized carbon atom by the $–NH_2$ group of N-(picolinylidene)hydrazine follows. Subsequently there is a proton transfer from the $–NH_2^+$ to the azomethine-N. The net result is formation of bis(picolinylidenehydrazyl)(2-pyridyl)methane (L^1) by the addition of N-(picolinylidene)hydrazine to one of the polarized azomethine group of N,N'-bis(picolinylidene)hydrazine (Scheme 2.2). This type of addition reaction to metal coordinated azomethine group is not uncommon.[23] In the final complex formation step, the bond between the metal center and the reduced azomethine-N is dissociated and both the 2–pyridinealdimine moieties of L^1 coordinate Mn^{2+} to form two new five membered chelate rings. As a result a

Scheme 2.2.

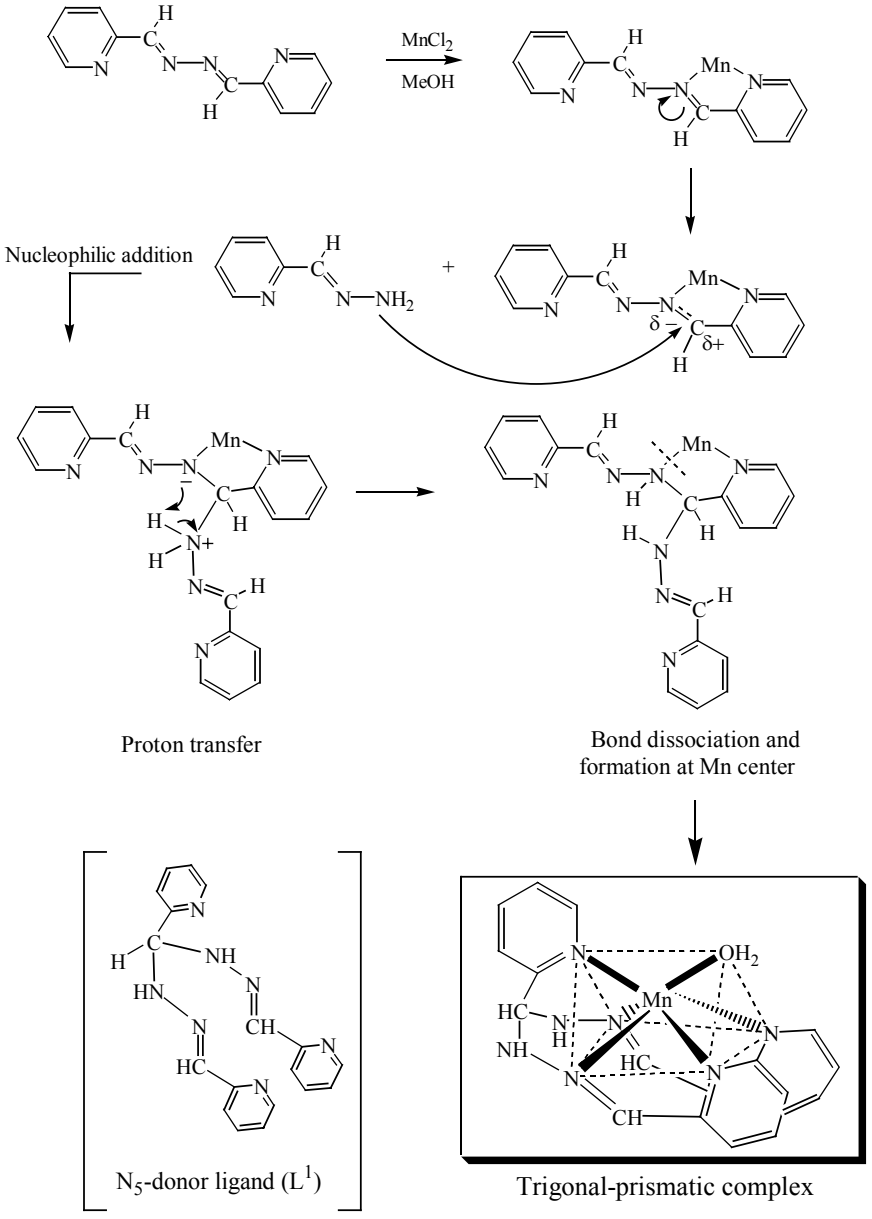
MnCl2
MeOH
Nucleophilic addition
Proton transfer
Bond dissociation and
formation at Mn center
N5-donor ligand (L1)
Trigonal-prismatic complex

bicyclic fragment, in which each cycle is six-membered and the Mn-atom, the pyridine-N and its adjacent C-atom, and the methane-C are common to both cycles, is formed (Scheme 2.2). This molecular structure is confirmed by X-ray crystallography. In absence of Mn^{2+} one mole equivalent each of N,N′-bis(picolinylidene)hydrazine, and N-(picolinylidene)hydrazine do not react to yield the ligand, L^1. This observation confirms the metal activated pathway for the formation of L^1.

2.4.3. Spectral features of 1 and 2

The infrared spectra of the complexes (Figure 2.2) display a broad band at ~3440 cm^{-1} due to the lattice water molecule in **1** and the coordinated as well as lattice water molecules[24] in **2**. In each complex, the strong band observed at ~1600 cm^{-1} is most likely associated with the metal coordinated C=N moieties of the ligand.[25] Three medium to strong bands observed in the range 1437–1549cm^{-1} are possibly due to the C=C stretches from the pyridine rings of the ligand.[26] A medium intensity band at 1628 cm^{-1} observed only in the spectrum of **1** is most likely due to the uncoordinated C=N fragments of the ligands.

The electronic absorption spectral data of the complexes in methanol solution are listed in Table 2.5, and a representative spectrum is shown in Figure 2.3. The $[MnL_2Cl_2]\cdot 0.125H_2O$ complex displays a strong absorption at 298 nm followed by the shoulders and another medium to strong absorptions at 213 nm. The complex $[MnL^1(H_2O)]I_2\cdot 4H_2O$ also displays a strong absorption at 297 nm followed by a shoulder and another strong absorption at 221 nm. All these absorptions are most likely due to ligand-to-metal charge transfer and intraligand transitions.[27]

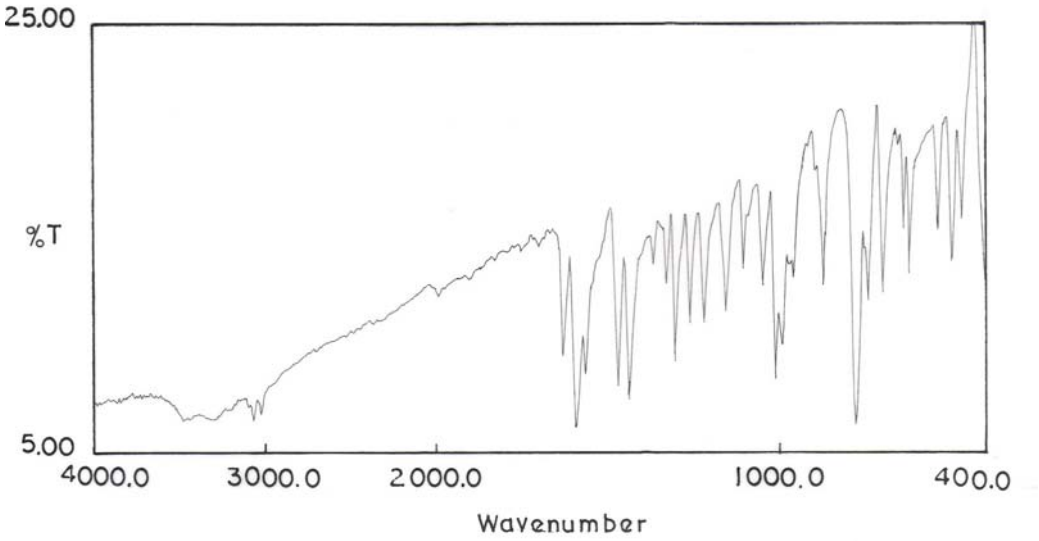

Figure 2.2. Infrared spectrum of $[MnL^1(H_2O)]I_2 \cdot 4H_2O$.

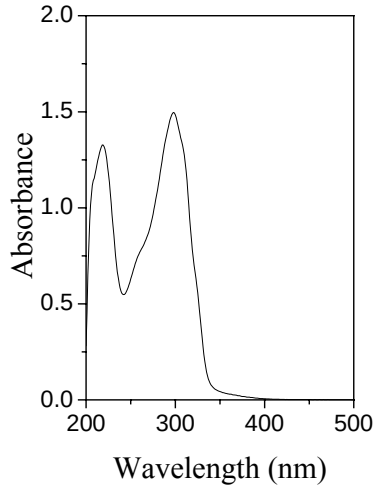

Figure 2.3. Electronic spectrum of $[MnL^1(H_2O)]I_2 \cdot 4H_2O$ in methanol solution.

Table 2.5. Electronic spectral data

Complex	λ_{max} (nm) (ε ($M^{-1}cm^{-1}$))
1	308(41,964)^{sh}, 298(41,857), 258(23,750)^{sh}, 213(18,267)
2	297(51,200), 262(27400),^{sh} 221(47,600)

sh = Shoulder.

The ESR spectra of the complexes were collected at the room temperature (298 K) in powder phase and also at 77 K in frozen methanol solutions. The spectra of the complexes in powder phase as well as in frozen solutions are very similar. A representative spectrum is shown in Figure 2.4. The spectral features are typical for high-spin d^5 manganese(II) systems.[28] Room temperature powder

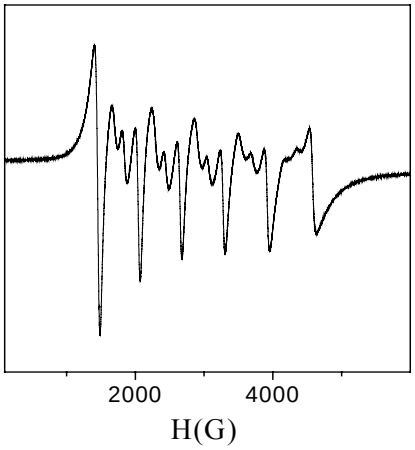

Figure 2.4. X–band ESR spectrum of $[MnL_2CL_2]\cdot 0.125H_2O$ in frozen methanol-toulene (1:1) solution.

spectrum shows a broad weak signal at lower field (g = 3.42–3.80) followed by a strong resonance in the range g = 2.01–2.07. In frozen (77 K) methanol solution, the complexes display a broad weak signal at g = 2.88 (**1**), 2.94 (**2**) and a strong signal at g ~ 1.99. In these spectra, the higher field signal shows the ^{55}Mn hyperfine structure with an average coupling constant of 86–96 G.

2.4.4. Description of molecular structures

The structures of $[MnL_2Cl_2]$ and $[MnL^1(H_2O)]^{2+}$ are shown in Figures 2.5 and 2.6, respectively. The selected bond parameters associated with the metal ions are listed in Table 2.6. The coordination geometry around the metal center in $[MnL_2Cl_2]$ and $[MnL^1(H_2O)]^{2+}$ can be best described as distorted octahedral and trigonal prismatic, respectively. In both the complexes, the neutral ligands (L and L^1) coordinate the metal ion *via* pyridyl-N and imine-N atoms.

$[MnL_2Cl_2]\cdot 0.125H_2O$

In this complex, the manganese(II) atom is hexa-coordinated. Each ligand (L) coordinates the metal ion *via* the pyridine-N and the imine-N atoms and forms a five-membered chelate ring. The imine-N atoms are *cis* to each other, while the pyridine-N atoms are *trans* to each other. The remaining two cis coordination sites are occupied by the two chloride ions (Figure 2.5). The N_4Cl_2 coordination environment around the metal ion can be described as distorted octahedral. The $N_{pyridine}$–Mn–$N_{pyridine}$ angle (156.65(10)°) is significantly deviated from the ideal value of the 180°. The two *trans* N_{imine}–Mn–Cl bond angles (163.05(8)–162.11(7)°) are also deviated form the ideal value but to a lesser extent. The chelate bit angles (70.77(10)° and 70.43(10)°) in the two five-

membered rings are essentially identical. The other *cis* angles are in the range 76.93(9)–104.32(4)° (Table 2.6). The Mn–$N_{pyridine}$, Mn–N_{imine} and Mn–Cl bond distances are consistent with the metal +2 oxidation state of the metal ion.[29-31] In this complex, each ligand coordinates the metal ion in bidentate manner and the uncoordinated 2-pyridinealdimine part is hanging approximately in trans configuration by making a twist about the N–N bond. This twist is reflected by the C(6)–N(2)–N(3)–C(7) and C(18)–N(6)–N(7)–C(19) torsion angles (146.1° and 133.6° respectively).

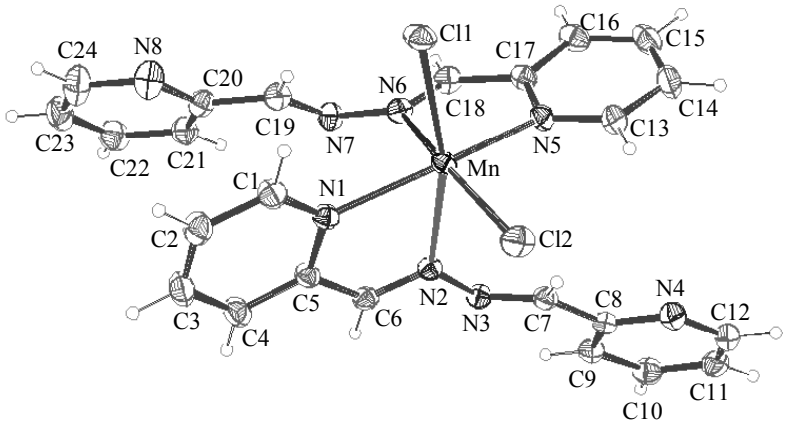

Figure 2.5. The structure of $[MnL_2Cl_2]$. All non-hydrogen atoms are represented by their 30% probability thermal ellipsoids.

$[MnL^1(H_2O)]I_2{\cdot}4H_2O$

In this complex, the metal ion is in trigonal prismatic N_5O coordination sphere. The L^1 ligand coordinates the metal ion *via* the pyridine-N and the imine-N atoms forming two, five-membered chelate rings and a bicyclic fragment that consists of two, six-membered chelate rings with four common atoms. The sixth

coordination site is occupied by a water O-atom. The manganese(II) to pyridine-N distances are in the range 2.260(4)–2.270(4) Å. These distances are comparable with the distances reported for other manganese(II) complexes containing the same coordinating atom. The metal to imine-N distances (2.274(4) and 2.272(4) Å) are similar to the distances observed for manganese(II) Schiff base complexes.[31a,c,d] The manganese(II) to water oxygen distance (2.113(4) Å) is unexceptional.[31b,d,32] The pair of picolinylidenehydrazyl arms and the pyridyl arm emanating from the methane C-atom of L^1 are ideally disposed to occupy five vertices of a trigonal prism (Scheme 2.2, Figure.2.6). The bond angles at the methane C-atom involving the non-hydrogen atoms are within 110.4(5)–116.0(5)º. The picolinylidenehydrazyl arms provide two imine-N (N3 and N6) and two pyridine-N (N4 and N7) centres. These four N-atoms form the square base of the trigonal prism. The N-atom (N1) of the pyridyl arm and the water oxygen (O1) occupies the remaining two vertices to complete the trigonal prismatic coordination sphere around the metal ion (Figure 2.7). Thus one pyridine-N and two imine-N atoms (N1, N3, N6) occupy one trigonal face and the remaining two pyridine-N atoms (N7, N4) and the water O-atom (O1) reside on the opposite trigonal face (Figure 2.7). The torsion angles involving opposing corners and the centroids of the trigonal faces are 2.93, 3.10 and 7.03° respectively. For an ideal trigonal prism these angles are 0°. The observed deviations from 0° are due to the trigonal faces not being exactly equilateral in the present complex. The two trigonal faces are also not parallel. The dihedral angle between them is 11.1(3)°.

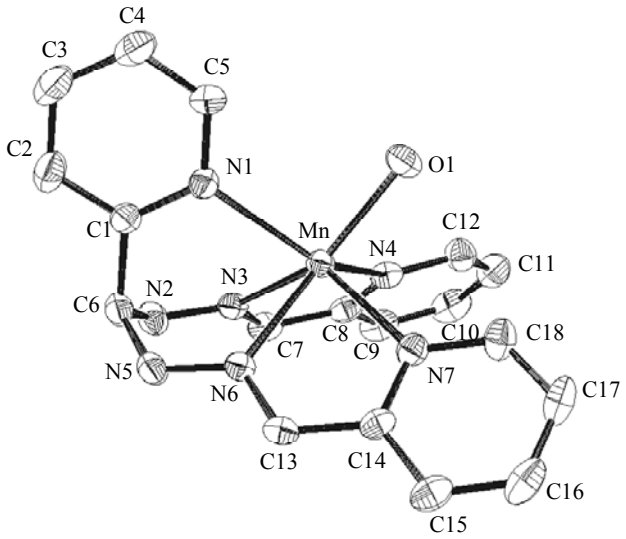

Figure 2.6. The structure of $[MnL^{1}(H_2O)]^{2+}$. All atoms are represented by their 30% probability thermal ellipsoids. Hydrogen atoms are omitted for clarity.

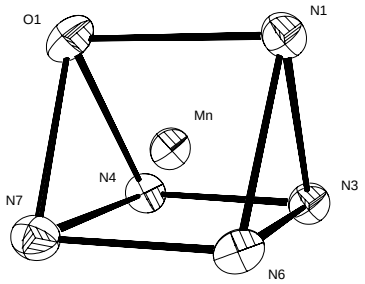

Figure 2.7. Trigonal prismatic geometry.

Table 2.6. Selected bond distances (Å) and angles (°)
$[MnL_2CL_2]\cdot 0.125H_2O$

Mn-N(1)	2.253(3)	Mn-N(5)	2.272(3)
Mn-N(2)	2.371(3)	Mn-N(6)	2.389(3)
Mn-Cl(2)	2.4001(10)	Mn-Cl(1)	2.4288(11)
N(1)-Mn-N(5)	156.65(10)	N(5)-Mn-N(2)	92.90(10)
N(1)-Mn-N(6)	89.22(10)	N(5)-Mn-N(6)	70.43(10)
N(1)-Mn-Cl(1)	97.45(8)	N(5)-Mn-Cl(1)	93.90(8)
N(1)-Mn-N(2)	70.77(10)	N(5)-Mn-Cl(2)	98.83(8)
N(1)-Mn-Cl(2)	98.04(7)	N(6)-Mn-Cl(1)	89.80(7)
N(2)-Mn-N(6)	76.93(9)	N(6)-Mn-Cl(2)	163.05(8)
N(2)-Mn-Cl(1)	162.11(7)	Cl(2)-Mn-Cl(1)	104.32(4)
N(2)-Mn-Cl(2)	90.95(7)		

$[MnL^1(H_2O)]I_2\cdot 4H_2O$

Mn-O(1)	2.113(4)	Mn-N(4)	2.260(4)
Mn-N(1)	2.270(4)	Mn-N(6)	2.272(4)
Mn-N(3)	2.274(4)	Mn-N(7)	2.262(5)
O(1)-Mn-N(1)	90.89(16)	N(1)-Mn-N(7)	130.33(16)
O(1)-Mn-N(3)	137.75(15)	N(3)-Mn-N(4)	71.30(16)
O(1)-Mn-N(4)	86.21(16)	N(3)-Mn-N(6)	76.74(15)
O(1)-Mn-N(6)	142.66(15)	N(3)-Mn-N(7)	128.54(16)
O(1)-Mn-N(7)	88.02(16)	N(4)-Mn-N(6)	125.85(16)
N(1)-Mn-N(3)	80.56(16)	N(4)-Mn-N(7)	96.06(16)
N(1)-Mn-N(4)	133.41(16)	N(6)-Mn-N(7)	71.59(17)
N(1)-Mn-N(6)	80.14(17)		

2.4.5. Non-covalent interactions and self-assembly

The molecules of $[MnL_2Cl_2]$ form a chain like arrangement in the crystal lattice *via* intermolecular hydrogen bonding interactions (Table 2.7). In this chain

(Figure 2.8), each molecule is connected to its one neighbour by a pair of reciprocal C–H···N interactions involving metal coordinated C–H (C18–H18) and an uncoordinated azomethine N-atom (N_3) and to its second neighbour by a pair of another reciprocal C–H···N interactions involving the *ortho*-C–H (C1–H1) of a metal coordinated pyridine and an uncoordinated pyridine N-atom (N8). The O-atom of the water molecule is somewhat closer to the C–H groups (C11–H11 and C10–H10) of one of the uncoordinated pyridine rings (Table 2.7). Possibly very weak C–H···O interactions are present. These O-atoms are sitting in between the parallel chains of $[MnL_2Cl_2]$ and are involved in four C–H···O interactions with the symmetry related complex molecules belong to adjacent chains. As a result a two-dimensional network is generated (Figure 2.9).

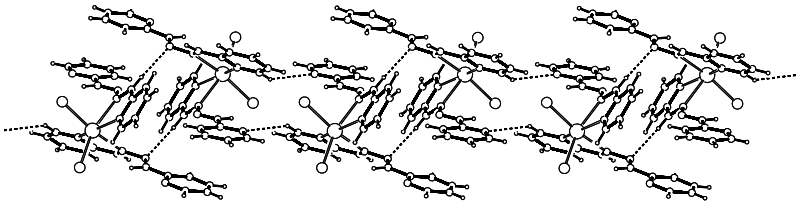

Figure 2.8. One dimensional self-assembly of $[MnL_2Cl_2]$ viewed along *b* axis.

In the crystal lattice of **2,** the H_2O molecules and iodide ions form two types of helical chains *via* O–H···O, O–H···I hydrogen bonding interactions. The relevant data are given in the Table 2.7. The first type of helix is constructed by three water (O2, O3 and O4) molecules and one iodide (I_2) and the second type of helix is formed by alternating H_2O and iodide ion. In the former helical chain of

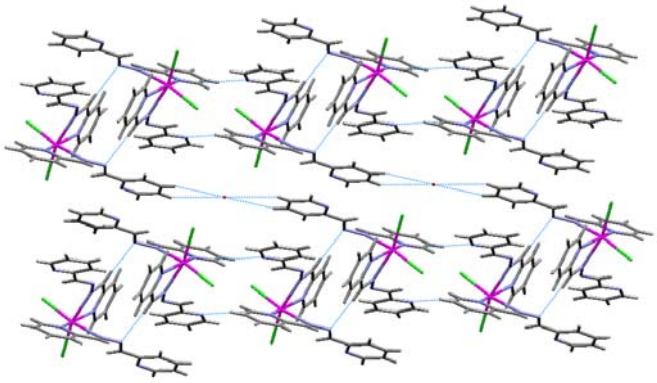

Figure 2.9. Two dimensional network of $[MnL_2Cl_2]$ and water molecules viewed down *a* axis.

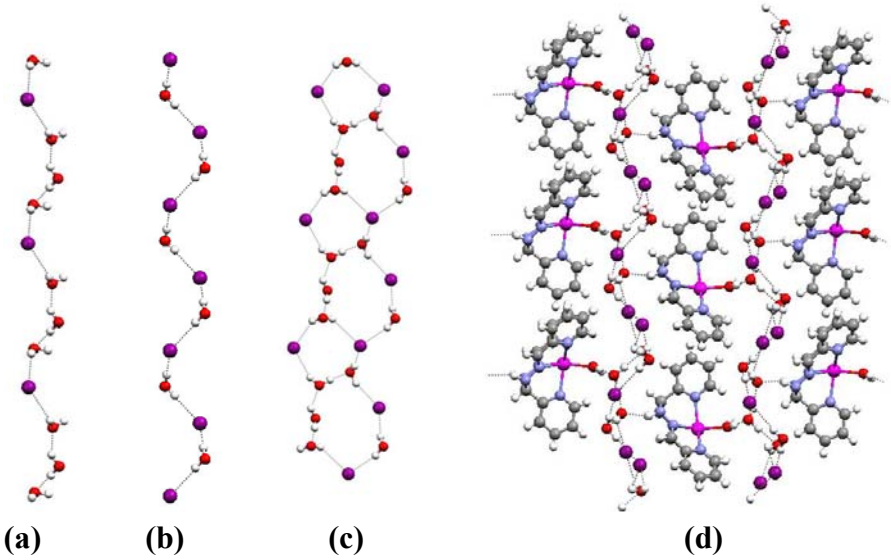

Figure 2.10. **(a)** and **(b)** Water-iodide helical chains along *b* axis. **(c)** Water-iodide tapes along *b* axis. **(d)** Two dimensional network of complex and water-iodide tapes.

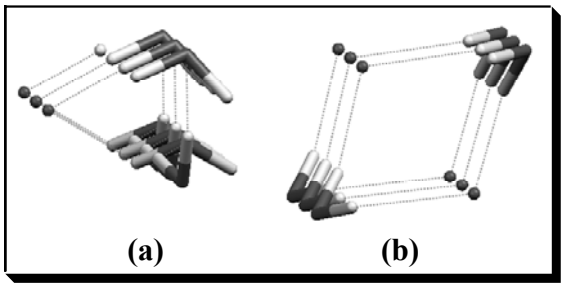

Figure 2.11. Helical channels (a) $\{(H_2O)_3\ I^-\}$and (b) $\{(H_2O)\ I^-\}$ viewed down *b* axis.

Table 2.7. Hydrogen bonding parameters

Complex	Interaction	H···A (Å)	D···A (Å)	D–H···A (^{o})
1	C1 – H1··· N8	2.61	3.34	139
	C18 – H18··· N3	2.60	3.51	169
	C10 – H10··· O1	3.52	4.17	130
	C11 – H11··· O1	3.47	4.14	131
2				
	O2 – H2a···O4	1.81	2.76	174
	O2 – H2b···O3	1.96	2.75	140
	O3 – H3a···O5	1.69	2.65	173
	O3 – H3b···I2	2.81	3.54	140
	O4 – H4a···I2	2.75	3.56	143
	O4 – H4b···I1	2.96	3.54	130
	O5 – H5a···I1	2.60	3.55	168
	O5 – H5b···I1	2.56	2.99	165
	O1 – H1b···O2	1.69	2.63	170
	N5 – H5a···O3	2.14	3.55	158

{$(H_2O)_3$ I^-}unit, the three water molecules form a linear trimer (O···O distances 2.63–2.76 Å; O–H···O angles, 140–174°).[33] The terminal two water molecules of this water trimer are again hydrogen bonded with two iodide ions (Figure 2.10a). In the later helical chain of {(H_2O) I^-} unit, each water molecule participates in two hydrogen bonding interactions with iodide ions and an infinite helix is formed (Figure 2.10b). These two parallel helices are further connected *via* O3–H3b···O5 and O4–H4b···I1 interactions and form the water-iodide tapes having an alternate five and seven membered (water-iodide) cycles (Figure 2.10c). Each water molecule in this tape participates in hydrogen bonding interactions. The complex cations act as bridges between the parallel infinite water-iodide tapes *via* hydrogen bonding interactions (O1–H1b···O2 and N5–H5a···O3) involving the coordinated water molecule and one of the two secondary amine N–H groups. As a result a two-dimensional hydrogen bonded network of **2** is formed in the crystal lattice (Figure 2.10d).

2.5. Conclusions

Though our aim was to prepare a diazine bridged dimanganese(II) helical complex, we have succeeded in isolating an octahedral and trigonal prismatic mononuclear manganese(II) complexes. The tetradentate ligand N,N'-bis(picolinylidene)hydrazine (L) acts as bidentate ligand in the octahedral $[MnL_2Cl_2]$ complex. In $[MnL^1(H_2O)]^{2+}$, the metal is in trigonal prismatic N_5O coordination sphere. Here, L^1 is N_5-donor bis(picolinylidenehydrazyl)(2-pyridyl)methane. This pentadentate N_5 donor ligand (L^1) was produced by manganese(II) activated addition of N-(picolinylidene)hydrazine to the tetradentate diazine ligand (L) N,N'-bis(picolinylidene)hydrazine. Although the

ligand is pentadentate, it is rigid enough to impose a trigonal prismatic coordination sphere around the metal ion together with the monodentate water molecule.

The complexes crystallize as $[MnL_2Cl_2]\cdot 0.125H_2O$ (**1**) and $MnL^1(H_2O)]I_2\cdot 4H_2O$ (**2**). In the crystal lattice, **1** forms a two-dimensional structure *via* inter molecular C–H···N and C–H···O interactions. In the crystal lattice of $[MnL^1(H_2O)]I_2\cdot 4H_2O$ the water and iodide ions form infinite tapes *via* O–H···O and O–H···I hydrogen bonds. These infinite tapes are further connected by the complex cations through O–H···O and N–H···O interactions and a two dimensional array is formed.

2.6. References

1. (a) W. J. Stratton, D. H. Busch, *J. Am. Chem. Soc.*, **1958**, *80*, 1286. (b) W. J. Stratton, D. H. Busch, *J. Am. Chem. Soc.*, **1958**, *80*, 3191. (c) W. J. Stratton, D. H. Busch, *J. Am. Chem. Soc.*, **1960**, *82*, 4834.
2. P. D. W. Boyd, G. M. Sheldrick, *J. Chem. Soc.*, *Dalton Trans.,* **1974**, 1097
3. (a) Z. Xu, L. K. Thompson, D. O. Miller, H. J. Clase, J. A. K. Howard, A. E. Goeta, *Inorg. Chem.,* **1998,** *37,* 3620. (b) J. Hamblin, A. Jackson, N. W. Alcock, M. J. Hannon, *J. Chem. Soc., Dalton Trans.,* **2002**, 1635. (c) G. Dong, P. K. liang, D. C. ying, H. Cheng, M. Q. jin, *Inorg. Chem.,* **2002** *41***,** 5978b. (d) G. Dong, P. K. liang, D. C. ying, Z. Y. Gang, M. Q. jin, *Chem. Lett.*, **2002**, 1014.
4. N. A. Law, M. T. Caudle, V. L. Pecoraro, *Adv. Inorg. Chem.*, **1999**, *46*, 305.
5. (a) A. Zouni, H. T. Witt, J. Kern, P. Fromme, N. Krauß, W. Saenger, P. Orth, *Nature*, **2001**, *409*, 739. (b) N. Kamiya, J. R. Shen, *Proc. Natl. Acad. Sci. USA*, **2003**, *100*, 98.

6. (a) Y. Kono, I. Fridovich, *J. Biol. Chem.*, **1983**, *258*, 6015. (b) W. F. Beyer Jr., I. Fridovich, *Biochemistry*, **1985**, *24*, 6460. (c) V. V. Barynin, A. A. Vagin, W. R. M. Adamyan, A. I. Grebenko, S. V. Khangulov, A. N. Popov, M. E. Andrianova, B. K. Vainshtein, *Dokl. Akad. Nauk.*, **1986**, *288*, 877. (d) V. V. Barynin, P. D. Hempstead, A. A. Vagin, S. V. Antonyuk, W. R. M. Adamyan, V. S. Lamzin, P. M. Harrison, P. J. Artymiuk, *J. Inorg. Biochem.*, **1997**, *67*, 196. (e) G. S. Allgood, J. J. Perry, *J. Bacteriol.*, **1986**, *168*, 563 (f) J. W. Whittaker, in *Metal Ions in Biological Systems*, ed. A. Sigel, H. Sigel, Marcel Dekker, New York, **2000**, *37*, 587.
7. (a) R. Eisenberg, J. A. Ibers, *Inorg. Chem.*, **1966,** *5,* 411. (b) R. Eisenberg, *Prog. Inorg. Chem.*, **1970,** *12*. 295.
8. (a) D. L. Kepert, *Prog. Inorg. Chem.*, **1977,** *23,* 1. (b) J. L. Martin, J. Takats, *Can. J. Chem*. **1989,** *67,* 1914.
9. P. M. Morse, G. S. Girolami, *J. Am. Chem. Soc*., **1989,** *111*, 4114.
10. J. C. Friese, A. Krol, C. Puke, K. Kirschbaum, D. M. Giolando, *Inorg. Chem*., **2000,** *39,* 1496 and references therein.
11. M. Kaupp, *Chem. Eur. J*., **1998,** *4,* 1678.
12. W.O. Gillum, J. C. Huffman, W. E. Streib, R. A. D. Wentworth, *J. Chem. Soc., Chem. Commun.,* **1969,** 843.
13. M. R. Churchill, A. H. Reis Jr., *J. Chem. Soc., Chem. Commun*., **1970**, 879.
14. E. Larsen, G. N. La Mar, B. E. Wagner, J. E. Parks, R. H. Holm, *Inorg. Chem*., **1972**, *11,* 2652.
15. K. A. Hilfiker, M. W. Brechbiel, R. D. Rogers, R. P. Planalp, *Inorg. Chem*., **1997,** *36,* 4600.
16. R. L. Paul, A.J. Amoroso, P. L. Jones, S. M. Couchman, Z. R. Reeves, L. H. Rees, J. C. Jeffery, J. A. M. Cleverty, M. D. Ward, *J. Chem. Soc., Dalton Trans*., **1999,** 1563.

17. W. E. Hatfield, E. A. Boudreaux, L. N. Mulay (Eds.), *Theory and Applications of Molecular Paramagnetism*, John Wiley, New York, **1976**, 491.
18. A. C. T. North, D. C. Philips, F. S. Mathews, *Acta Crystallogr., Sect. A,* **1968,** *24*, 351.
19. L. J. Farrugia, *J. Appl. Crystallogr*., **1999**, *32*, 837.
20. G. M. Sheldrick, SHELX-97, University of Göttingen, Göttingen, Germany, **1997**.
21. (a) P. McArdle, J. *Appl. Crystallogr*., **1995** *28*, 65. (b) A. L. Spek, Platon, *Molecular Graphics Software,* University of Glasgow, U. K, 2001.
22. W. J. Geary, *Coord. Chem. Rev.,* **1971,** *7,* 81.
23. N. R. Sangeetha, S. N. Pal, S. Pal, *Polyhedron,* **2000**, *19*, 2713, and references therein.
24. K. Nakamoto, *Infrared and Raman Spectra of Inorganic and Coordination Compounds*, John Wiley, New York, **1986**, p. 228.
25. J. Saroja, V. Manivannan, P. Chakraborty, S. Pal, *Inorg. Chem.*, **1995,** *34,* 3099
26. W. Kemp, *Organic Spectroscopy*, Macmillan, Hampshire, **1987**, p. 56.
27. C. J. Carrano, M. W. Carrano, K. Sharma, G. Backes, J. Sanders-Loehr, *Inorg. Chem*., **1990**, *29,* 1865.
28. R.D. Dowsing, J.F. Gibson, *J. Chem. Phys*., **1969**, *50*, 294.
29. M. V. Triller, W. Y. Hsien, V. L. Pecorara, A. Rompel, B. Krebs, *Inorg. Chem*., **2002**, *41*, 5544.
30. Z. Xu, L. K. Thompson, D. A. Black, C. Ralph, D. O. Miller, M. A. Leech, J. A. K. Howard, *J. Chem. Soc., Dalton Trans*., **2002,** 2042.
31. (a) A. Choudhury, B. Geetha, N. R. Sangeetha, V. Kavita, V. Susila, S. Pal, *J. Coord. Chem*., **1999,** *48,* 87. (b) M. E. de Vries, R. M. La Crois, G. Roelfes, H. Kooijman, A. L. Spek, R. Hage, B. L. Feringa, *Chem. Commun.,*

1997, 1549. (c) E. Gallo, E. Solari, S. De Angelis, C. Floriani, N. Re, A. C. Villa, C. Rizzoli, *J. Am. Chem. Soc.,* **1993**, *115*, 9850. (d) O. Jimenez-Sandoval, D. R. Rosales, M. D. J. R. Hoz, M. E. S. Torres, R. Z. Ulloa, *J. Chem. Soc., Dalton Trans*., **1998,** 1551.

32. N. Nakasuka, S. Azuma, C. Katayama, M. Honda, J. Tanaka, M. Tanaka, *Acta Crystallogr. Sect. C,* **1985,** *41,* 1176.
33. A. Mukherjee, M. K. Saha, M. Nethaji, A. R. Chakravarty, *Chem*. *Commun*., **2004**, 716. (b) R. Q. Zoua, L. Z. Cai, G. C. Guoa, *J*. *Mol*. Struct., **2005**, *737*, 125.

Chapter 3

Self-Assembled Dinuclear Triple Helicates with Dianionic Diazine Ligands[§]

3.1. Abstract

A series of dinuclear complexes of Mn(III), Fe(III) and Co(III) with two diazine Schiff bases, H_2salhn and H_2mesalhn, are reported. The Schiff bases are prepared by condensation reactions of hydrazine with salicylaldehyde (H_2salhn) and with 2-hydroxy acetophenone (H_2mesalhn) in 1:2 mole ratio. The X-ray crystallographic characterization reveals triple helical structures of [Co_2(μ-salhn)$_3$], [Co_2(μ-mesalhn)$_3$], and [Fe_2(μ-mesalhn)$_3$]. In each complex, three dinucleating O,N,N,O donor ligands provide three diazine (=N–N=) bridges between the metal ions and facial O_3N_3 coordination spheres around them. The ligands are twisted along the N–N single bond and wrap the two metal ions in a helical fashion to generate the triple helical structure. The dicobalt(III) complex of mesalhn^{2-} is D_3-symmetric, while the diiron(III) analogue is very close to that. On the other hand, the dicobalt(III) complex of salhn^{2-} is significantly deviated from the ideal D_3-symmtery due to the large range covered by the twist angles of the three ligands. In the crystal lattice of these complexes, intermolecular C–H···O, C–H···N, O–H···O, C–H···Cl, and π–π interactions involving the complex and the solvent molecules lead to one- and two-dimensional supramolecular structures. [Fe_2(μ-mesalhn)$_3$] and [Co_2(μ-mesalhn)$_3$] are redox active and display two successive metal centered reductions on the cathodic side

[§] This work has been accepted for publication in *Inorg. Chem.*,

of Ag/AgCl reference electrode. Weak antiferromagnetic spin-coupling is operative between the two metal ions in $[Mn_2(\mu\text{-salhn})_3]$ ($J = -0.57(1)$ cm^{-1}) and in $[Fe_2(\mu\text{-mesalhn})_3]$ ($J = -2.82(4)$ cm^{-1}).

3.2. Introduction

As discussed in the preceding chapters, self assembled helical coordination complexes or helicates has become an area of immense research activity over the last decade.[1] The interest on such complexes is primarily due to their potential applications in enantioselective processes, designing optical devices and magnetic materials, probing DNA structures and understanding helical self-organization processes operative in nature.[1,2] Design and synthesis of such helicates requires ligands containing two or more metal chelating sites that are connected to each other by a spacer. If the coordination of metal ions to the chelating sites results into the twisting along the spacer a helical configuration of the ligand around the metal ions is produced. Metal ions that prefer tetrahedral coordination afford double helicates and metal ions that prefer octahedral coordination afford triple helicates with such ligands.[3] Bis Schiff bases derived from hydrazine fall in this class of ligands. Here the two chelating sites are connected directly by a single bond. These easy to prepare and inexpensive diazine ligands which provide the =N–N= fragment as the bridging unit between the two metal ions are extremely efficient in producing dinuclear metallo-helicates due to the twisting along the N–N single bond. The neutral N_4-donor Schiff base N,N′-bis(picolinylidene)hydrazine was the very first ligand of this type used to synthesize dinuclear complexes of bivalent transition metal ions.[4,5]

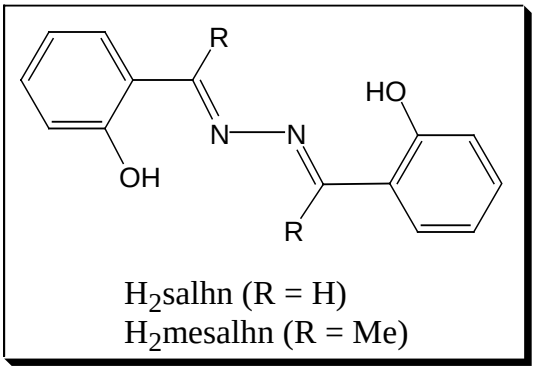

Figure 3.1

In recent times, a number of structurally characterized helical complexes have been reported with N,N′-bis(picolinylidene)hydrazine or its derivatives.[6] In contrast, there are very few reports on structurally characterized complexes with the very similar N_2O_2-donor Schiff base N,N′-bis(salicylidene)hydrazine (H_2salhn, two H's stand for the dissociable phenolic protons). The crystal structure of H_2salhn (Figure 3.1) is known.[7] The compound is in the usual *trans* configuration with two intramolecular O–H···N hydrogen bonds. Two complexes, $[(CO)_2Rh(\mu\text{-salhn})Rh(CO)_2]$[8] and $[\{Co_3L(CH_3COO)(CH_3O)_3\}_2(\mu\text{-salhn})]$[9] ($H_3L$ is 2,6-bis(salicylideneaminomethyl)-4-methylphenol), reported earlier contain the $salhn^{2-}$ as the bridging ligand. In both the complexes, diazine fragment of $salhn^{2-}$ is the only bridging unit between the two metal ions and it is in *trans* configuration as in the free Schiff base. Recently we have reported a diruthenium(III) complex, $[Ru_2Cl_2(PPh_3)_2(\mu\text{-Cl})_2(\mu\text{-salhn})]$, where due to the additional two chloride bridges and the *trans* arrangement of the terminal chlorides the $salhn^{2-}$ is in near *cis* configuration.[10] Before this diruthenium(III) complex, we reported a neutral diiron(III) complex of $salhn^{2-}$.[11] In $[Fe_2(\mu\text{-}$

salhn)$_3$] (**1**), the three ligands provide the three diazine bridges between the metal ions and each of the three ligands is twisted along the N–N bond. This complex is the first example of a helical species prepared from H_2salhn. Recently the structures of **1** and an analogous complex with a substituted derivative of salhn^{2-} have been reported once again by another research group.[12]

In the previous chapter, we have discussed the results obtained in our attempts to prepare triple helical dimanganese(II) complex with N,N′-bis(picolinylidene)hydrazine. In this chapter, we have described a series of neutral dinuclear manganese(III), iron(III), and cobalt(III) complexes with the diazine Schiff bases H_2salhn and H_2mesalhn. The complexes, [Mn_2(μ-salhn)$_3$] (**2**), [Co_2(μ-salhn)$_3$] (**3**), [Co_2(μ-mesalhn)$_3$] (**4**), and [Fe_2(μ-mesalhn)$_3$] (**5**), have been characterized by analytical, spectroscopic, cryomagnetic and electrochemical measurements. The X-ray structures are reported for the solvated crystals of **3**, **4**, and **5**. As observed for **1**,[11] the two pseudo-octahedral metal ions are bridged by three diazine (=N–N=) moieties from the three ligands and each ligand is twisted along the N–N single bond in these complexes. In the solid state, barring the molecules of **4** the molecules of the other two complexes (**3** and **5**) do not have the ideal D_3 symmetry.

3.3. Experimental section

3.3.1. Materials

The Schiff bases H_2salhn and H_2mesalhn were prepared in ~95% yield by condensation reactions of one mole equivalent of hydrazine and two mole equivalents of salicylaldehyde or 2-hydroxyacetophenone in methanol.[11,13] All

other chemicals and solvents used in this work were of analytical grade available commercially and were used without further purification.

3.3.2. Physical measurements

Microanalytical (C, H, N) data were obtained with a Thermo Finnigon Flash EA1112 series elemental analyzer. Infrared spectra were collected by using KBr pellets on a Jasco-5300 FT-IR spectrophotometer. A Shimadzu 3101-PC UV/vis/NIR spectrophotometer was used to record the electronic spectra. The proton NMR spectrum was recorded with the help of a Bruker 400 MHz spectrometer. The EPR spectra were recorded on a Jeol JES-FA200 spectrometer. Solution electrical conductivities were measured with a Digisun DI-909 conductivity meter. A CH-Instruments model 620A electrochemical analyzer was used for cyclic voltammetric experiments with dimethylformamide solutions of **2** and **3** and dichloromethane solutions of **4** and **5** containing tetrabutylammonium perchlorate (TBAP) as supporting electrolyte. The three electrode measurements were carried out at 298 K under a dinitrogen atmosphere with a platinum disk working electrode, a platinum wire auxiliary electrode and an Ag/AgCl reference electrode. Under identical conditions the $E_{1/2}$ (= $(E_{pa} + E_{pc})/2$) and the ΔEp (= $E_{pa} - E_{pc}$) values of Fc^+/Fc (Fc, ferrocene) couple were 0.57 V and 140 mV, respectively. The potentials reported in this work are uncorrected for junction contributions. The variable temperature (18–300 K) magnetic susceptibility measurements with powdered samples were performed using the Faraday technique with a set-up comprising a George Associates Lewis coil force magnetometer, a CAHN microbalance and an Air Products cryostat. $Hg[Co(NCS)_4]$ was used as the standard. Diamagnetic corrections calculated

from Pascal's constants[14] were used to obtain the molar paramagnetic susceptibilities.

3.3.3. Preparation of the complexes

$[Mn_2(\mu\text{-salhn})_3]$ (2)

To a suspension of H_2salhn (241 mg, 1 mmol) in methanol (20 mL) 112 mg (2 mmol) of KOH was added and the mixture was stirred at room temperature until a clear yellow solution was obtained. To this clear solution 235 mg (0.67 mmol) of $[Mn(acac)_3]$ was added and stirred at room temperature in air for 4 h. The brown solid separated was collected by filtration, washed with methanol and dried in air. Yield, 110 mg (40%).

Selected IR bands (cm^{-1}): 1601(vs), 1576(s), 1526(s), 1468(s), 1439(s), 1373(w), 1281(m), 1192(s), 1148(s), 1015(w), 976(w), 926(w), 903(m), 756(s), 685(w), 579(m), 457(m), 419(w).

$[Co_2(\mu\text{-salhn})_3]$ (3)

To a 5:1 mixture of methanol and dichloromethane (30 mL) 241 mg (1 mmol) of H_2salhn and 112 mg (2 mmol) of KOH were added and stirred at room temperature until a clear yellow solution was obtained. To this solution 159 mg (0.67 mmol) of $CoCl_2 \cdot 6H_2O$ was added and stirred at room temperature in air for 6 h. The complex precipitated as a brown solid was collected by filtration, washed with methanol and dried in air. Yield, 175 mg (63%).

Selected IR bands (cm^{-1}): 1608(vs), 1570(s), 1539(s), 1470(s), 1445(s), 1370(w), 1279(s), 1190(s), 1150(s), 1036(m), 961(m), 897(m), 860(m), 754(s), 685(m), 584(s), 486(m), 449(s), 415(w).

$[Co_2(\mu\text{-mesalhn})_3]$ (4)

H_2mesalhn (268 mg, 1 mmol) and KOH (112 mg, 2 mmol) were taken in 30 mL of methanol and stirred at room temperature. When a clear yellow solution was obtained solid $CoCl_2 \cdot 6H_2O$ (159 mg, 0.67 mmol) was added and stirred again in air at room temperature for 4 h. The complex was precipitated as a dark brown solid. It was collected by filtration, washed with cold methanol and dried in air. Yield, 220 mg (72%).

Selected IR bands (cm^{-1}): 1595(s), 1560(s), 1522(s), 1437(s), 1335(s), 1240(s), 1140(m), 1020(m), 937(m), 862(s), 754(s), 621(w), 577(m), 521(w), 446(m), 415(w).

$[Fe_2(\mu\text{-mesalhn})_3]$ (5)

H_2mesalhn (100 mg, 0.37 mmol) and $N(C_2H_5)_3$ (0.12 mL, 87 mg, 0.86 mmol) were taken in 10 mL of CH_3CN and refluxed for 10 min. To the resulting clear yellow solution 50 mg (0.31 mmol) of $FeCl_3$ was added and the mixture was refluxed for another 15 min. It was then cooled to room temperature and stirred in air for 1 h. The complex separated as a brown crystalline material was collected by filtration, washed with cold methanol and dried in air. Yield, 75 mg (67%).

Selected IR bands (cm^{-1}): 1595(s), 1564(s), 1530(s), 1437(s), 1327(s), 1240(s), 1149(w), 977(w), 1034(m), 916(m), 860(m), 756(s), 611(m), 527(w), 497(w), 422(w).

3.3.4. X–ray crystallography

Single crystals of $[Co_2(\mu\text{-salhn})_3]$ (**3**) were grown by slow evaporation of a dimethylformamide-acetonitrile (1:1) solution. On the other hand, single crystals of both $[Co_2(\mu\text{-mesalhn})_3]$ (**4**) and $[Fe_2(\mu\text{-mesalhn})_3]$ (**5**) were obtained by slow evaporation of dichloromethane-acetonitrile (1:1) solutions of the complexes. The complex $[Co_2(\mu\text{-salhn})_3]$ (**3**) crystallizes as **3**·$2(CH_3)_2NCHO\cdot H_2O$ in the $P\bar{1}$ space group. Whereas $[Co_2(\mu\text{-mesalhn})_3]$ (**4**) and $[Fe_2(\mu\text{-mesalhn})_3]$ (**5**) crystallize as **4**·$2H_2O$ and **5**·$2CH_2Cl_2$ in the space groups $R\bar{3}$ and $P\bar{1}$, respectively. Unit cell parameters and the intensity data for **3**·$2(CH_3)_2NCHO\cdot H_2O$ and **5**·$2CH_2Cl_2$ were obtained on a Bruker-Nonius SMART APEX CCD single crystal diffractometer, equipped with a graphite monochromator and a Mo $K\alpha$ fine-focus sealed tube (λ = 0.71073 Å) operated at 2.0 kW. The detector was placed at a distance of 6.0 cm from the crystal. Data were collected at 298 K with a scan width of 0.3° in ω and an exposure time of 30 sec/frame. The SMART software was used for data acquisition and the SAINT-Plus software was used for data extraction.[15] In each case, an absorption correction was performed with the help of SADABS program.[16] Unit cell parameters for **4**·$2H_2O$ were determined by the least-squares fit of 25 reflections having 2θ values in the range 18–21° on an Enraf-Nonius Mach-3 single crystal diffractometer using graphite monochromated Mo $K\alpha$ radiation (λ = 0.71073 Å). The data were collected by ω -scan method. The stability of the crystal was monitored by measuring the

intensities of three check reflections after every 1.5 h during the data collection. No decay was observed during the 110 h exposure to X-ray. The ψ-scans[17] of 4 reflections having θ and χ values within 4–13° and 82–87°, respectively were used for an empirical absorption correction. The programs of the WinGX package[18] were used for data reduction and absorption correction. In each case, the structure was solved by direct methods and refined on F^2 by full-matrix least-squares procedures. All non-hydrogen atoms were refined with anisotropic thermal parameters. Hydrogen atoms were included in the structure factor calculation at idealized positions by using riding model, but not refined. The SHELX-97 programs[19] were used for structure solution and refinement. The ORTEX6a[20] and Platon[21] packages were used for molecular graphics. Significant crystallographic data for **3**·2$(CH_3)_2NCHO·H_2O$, **4**·2H_2O and **5**·2CH_2Cl_2 are summarized in Table 3.1. Atomic coordinates and equivalent isotropic displacement parameters for **3**·2$(CH_3)_2NCHO·H_2O$, **4**·2H_2O and **5**·2CH_2Cl_2 are provided in Tables 3.2, 3.3 and 3.4, respectively.

Table 3.1. Crystallographic data for **3**·2$(CH_3)_2NCHO·H_2O$, **4**·2H_2O, and **5**·2CH_2Cl_2

Complex	**3**·2$(CH_3)_2NCHO·H_2O$	**4**·2H_2O	**5**·2CH_2Cl_2
Chemical formula	$Co_2C_{48}H_{46}N_8O_9$	$Co_2C_{48}H_{46}N_6O_8$	$Fe_2Cl_4C_{50}H_{46}N_6O_6$
Formula weight	996.79	952.77	1080.43
Space group	Triclinic- $P\bar{1}$	Trigonal-$R\bar{3}$	Triclinic-$P\bar{1}$
a, Å	12.5167(8)	14.282(2)	11.931(3)
b, Å	14.8098(9)	14.282(2)	13.555(4)
c, Å	15.1124(9)	37.451(6)	15.319(4)
α, deg.	62.845(1)	90	82.267(5)
β, deg.	66.846(1)	90	88.161(4)
γ, deg.	65.940(1)	120	76.548(4)
V, Å^3	2200.8(2)	6616(2)	2387.6(11)
Z	2	6	2
μ mm^{-1}	0.822	0.814	0.889
Reflections collected/unique	18608/7991	10507/3379	25088/9506
Reflections $I > 2\sigma(I)$	4560	1351	4826
No. of parameters	608	195	619
$R1$,[a] w$R2$[b] [($I > 2\sigma$ (I)]	0.0510, 0.1029	0.0840, 0.1834	0.0786, 0.1454
$R1$,[a] w$R2$[b] (all data)	0.1025, 0.1162	0.2113, 0.2415	0.1617, 0.1743
Goodness-of-fit[c]	0.867	0.981	0.990
Largest peak, hole [e Å^{-3}]	0.376 and -0.267	0.871 and -0.274	0.583 and -0.375

[a] $R1 = \Sigma(||F_o|| - ||F_c||)/\Sigma|F_o|$. [b] $wR2 = [\Sigma(w(|F_o|^2 - |F_c|^2)^2)/\Sigma(w|F_o|^2)]^{1/2}$. [c] GOF = $[\Sigma w(|F_o|^2 - |F_c|^2)^2]/(n - p)^{1/2}$, where n is the number of reflections, and p is the number of refined parameters.

Table 3.2. Atomic coordinates (x 10^4) and equivalent isotropic displacement parameters (Å^2 x 10^3) for $[Co_2(\mu\text{-salhn})_3]\cdot 2(CH_3)_2NCHO\cdot H_2O$

Atom	x	y	z	U(eq)
Co(1)	3385(1)	855(1)	3084(1)	32(1)
Co(2)	5192(1)	-1464(1)	2685(1)	32(1)
O(1)	2872(2)	1069(2)	4355(2)	40(1)
O(2)	5208(2)	-1939(2)	1701(2)	41(1)
O(3)	3674(2)	2194(2)	2427(2)	40(1)
O(4)	5259(2)	-2839(2)	3657(2)	39(1)
O(5)	1799(2)	1565(2)	2923(2)	39(1)
O(6)	6887(2)	-1907(2)	2320(2)	43(1)
O(8)	8775(6)	-5397(6)	8252(5)	143(2)
O(7)	8045(4)	-6920(4)	4341(4)	102(1)
O(9)	7641(6)	-4753(6)	9868(5)	177(3)
N(1)	2941(3)	-445(2)	3737(2)	31(1)
N(2)	3467(3)	-1126(2)	3167(2)	32(1)
N(3)	4973(3)	136(2)	3294(2)	33(1)
N(4)	5280(3)	-975(2)	3623(2)	34(1)
N(5)	3972(3)	692(2)	1774(2)	33(1)
N(6)	5101(3)	-81(2)	1637(2)	33(1)
N(7)	9368(6)	-4513(5)	6600(6)	114(2)
N(8)	7249(4)	-5524(4)	3063(4)	76(1)
C(1)	2051(3)	693(3)	5153(3)	37(1)
C(2)	1560(3)	1104(3)	5952(3)	44(1)
C(3)	709(4)	713(4)	6827(3)	52(1)
C(4)	317(4)	-102(4)	6966(3)	54(1)
C(5)	792(4)	-537(4)	6214(3)	50(1)
C(6)	1662(3)	-167(3)	5316(3)	38(1)
C(7)	2200(3)	-740(3)	4634(3)	37(1)
C(8)	2780(3)	-1484(3)	3043(3)	34(1)
C(9)	3179(3)	-2114(3)	2426(3)	37(1)
(10)	2321(4)	-2508(3)	2432(3)	48(1)
C(11)	2602(5)	-3042(4)	1796(4)	59(1)
C(12)	3745(5)	-3200(4)	1150(3)	60(1)
C(13)	4608(4)	-2837(3)	1130(3)	51(1)

C(14)	4352(4)	-2281(3)	1770(3)	38(1)
C(15)	4707(3)	2395(3)	2134(3)	37(1)
C(16)	4773(4)	3434(3)	1521(3)	43(1)
C(17)	5810(5)	3701(4)	1197(4)	61(1)
C(18)	6870(5)	2951(4)	1468(5)	82(2)
C(19)	6842(5)	1954(4)	2055(4)	71(2)
C(20)	5761(4)	1651(3)	2409(3)	47(1)
C(21)	5854(3)	552(3)	2961(3)	42(1)
C(22)	5599(3)	-1548(3)	4476(3)	36(1)
C(23)	5893(3)	-2662(3)	4878(3)	36(1)
C(24)	6337(4)	-3203(3)	5771(3)	51(1)
C(25)	6615(5)	-4251(4)	6196(3)	61(1)
C(26)	6456(4)	-4845(3)	5779(3)	55(1)
C(27)	6011(4)	-4349(3)	4935(3)	44(1)
C(28)	5705(3)	-3249(3)	4450(3)	35(1)
C(29)	1536(3)	2107(3)	2039(3)	35(1)
C(30)	370(3)	2837(3)	2019(3)	46(1)
C(31)	32(4)	3416(4)	1126(3)	52(1)
C(32)	788(4)	3320(4)	205(3)	56(1)
C(33)	1901(4)	2618(3)	187(3)	49(1)
C(34)	2306(3)	2003(3)	1090(3)	37(1)
C(35)	3456(3)	1238(3)	1019(3)	35(1)
C(36)	5993(3)	231(3)	902(3)	37(1)
C(37)	7214(3)	-416(3)	769(3)	39(1)
C(38)	8094(4)	18(4)	-117(3)	50(1)
C(39)	9296(4)	-537(4)	-259(3)	58(1)
C(40)	9663(4)	-1500(4)	457(3)	55(1)
C(41)	8867(4)	-1938(4)	1324(3)	50(1)
C(42)	7603(3)	-1426(3)	1498(3)	37(1)
C(43)	7317(6)	-6475(6)	3780(5)	89(2)
C(44)	8043(7)	-4917(6)	2844(5)	115(2)
C(45)	6360(7)	-4991(8)	2481(6)	129(3)
C(46)	8776(8)	-4553(7)	7512(9)	117(3)
C(47)	10010(9)	-5485(7)	6304(7)	151(3)
C(48)	9386(9)	-3457(6)	5775(7)	162(4)

Table 3.3. Atomic coordinates (x 10^4) and equivalent isotropic displacement parameters (Å^2 x 10^3) for $[Co_2(\mu\text{-mesalhn})_3]\cdot 2H_2O$

Atom	x	y	z	U(eq)
Co(1)	6667	3333	1575(1)	52(1)
Co(2)	6667	3333	645(1)	58(1)
O(1)	6758(4)	4420(4)	1876(1)	60(1)
O(2)	5980(5)	2129(4)	346(1)	74(1)
O(3)	6667	3333	2998(6)	227(8)
O(4)	3333	6667	2765(9)	328(15)
N(1)	5588(4)	3384(4)	1273(1)	52(1)
N(2)	5406(4)	2851(4)	941(1)	54(1)
C(1)	5935(6)	4558(5)	1935(2)	56(2)
C(2)	5803(6)	4874(6)	2274(2)	69(2)
C(3)	5000(7)	5084(6)	2351(2)	81(3)
C(4)	4258(7)	4989(6)	2081(3)	87(3)
C(5)	4360(6)	4663(6)	1749(2)	72(2)
C(6)	5167(5)	4427(5)	1671(2)	54(2)
C(7)	5144(5)	3978(5)	1322(2)	54(2)
C(8)	4459(6)	1982(6)	897(2)	59(2)
C(9)	4164(6)	1394(6)	561(2)	61(2)
C(10)	3070(7)	683(6)	498(2)	79(2)
C(11)	2730(8)	100(8)	189(3)	97(3)
C(12)	3482(9)	209(8)	-59(3)	99(3)
C(13)	4551(8)	912(7)	-3(2)	86(3)
C(14)	4932(7)	1534(6)	309(2)	67(2)
C(15)	4598(6)	4191(6)	1018(2)	68(2)
C(16)	3663(6)	1556(6)	1204(2)	70(2)

Table 3.4. Atomic coordinates (x 10^4) and equivalent isotropic displacement parameters (Å^2 x 10^3) for $[Fe_2(\mu\text{-mesalhn})_3]\cdot 2CH_2Cl_2$

Atom	x	y	z	U(eq)
Fe(1)	4352(1)	3196(1)	3686(1)	31(1)
Fe(2)	3372(1)	2622(1)	1472(1)	35(1)
Cl(1)	7669(2)	5285(2)	2853(1)	107(1)
Cl(2)	8330(2)	4745(2)	4673(1)	87(1)
Cl(3)	1368(2)	1314(2)	-1022(2)	124(1)
Cl(4)	3248(2)	2268(2)	-1469(1)	105(1)
O(1)	4122(3)	4539(3)	3960(2)	40(1)
O(2)	4420(3)	1725(3)	816(2)	44(1)
O(3)	3789(3)	2581(3)	4747(2)	41(1)
O(4)	2885(4)	3688(3)	542(2)	50(1)
O(5)	5943(3)	2836(3)	3965(2)	41(1)
O(6)	2090(3)	2019(3)	1462(2)	48(1)
N(1)	4665(3)	3907(3)	2351(3)	32(1)
N(2)	4870(4)	3204(3)	1721(3)	31(1)
N(3)	2575(4)	3391(3)	3219(3)	32(1)
N(4)	2423(4)	3742(3)	2300(3)	33(1)
N(5)	4739(4)	1727(3)	3148(3)	32(1)
N(6)	3798(4)	1557(3)	2698(3)	32(1)
C(1)	4212(4)	5436(4)	3552(3)	30(1)
C(2)	4156(5)	6215(4)	4071(4)	42(2)
C(3)	4206(6)	7177(5)	3714(4)	58(2)
C(4)	4294(6)	7401(5)	2815(4)	64(2)
C(5)	4377(6)	6655(5)	2293(4)	57(2)
C(6)	4363(4)	5645(4)	2631(3)	33(1)
C(7)	4552(4)	4867(4)	2042(3)	32(1)
C(8)	5922(5)	2911(4)	1461(3)	36(1)
C(9)	6210(5)	2243(4)	771(3)	40(1)
C(10)	7283(6)	2167(5)	353(4)	64(2)
C(11)	7605(6)	1596(6)	-315(5)	73(2)
C(12)	6848(6)	1063(5)	-584(4)	63(2)
C(13)	5806(5)	1117(4)	-205(4)	47(2)
C(14)	5440(5)	1722(4)	470(3)	40(1)

C(15)	4644(6)	5206(4)	1069(3)	53(2)
C(16)	6874(5)	3258(5)	1850(4)	51(2)
C(17)	2777(5)	2588(4)	5097(3)	35(1)
C(18)	2681(6)	2394(4)	6011(4)	47(2)
C(19)	1663(7)	2396(5)	6430(4)	58(2)
C(20)	674(6)	2577(5)	5949(4)	62(2)
C(21)	716(5)	2772(4)	5040(4)	50(2)
C(22)	1760(5)	2789(4)	4597(3)	36(1)
C(23)	1701(5)	3104(4)	3638(3)	35(1)
C(24)	1850(5)	4676(5)	2081(4)	38(1)
C(25)	1610(5)	5067(5)	1144(4)	45(2)
C(26)	778(5)	5982(5)	947(4)	59(2)
C(27)	440(6)	6360(6)	100(5)	72(2)
C(28)	889(6)	5834(6)	-579(5)	67(2)
C(29)	1709(6)	4947(6)	-418(4)	60(2)
C(30)	2083(5)	4542(5)	441(4)	45(2)
C(31)	633(5)	3110(5)	3156(4)	51(2)
C(32)	1442(5)	5367(5)	2767(4)	54(2)
C(33)	6769(5)	2006(4)	4007(3)	37(1)
C(34)	7766(5)	1989(5)	4457(4)	44(2)
C(35)	8665(6)	1178(6)	4511(5)	63(2)
C(36)	8640(6)	339(6)	4108(5)	78(2)
C(37)	7671(6)	330(5)	3655(5)	64(2)
C(38)	6719(5)	1153(4)	3579(3)	37(1)
C(39)	5719(5)	1068(4)	3107(3)	36(1)
C(40)	3273(5)	880(4)	3093(4)	38(1)
C(41)	2311(5)	635(5)	2654(4)	44(2)
C(42)	1919(6)	-233(5)	3026(5)	61(2)
C(43)	1041(7)	-511(6)	2666(6)	83(3)
C(44)	490(7)	90(7)	1933(6)	82(3)
C(45)	843(5)	926(5)	1557(4)	57(2)
C(46)	1778(5)	1214(5)	1881(4)	41(2)
C(47)	5842(5)	199(4)	2563(4)	51(2)
C(48)	3630(6)	333(5)	3999(4)	56(2)
C(49)	7196(6)	5049(6)	3932(4)	70(2)
C(50)	2508(7)	1711(7)	-637(5)	92(3)

3.4. Results and discussion

3.4.1. Synthesis, structure, and physical properties

The complexes have been synthesized in moderate to good yields by reacting the metal ion starting material, the corresponding Schiff base and the base (KOH or $N(C_2H_5)_3$) in ~2:3:6 mole ratio. The elemental analysis data are (Table 3.5) satisfactory with the general molecular formula $[M_2(\mu\text{-salhn})_3]$ (M = Mn (**2**), Co (**3**)) and $[M_2(\mu\text{-mesalhn})_3]$ (M = Co (**4**), Fe(**5**)). The trivalent metal ion starting materials, $[Mn(acac)_3]$ and $FeCl_3$, have been used for the synthesis of **2** and **5**, respectively. On the other hand, for the synthesis of **3** and **4** cobaltous chloride has been used as the starting material. As the reactions were performed under aerobic condition, the oxygen in air is the likely oxidizing agent during the synthesis of the two dicobalt(III) complexes. Despite our several attempts we could not prepare $[Mn_2(\mu\text{-mesalhn})_3]$. Both **4** and **5** are soluble in low-polar solvents such as dichloromethane and chloroform. However, **2** and **3** are insoluble in nature. They are sparingly soluble in dimethylformamide and dimethylsulfoxide only. In these solvents, the solubility of the former is slightly better than that of the later. All the complexes are electrically non-conducting in solutions. As expected the dicobalt(III) complexes **3** and **4** are diamagnetic. On the other hand, the dimanganese(III) complex **(2)** and the diiron(III) complex (**5)** are paramagnetic.

3.4.2. Infrared spectral properties

In the infrared spectrum, none of the complexes displays the free Schiff base phenolic OH stretch. Thus the ligands are dianionic in each complex. This

observation together with the elemental analysis data and the electrically non-conducting nature of the complexes suggest the +3 oxidation state of the metal ions in these complexes. The intense band observed in the range 1608–1595 cm^{-1} is assigned to the C=N stretch. The C=N stretches for H_2salhn and H_2mesalhn appear at 1624 and 1622 cm^{-1}, respectively.[11,13c] Thus there is a substantial low energy shift of the C=N stretch due to metal coordination. The infrared spectra of the complexes of $salhn^{2-}$ (**1**,[11] **2**, and **3**) are essentially identical except for small shifts of frequencies (Figure 3.2). The similarities in the IR-spectra indicate that molecular structures of **2** and **3** are very similar to that of **1**.[11] There is a similar 1:1 correlation in the infrared spectra of the complexes of $mesalhn^{2-}$ (**4** and **5**) suggesting similar molecular structures of both the complexes. The X-ray structural studies (*vide infra*) confirm the above observations.

Table 3.5. Elemental analysis data[a]

Complex	**%C**	**%H**	**%N**
$Mn_2(\mu\text{-salhn})_3]$ (**2**)	61.15(61.17)	3.83(3.67)	9.96(10.19)
$Co_2(\mu\text{-salhn})_3]$ (**3**)	60.21(60.59)	3.42(3.63)	9.78(10.09)
$Co_2(\mu\text{-mesalhn})_3]$ (**4**)	62.72(62.89)	4.45(4.62)	8.91(9.17)
$Fe_2(\mu\text{-mesalhn})_3]$ (**5**)	63.14(63.31)	4.55(4.65)	9.11(9.23)

[a] Calculated values are in parentheses

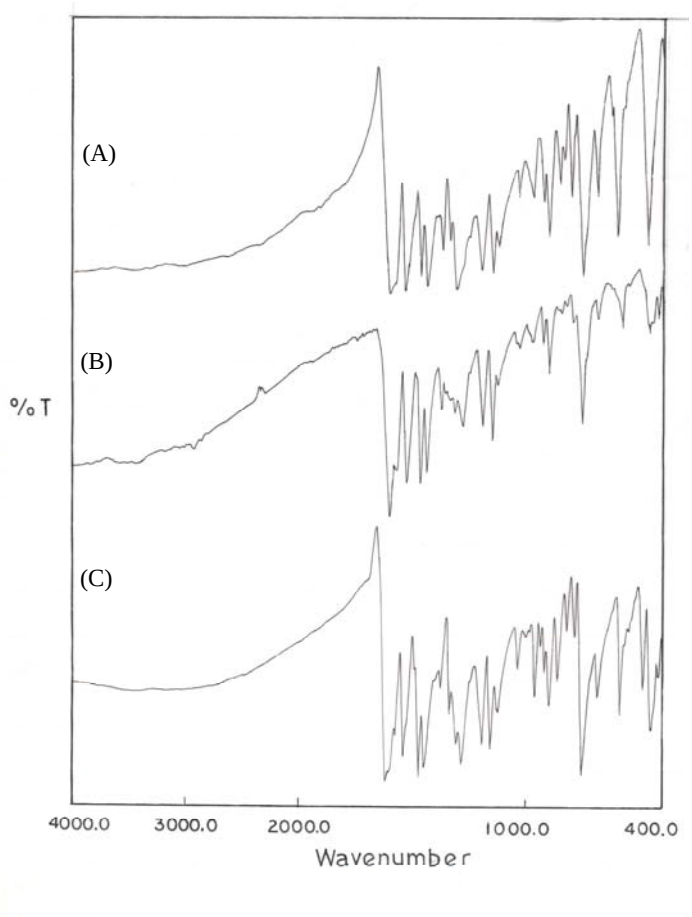

Figure 3.2. Infrared spectra of **1** (A), **2** (B) and **3** (C) in KBr disks.

3.4.3. NMR spectral properties

The proton NMR spectrum of complex **4** is recorded in $CDCl_3$. Although both the dicobalt(III) complexes **3** and **4** are diamagnetic, we could not able to record the proton NMR spectrum of **3** due to its very poor solubility. The complex **4** displays a singlet at 2.05 δ due to the methyl group protons.

Appearance of a solitary signal for the methyl group protons suggest that not only all the three ligands but both halves of each mesalhn^{2-} in [Co_2(mesalhn)$_3$] are magnetically equivalent at least on the NMR time scale. The aromatic protons appear as two multiplets centered at ~6.48 and ~7.16 δ.

3.4.4. Electronic spectral properties

The electronic spectral profiles of the complexes are very similar (Table 3.6). All the complexes display multiple bands in the range 515–350 nm due to ligand-to-metal charge transfer transitions.[11] A representative spectrum is shown in Figure 3.3. The intense bands observed below 350 nm are likely to be due to intraligand transitions.

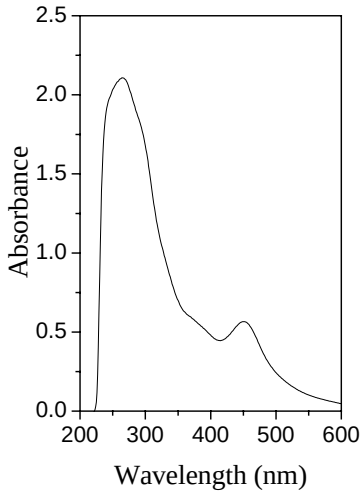

Figure 3.3. Electronic spectrum of **4** in CH_2Cl_2 solution.

Table 3.6. Electronic spectral data

Complex	λ_{max} (nm) (ε ($M^{-1}cm^{-1}$))
2[a]	420 (10600)[sh], 370 (31000)[sh], 356 (34700), 295 (38600)
3[a]	457, 420[sh], 331, 300
4[b]	450 (14900), 370 (15500)[sh], 290 (54000),[sh] 265 (83400)
5[b]	515 (5800)[sh], 440 (7700)[sh], 348 (27500)[sh], 274 (41300)

[a]In dimethylformamide. [b]In dichloromethane. [sh]Shoulder.

3.4.5. EPR Spectra

The EPR silent nature of the dimanganese(III) complex (**2**) is consistent with the d^4 configuration of the metal ions in this complex. In principle, the diiron(III) complex (**5**) can have spin states 5, 4, 3, 2, 1 and 0. Except the lowest energy singlet state the other states can give rise to EPR signals. As observed for **1**[11] the room temperature powder EPR spectrum of **5** displays a broad signal at g ~ 2. Cooling to low temperature (120 K) causes only the sharpening of this signal.

3.4.6. Electrochemical properties

Electron transfer characteristics of all the complexes have been investigated with the help of cyclic voltammetry. Due to solubility reason, the cyclic voltammograms of the dimanganese(III) and dicobalt(III) complexes (**2** and **3**) of $salhn^{2-}$ were recorded using dimethylformamide solutions. None of the two

complexes display any response within ±1.5 V (vs. Ag/AgCl). In **2**, it is very likely that the +3 oxidation state of each metal ion is well-stabilized by the three salicylaldiminate ligands and hence reduction to +2 state is very difficult. Considering that **4** is redox active (*vide infra*), the absence of any response for **3** is unexpected. Possibly very low concentration of **3** due to its poor solubility is responsible for not observing any redox response in the cyclic voltammogram. However, it may be noted that the analogous diiron(III) complex (**1**) in dichloromethane displays two quasi-reversible metal centered reduction responses at –0.52 and –0.80 V (vs. SCE). As observed for **1**, the complexes of $mesalhn^{2-}$ (**4** and **5**) in dichloromethane display two reductions on the cathodic side of the Ag/AgCl reference electrode. For the dicobalt(III) complex (**4**) both the responses are irreversible (Figure 3.4a). The values of the cathodic peak potentials (E_{pc}) are –0.99 and –1.40 V. On the other hand, the responses observed for the diiron(III) complex (**5**) are reversible (Figure 3.4b). The $E_{1/2}$ values are –0.54 and –0.98 V. The corresponding ΔE_p values are 70 and 80 mV, respectively. The one electron stoichiometry of these responses has been confirmed by comparing the current heights with known one-electron redox processes under identical conditions.[10,11] The gap between the two reduction potentials is essentially identical for both complexes. The first response is assigned to the M^{III}_2 to $M^{III}M^{II}$ reduction and the second response is assigned to the $M^{III}M^{II}$ to M^{II}_2 reduction process. The potentials of **4** are shifted by ~0.4 V to the cathodic side compared to the potentials of **5**. This shift is most likely due to the larger ligand field stablilization in the low-spin dicobalt(III) complex (**4**) than that in the high-spin diiron(III) complex (**5**).

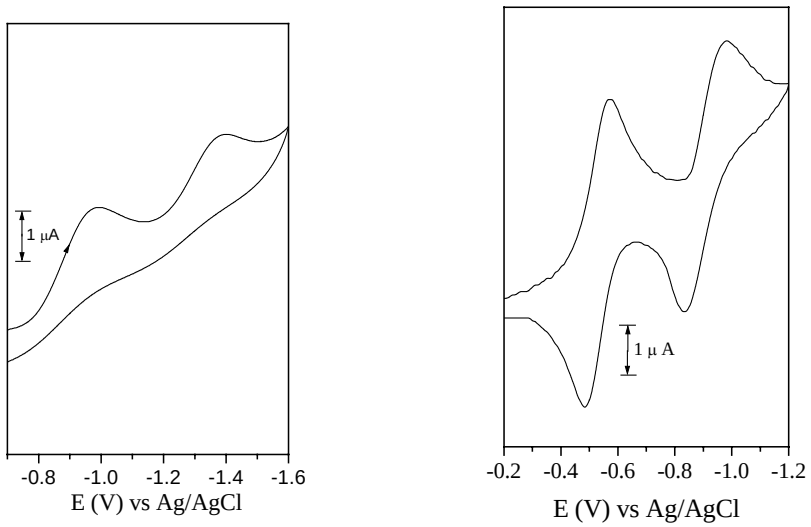

(a) (b)

Figure 3.4. Cyclic voltammograms (scan rate 50 mVs^{-1}) of (a) **4** and (b) **5** solutions (0.1 M TBAP) at a platinum electrode at 298 K.

For a weakly coupled (*vide infra*) dinuclear complex the difference in the metal centered redox potentials can be calculated with the help of an electrostatic model.[22] The $\Delta E_{1/2}$ values calculated for the diiron(III) complexes **1** and **5** by using the electrostatic equation $\Delta E_{1/2} = q^2/4\pi\varepsilon_0 Dr$ (r is the distance between the metal centers obtained in the X-ray structures) and assuming a continuous dielectric with a dielectric constant equal to that of the solvent dichloromethane used for cyclic voltammetry are 0.40 and 0.41 V, respectively. The experimental $\Delta E_{1/2}$ values are 0.28[11] and 0.44 V for **1** and **5**, respectively. The $\Delta E_{1/2}$ value (0.45 V) calculated for **4** is very close to the difference (0.41 V) in the two cathodic peak potentials (E_{pc}) observed in it's cyclic voltammogram. Thus for

$[Fe_2(salhn)_3]$ (**1**) the magnitude of the dielectric constant in the intermetallic space is higher than that of the solvent. On the other hand, for the complexes of $mesalhn^{2-}$ (**4** and **5**) the dielectric medium in the region between the two metal centers is similar to that provided by the solvent around the complex molecules.

3.4.7. Magnetic properties of 2 and 5

The magnetic susceptibilities of the dimanganese(III) and the diiron(III) complexes (**2** and **5**) were measured in the temperature range 18–300 K at a constant magnetic field of 5 kG with powdered samples of the complexes. For each complex the effective magnetic moment (μ_{eff}) decreases gradually with the decrease of temperature indicating antiferromagnetic interaction between the two metal ions (Figure3.5). At 300 K the μ_{eff} value (6.78 μ_B) of **2** is very close to the spin-only moment (6.93 μ_B) of a dimer containing two metal ions with S = 2 spin states. The moment of **2** decreases to 6.15 μ_B at 18 K. In contrast, the change in the μ_{eff} value on cooling is more dramatic in the case of **5**. The μ_{eff} value (7.85 μ_B) at 300 K is slightly smaller than the spin-only moment (8.37 μ_B) expected for a diiron(III) complex where both the metal ions are high spin (S = 5/2). At 18 K the μ_{eff} value decreases to 3.85 μ_B. The data were fitted using the expressions for χ_M vs T derived from the isotropic spin-exchange Hamiltonian $H = -2JS_1 \cdot S_2$, where $S_1 = S_2 = 2$ (for **2**) and $S_1 = S_2 = 5/2$ (for **5**).[23] The best least-squares fits[24] were obtained with $J = -0.57(1)$ cm^{-1} and $g = 1.958(3)$ (for **2**) and $J = -2.82(4)$ cm^{-1} and $g = 1.944(9)$ (for **5**).

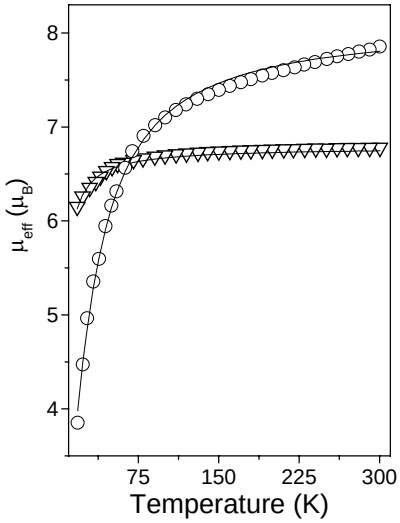

Figure 3.5. Temperature dependence of the effective magnetic moments of $[Mn_2(salhn)_3]$ (∇)] and $[Fe_2(mesalhn)_3]$ (O). The continuous lines were generated from the best least-squares fit parameters given in the text.

Very weak to strong intramolecular antiferromagnetic coupling has been observed for dicopper(II) complexes containing one or two =N–N= bridges.[6a–c,e] The extent of twisting of the dinucleating ligand along the N–N single bond, largely determines the magnitude of the antiferromagnetic spin-exchange between the metal centers in these complexes. It has been found that if the twist angle is ~70^o, effective orthogonality between the magnetic orbitals of the Cu(II) centers and that between the nitrogen p-orbitals involved in the spin-exchange process is attained.[6b-d] Except these dicopper(II) complexes magnetic properties of very few dinuclear complexes of other 3d metal ions containing the diazine bridge are reported. These are the diiron(III) complex[11] of $salhn^{2-}$ (**1**) and some dimetal(II) (M = Ni,[4d,e,6d] Co[4e] and Mn[6d]) complexes with N,N′-bis(picolinylidene)hydrazine

or its derivatives. All these complexes contain three =N–N= bridges between the metal ions and exhibit no spin-exchange or very weak intramolecular spin-exchange. In the dimanganese(II) and dinickel(II) complexes, the average dihedral angles between the two chelate rings formed by each dinucleating ligand are ~68 and ~70°, respectively.[6d] These twist angles are very similar to the twist angle found as the orthogonal limit for the dicopper(II) complexes which contain similar neutral ligands. Among the present series of weakly antiferromagnetic triple helicates (**1**, **2**, and **5**) with the dianionic ligands salhn^{2-} and mesalhn^{2-}, the X-ray structure of **2** could not be determined due to the lack of single crystals. Although in **1** the twist angles (26.6–56.8°) are significantly lower than the orthogonal limit (70°) reported before but for **5** these (59.88–66.49°) are close to the orthogonal limit.

3.4.8. Description of molecular structures

The molecular structures of [Co_2(μ-salhn)$_3$] (**3**), [Co_2(μ-mesalhn)$_3$] (**4**), and [Fe_2(μ-mesalhn)$_3$] (**5**) are illustrated in Figures 3.6, 3.7 and 3.8 respectively. The selected bond parameters associated with the metal ions are listed in Tables 3.7, 3.8, and 3.9. In all the complexes, each of the three ligands coordinates the two metal ions via the two phenolate-O and the two imine-N atoms. Thus the metal ions are in facial O_3N_3 coordination spheres and connected by three diaza (=N–N=) bridges. The Co···Co distances in **3** and **4** are 3.4301(7) and 3.4814(22) Å, respectively. In comparison, the Fe···Fe distance in **5** is significantly longer (3.8541(13) Å). The M–O(phenolate) and M–N(imine) bond lengths (Tables 3.7–3.9) in the dicobalt complexes (**3** and **4**) as well as in the diiron complex (**5**) are consistent with the +3 oxidation state of the metal ions.[9,11,12,25] In each

complex, the ligands are twisted along the N–N single bonds to accommodate the two metal ions. As a result the triple helical structure is generated. Both the complexes of salhn^{2-} (**1** and **3**) crystallize in the space group $P\bar{1}$ and the asymmetric unit contains one full complex molecule in each case. The extent of twisting is very different for the three ligands in both **1** and **3** (Figure 3.6). In **1**, the dihedral angles between the two salicylaldimine moieties of the three ligands are in the range 26.6–56.8°.[11] These dihedral angles are 31.78(12)°, 39.49(7)°, and 59.41(10)^{o} in **3**. Thus although the three bridging salhn^{2-} in **1** and **3** are C_2-symmetric but not identical and hence [M_2(μ-salhn)$_3$] (M = Fe(III) and Co(III))

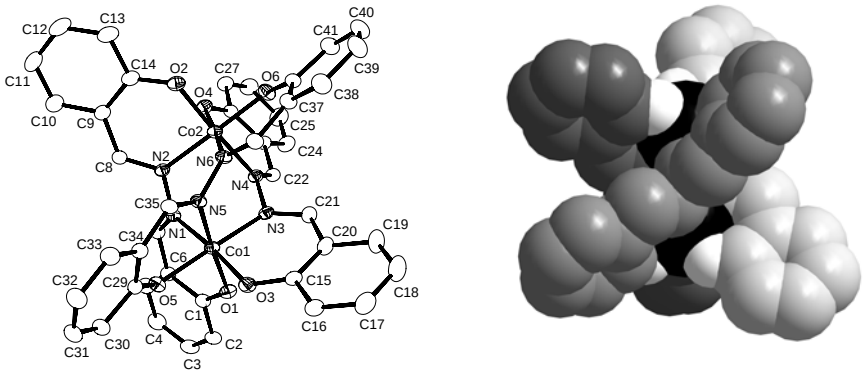

(a) **(b)**

Figure 3.6. Molecular structure of [Co_2(salhn)$_3$]. Hydrogen atoms are omitted for clarity. (a) ORTEP diagram with the atom labeling scheme. All atoms are represented by their 25% probability thermal ellipsoids. (b) Space filling representation of the triple helical structure.

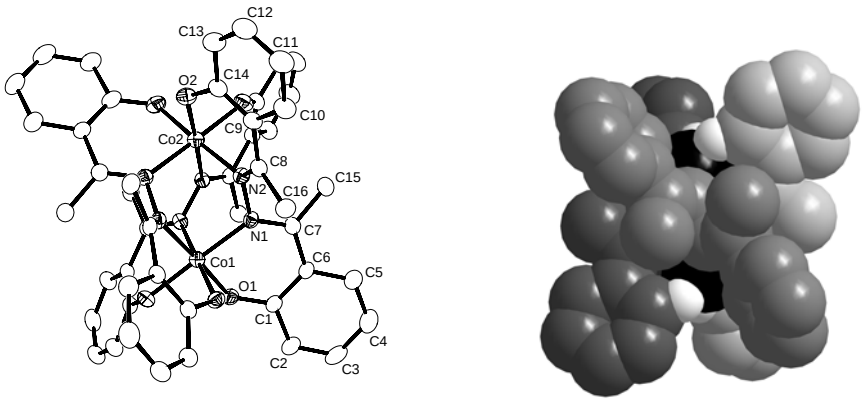

(a) **(b)**

Figure 3.7. Molecular structure of $[Co_2(mesalhn)_3]$. Hydrogen atoms are omitted for clarity. (a) ORTEP diagram with the atom labeling scheme. All atoms are represented by their 20% probability thermal ellipsoids. (b) Space filling representation of the triple helical structure.

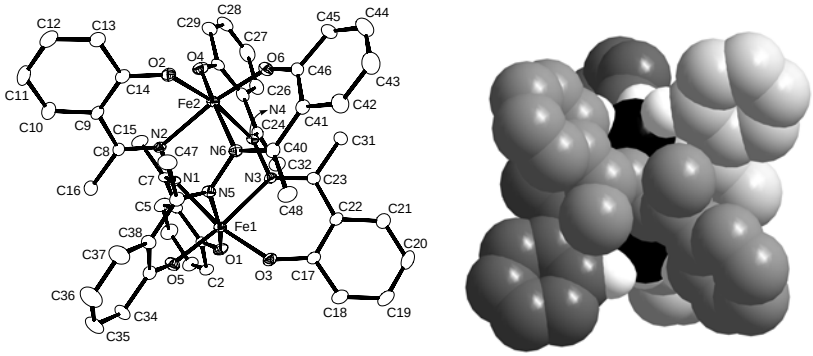

(a) **(b)**

Figure 3.8. Molecular structure of $[Fe_2(mesalhn)_3]$.(a) ORTEP diagram with the atom labeling scheme. All atoms are represented by their 25% probability thermal ellipsoids. (b) Space filling representation of the triple helical structure. Hydrogen atoms are omitted for clarity.

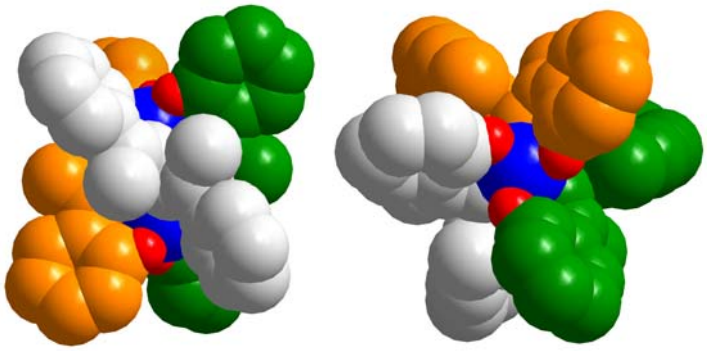

(a) **(b)**

Figure 3.9. Ideal D_3 symmetry in $[Co_2(mesalhn)_3]$ (**4**): (a) viewed perpendicular to the threefold axis (b) viewed parallel to the threefold axis

does not possess the ideal D_3 symmetry expected for a perfect triple helicate. In contrast, **4** crystallizes in the trigonal space group $R\bar{3}$ and the crystallographic three-fold axis coincides with the molecular three-fold axis that passes through the two metal ions. Consequently both the metal centers have 1/3 occupancy and only one of the three ligands is present in the asymmetric unit. The dihedral angle between the two chelating fragments of $mesalhn^{2-}$ is 47.70(13)°. Thus the extent of the helical twist along the N–N single bond is identical for all the three $mesalhn^{2-}$ in **4** and the molecules have the idealized D_3 symmetry (Figure 3.9). On the other hand, the diiron(III) complex of $mesalhn^{2-}$ (**5**) crystallizes in the space group $P\bar{1}$ and the asymmetric unit contains one complete molecule of the complex. As observed for **1** and **3** the extent of helical twist of the three ligands along the N–N single bond is different. However, here the dihedral angles (59.88(11)°, 64.02(10)°, and 66.49(12)°) between the two chelating fragments of the three $mesalhn^{2-}$ span significantly smaller range than that observed for **1** and

3. Thus the molecules of **5** are much closer to the ideal D_3 symmetry (Figure 3.8) compared to the molecules of **1** and **3**. Interestingly the dihedral angles indicate that the helical twist of mesalhn^{2-} in **4** is significantly smaller than the average helical twist of mesalhn^{2-} in **5**. As a consequence the Fe···Fe distance in **5** is longer by ~0.4 Å than the Co···Co distance in **4**.

Table 3.7. Selected bond distances (Å) and angles (°) for 3·2(CH$_3$)$_2$NCHO·H$_2$O

Co(1)-O(1)	1.903(2)	Co(2)-O(2)	1.903(2)
Co(1)-O(3)	1.885(2)	Co(2)-O(4)	1.881(2)
Co(1)-O(5)	1.883(3)	Co(2)-O(6)	1.874(3)
Co(1)-N(1)	1.922(3)	Co(2)-N(2)	1.913(3)
Co(1)-N(3)	1.911(3)	Co(2)-N(4)	1.917(2)
Co(1)-N(5)	1.914(3)	Co(2)-N(6)	1.925(3)
O(1)-Co(1)-O(3)	87.84(10)	O(2)-Co(2)-O(4)	88.74(10)
O(1)-Co(1)-O(5)	89.07(11)	O(2)-Co(2)-O(6)	88.61(11)
O(1)-Co(1)-N(1)	92.15(10)	O(2)-Co(2)-N(2)	92.56(10)
O(1)-Co(1)-N(3)	88.97(11)	O(2)-Co(2)-N(4)	176.20(11)
O(1)-Co(1)-N(5)	176.31(11)	O(2)-Co(2)-N(6)	87.93(11)
O(3)-Co(1)-O(5)	86.77(11)	O(4)-Co(2)-O(6)	86.75(11)
O(3)-Co(1)-N(1)	174.73(12)	O(4)-Co(2)-N(2)	88.19(12)
O(3)-Co(1)-N(3)	93.49(11)	O(4)-Co(2)-N(4)	92.67(11)
O(3)-Co(1)-N(5)	89.04(11)	O(4)-Co(2)-N(6)	176.58(10)
O(5)-Co(1)-N(1)	87.97(11)	O(6)-Co(2)-N(2)	174.78(12)
O(5)-Co(1)-N(3)	178.00(11)	O(6)-Co(2)-N(4)	87.95(11)
O(5)-Co(1)-N(5)	92.72(11)	O(6)-Co(2)-N(6)	93.92(12)
N(1)-Co(1)-N(3)	91.78(12)	N(2)-Co(2)-N(4)	91.02(11)
N(1)-Co(1)-N(5)	91.14(11)	N(2)-Co(2)-N(6)	91.21(12)
N(3)-Co(1)-N(5)	89.27(12)	N(4)-Co(2)-N(6)	90.70(11)

Table 3.8. Selected bond distances (Å) and angles (º) for 4·2H_2O[a]

Co(1)-O(1)	1.870(4)	Co(2)-O(2)	1.867(5)
Co(1)-N(1)	1.942(5)	Co(2)-N(2)	1.924(5)
O(1)–Co(1)–N(1)	92.7(2)	O(2)–Co(2)–N(2)	92.8(2)
O(1)–Co(1)–O(1A)	87.4(2)	O(2)–Co(2)–O(2A)	87.7(2)
O(1)–Co(1)–N(1A)	90.4(2)	O(2)–Co(2)–N(2A)	177.0(2)
O(1)–Co(1)–N(1B)	177.8(2)	O(2)–Co(2)–N(2B)	89.3(2)
N(1)–Co(1)–N(1B)	89.5(2)	N(2)–Co(2)–N(2B)	90.2(2)

[a] Symmetry transformations: A = –x + y + 1, –x + 1, z; B = –y + 1, x – y, z.

Table 3.9. Selected bond distances (Å) and angles (º) for 5·2CH_2Cl_2

Fe(1)-O(1)	1.880(4)	Fe(2)-O(2)	1.896(4)
Fe(1)-O(3)	1.901(4)	Fe(2)-O(4)	1.887(4)
Fe(1)-O(5)	1.895(4)	Fe(2)-O(6)	1.896(4)
Fe(1)-N(1)	2.200(4)	Fe(2)-N(2)	2.178(4)
Fe(1)-N(3)	2.205(4)	Fe(2)-N(4)	2.196(4)
Fe(1)-N(5)	2.201(4)	Fe(2)-N(6)	2.204(4)
O(1)-Fe(1)-O(3)	98.88(16)	O(2)-Fe(2)-O(4)	97.51(17)
O(1)-Fe(1)-O(5)	94.72(16)	O(2)-Fe(2)-O(6)	98.70(16)
O(1)-Fe(1)-N(1)	83.53(15)	O(2)-Fe(2)-N(2)	84.38(16)
O(1)-Fe(1)-N(3)	94.66(16)	O(2)-Fe(2)-N(4)	170.10(16)
O(1)-Fe(1)-N(5)	170.11(15)	O(2)-Fe(2)-N(6)	91.51(16)
O(3)-Fe(1)-O(5)	98.46(16)	O(4)-Fe(2)-O(6)	97.23(18)
O(3)-Fe(1)-N(1)	168.52(16)	O(4)-Fe(2)-N(2)	91.60(17)
O(3)-Fe(1)-N(3)	83.79(16)	O(4)-Fe(2)-N(4)	83.91(17)
O(3)-Fe(1)-N(5)	91.00(16)	O(4)-Fe(2)-N(6)	170.79(17)

O(5)-Fe(1)-N(1)	92.50(16)	O(6)-Fe(2)-N(2)	170.16(16)
O(5)-Fe(1)-N(3)	169.90(15)	O(6)-Fe(2)-N(4)	90.81(16)
O(5)-Fe(1)-N(5)	83.67(16)	O(6)-Fe(2)-N(6)	83.21(17)
N(1)-Fe(1)-N(3)	84.83(15)	N(2)-Fe(2)-N(4)	85.78(15)
N(1)-Fe(1)-N(5)	86.79(15)	N(2)-Fe(2)-N(6)	87.39(16)
N(3)-Fe(1)-N(5)	86.45(15)	N(4)-Fe(2)-N(6)	86.88(15)

3.4.9. Self-assembled supramolecular networks

Infinite 1D chain of $[Co_2(\mu\text{-salhn})_3]\cdot 2(CH_3)_2NCHO\cdot H_2O$

In the crystal lattice of **3**·2$(CH_3)_2$NCHO·H_2O, the $(CH_3)_2$NCHO molecules exist as dimers via C–H···O and C–H···N interactions involving the O- and the N-atoms of the amide group and the C–H fragments of two methyl groups in a reciprocal fashion with respect to the hydrogen bond donors and acceptors.[26] The C···O and C···N distances are 3.408(14) and 3.344(13) Å, respectively. The C–H···O and C–H···N angles are 164 and 152°, respectively. The water molecule is also involved in two hydrogen bonding interactions (O–H···O and C–H···O) as donor as well as acceptor with two $(CH_3)_2$NCHO molecules. The O···O and C···O distances are 2.679(10) and 3.573(11) Å, respectively. The O–H···O and C–H···O angles are 160 and 171°, respectively. The interactions involving the water molecule are roughly orthogonal to the interactions between the two $(CH_3)_2$NCHO molecules. Consequently, two dimers of $(CH_3)_2$NCHO are bridged by two water molecules and a rectangular structure is formed (Figure 4). These rectangular motifs are bridged by the dinuclear helicates due to two more C–H···O interactions involving the O-atoms of the $(CH_3)_2$NCHO molecules and the C–H fragments of one azomethine (–CH=N–) group (C···O, 3.177(16) Å; C–H···O,

162°) and one benzene ring (C···O, 3.438(11) Å; C–H···O, 157°). Self-organization via all these weak intermolecular interactions lead to a one-dimensional supramolecular arrangement of the **3**·2$(CH_3)_2NCHO·H_2O$ units in the crystal lattice (Figure 3.10).

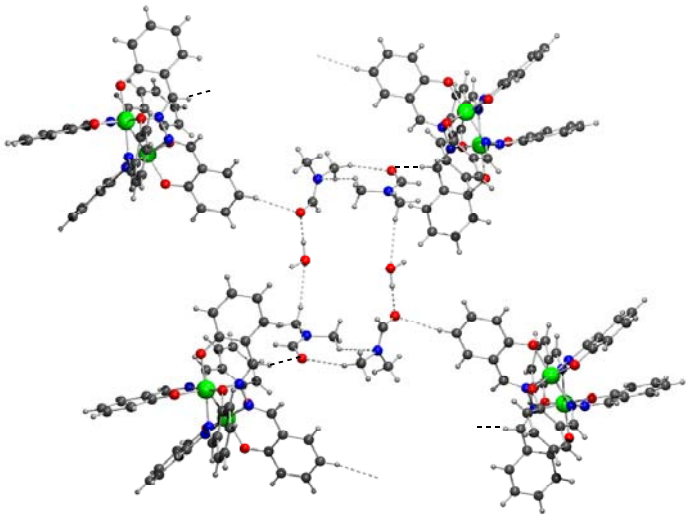

Figure 3.10. One-dimensional arrangement of $[Co_2(salhn)_3]·2(CH_3)_2NCHO·H_2O$.

Hexagonal packing of $[Co_2(\mu\text{-mesalhn})_3]·2H_2O$

Unlike **3**·2$(CH_3)_2NCHO·H_2O$, the crystal packing of **4**·2H_2O is apparently not directed by the trapped solvent molecules. Both the water molecules are disordered with 1/3 site occupancy on the special positions. One of the O-atoms is on the same three-fold axis that passes through the two Co centers and is very close to it's symmetry equivalent. The O···O distance in this water dimer is 2.51Å. The nearest (3.32 Å) H-atom to this O-atom is from an benzene ring

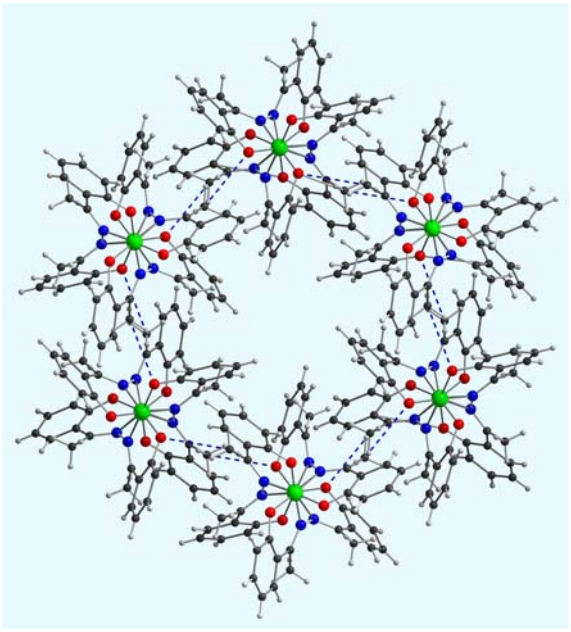

(a)

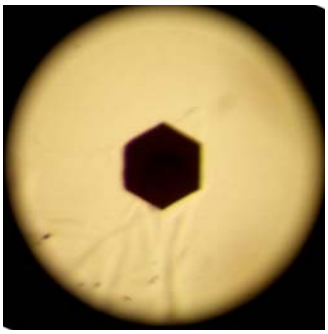

(c)

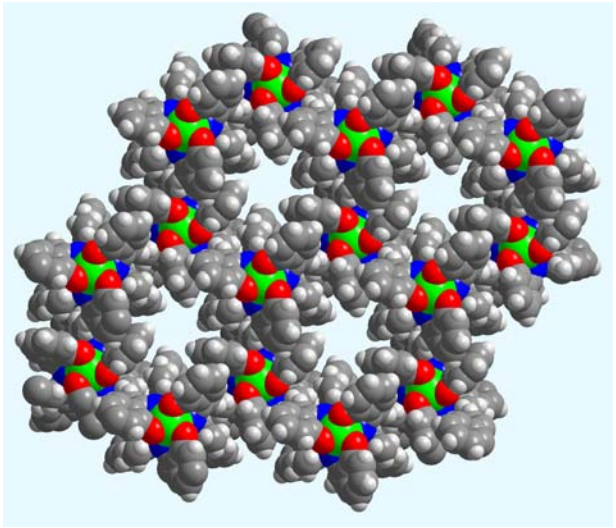

(b)

Figure 3.11. Projection of (a) hexagonal packing and (b) space filling representation of the two-dimensional layered structure of $[Co_2(mesalhn)_3]$ onto the *ab*-plane. (c) The hexagonal morphology of the single crystal of $[Co_2(mesalhn)_3]\cdot 2H_2O$.

(C2–H) of the ligand. On the other hand, the other O-atom is located on the three-fold axis that passes through the center of the hexagon formed by the complex molecules. In this case also the nearest (3.44 Å) H-atom belongs to the same benzene ring (C4–H). The packing of the D_3-symmetric molecules of **4** is shown in Figure 3.11. The molecules are arranged hexagonally along the *c*-axis, which is also parallel to the Co···Co molecular axis. Each molecule is connected to it's three neighbors via C–H···O interactions involving the hydrogen atom of a methyl group and one phenolate-O in a reciprocal fashion (Figure 3.11a). The C···O distance and the C–H···O angle are 3.467(9) Å and 161°, respectively. As a result a two-dimensional layered structure parallel to the *ab*-plane is formed (Figure 3.11b). Interestingly, the morphology of the single crystals of **4**·$2H_2O$ is also perfectly hexagonal (Figure 3.11c).

Two dimensional network of $[Fe_2(\mu\text{-mesalhn})_3]\cdot 2CH_2Cl_2$

The molecules of **5** form discrete dimers due to a pair of reciprocal C–H···O interactions involving a metal coordinated phenolate-O and an benzene ring C–H group (Figure 3.12). The C···O distance and the C–H···O angle are 3.416(6) Å and 134°, respectively. One of the two CH_2Cl_2 molecules present in the asymmetric unit acts as donor in a bifurcated hydrogen bonding interaction involving two metal coordinated phenolate-O atoms and as an acceptor in a C–H···Cl interaction involving a benzene ring C–H group.[26,27] The C···O distances and the C–H···O angles are 3.543(7) and 3.305(8) Å, and 140 and 133°.

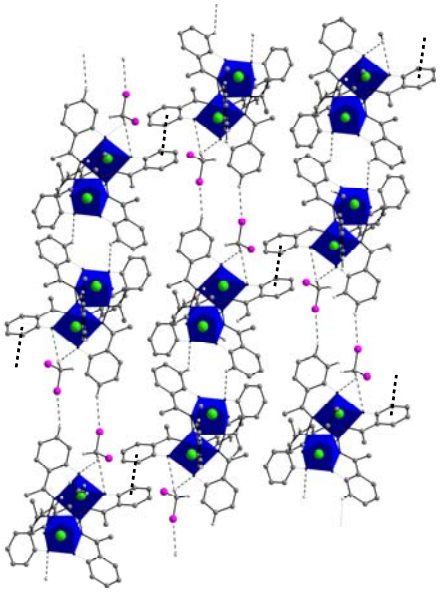

Figure 3.12. Two-dimensional network of $[Fe_2(mesalhn)_3]\cdot 2CH_2Cl_2$.For the clarity one of the CH_2Cl_2 molecules that does not participate in self organization process is not shown.

The C···Cl distance and C–H···Cl angle are 3.655(7) Å and 157^o, respectively. These weak interactions connect the C–H···O bridged dimers of **5** and a one-dimensional chain-like arrangement is formed (Figure 3.12). One of the benzene rings of each complex molecule in this chain is involved in π–π interaction with the benzene ring of a molecule that belongs to the adjacent chain. The interplanar distance and the centroid-to-centroid distances are 3.410 and 3.646(4) Å, respectively. As the successive molecules in a particular chain are inverse symmetry related, these π–π interactions alternate from one side to another side of each chain and a two-dimensional layered organization of the **5**·CH_2Cl_2 units is formed (Figure 3.12). The second CH_2Cl_2 molecule present in the asymmetric

unit does not participate in the self-assembly process to a supramolecular structure. It is simply connected to the complex molecule by a C–H···Cl interaction that involves an benzene ring C–H group. The C···Cl distance and the C–H···Cl angle are 3.425(9) Å and 122^{o}, respectively.

3.5. Conclusions

In this chapter, we are successful in synthesizing dinuclear triple helicates of trivalent metal ions (Mn(III), Fe(III), and Co(III)) with the Schiff bases derived from one mole equivalent of hydrazine and two mole equivalents of salicylaldehyde (H_2salhn) or 2-hydroxy acetophenone (H_2mesalhn) are described. All the complexes have the general formula [M_2(Rsalhn)$_3$] (R = H and Me). In these complexes, two pseudo-octahedral metal ions enforce the twisting of the two chelating sites of each ligand along the N–N single bond to generate the triple helical structure. The dicobalt(III) complex of mesalhn^{2-} has the ideal and the corresponding diiron(III) analogue has a very close to D_3-symmetric triple helical structure. On the other hand, although triple helical but as observed previously for the diiron(III) complexes of salhn^{2-}, the extent of twisting of the three ligands differ considerably in the dicobalt(III) complex of salhn^{2-}. In the crystal lattice, self-organization via non-covalent intermolecular interactions involving the complex and the solvent molecules provide one- and two-dimensional supramolecular structures. The diiron(III) and the dicobalt(III) complexes are redox active and display two metal centered reductions. The magnetic properties of both the dimanganese(III) and the diiron(III) complexes indicate the presence of weak antiferromagnetic spin-exchange.

3.6. References

(1) (a) J. M. Lehn, *Supramolecular Chemistry*; VCH: Weinheim, 1995. (b) C. Piguet, G. Bernardinelli, G. Hopfgartner, *Chem. Rev.*, **1997**, *97*, 2005. (c) A. Williams, *Chem. Eur. J.*, **1997**, *3*, 15. (d) M. Albrecht, *Chem. Rev.*, **2001**, *101*, 3457. (e) M. J. Hannon, L. Childs, J. *Supramol. Chem,*. **2004**, *16*, 7.

(2) (a) O. Kahn, *Molecular Magnetism*, VCH: Weinheim, 1993. (b) C. T. Chen, K. S. Suslick, *Coord. Chem. Rev.* **1993**, *128*, 293. (c) B. Kesanli, W. Lin, *Coord. Chem. Rev.*, **2003**, *246*, 305. (d) C. J. Matthews, S. T. Onions, G. Morata, L. J. Davis, S. L. Heath, D. J. Price, *Angew. Chem. Int. Ed.*, **2003**, *42*, 3166. (e) M. Va´zquez, A. Taglietti, D. Gatteschi, L. Sorace, C. Sangregorio, A. M. Gonza´lez, M. Maeiro, R. M. Pedrido, M. R. Bermejo, *Chem. Commun.*, **2003**, 1840. (f) B. Schoentjes, J. M. Lehn, *Helv. Chim., Acta* **1995**, *78*, 1. (g) I. Meistermann, V. Moreno, M. J. Prieto, E. Molderheim, E. Sletten, S. Khalid, M. Rodger, J. Perberdy, C. J. Isaac, A. Rodger, M. J. Hannon, *Proc. Natl. Acad. Sci., U.S.A.* **2002**, *99*, 5069.

(3) (a) J. M. Lehn, J. Siegel, J. Harrowfield, B. Chevrier, D. Moras, *Proc. Natl. Acad. Sci., U.S.A.*, **1987**, *84*, 2565. (b) E. C. Constable, *Tetrahedron*, **1992**, *48*, 10013. (c) R. Krämer, J. M. Lehn, A. M. Rigault, *Proc. Natl. Acad. Sci. U.S.A.* **1993**, *90*, 5394. (d) M. A. Houghton, A. Bilyk, M. M. Harding, P. Turner, T. W. Hambley, *J. Chem. Soc., Dalton Trans.*, **1997**, 2725.

(4) (a) W. J. Stratton, D. H. Busch, *J. Am. Chem. Soc.*, **1958**, *80*, 1286. (b) W. J. Stratton, D. H. Busch, *J. Am. Chem. Soc.* **1958**, *80*, 3191. (c) W. J. Stratton, D. H. Busch, *J. Am. Chem. Soc.* **1960**, *82*, 4834. (d) P. W. Ball, A. B. Blake, *J. Chem. Soc., A*, **1969**, 1415. (e) W. J. Stratton, *Inorg. Chem.*, **1970**, *9*, 517.

(5) Boyd, P. D. W. Gerloch, G. M. Sheldrick, *J. Chem. Soc., Dalton Trans.*, **1974**, 1097.

(6) (a) C. J. O'Connor, R. J. Romananch, D. M. Robertson, E. E. Eduok, F. R. Fronezek, *Inorg. Chem.*, **1983**, *22*, 449. (b) Z. Xu, L. K. Thompson, D. O. Miller, *Inorg. Chem.*, **1997**, *36*, 3985. (c) L. K. Thompson, Z. Xu, A. E. Goeta, J. A. K. Howard, H. J. Clase, D. O. Miller, *Inorg. Chem.*, **1998**, *37*, 3217. (d) Z. Xu, L. K. Thompson, D. O. Miller, H. J. Clase, J. A. K. Howard, A. E. Goeta, *Inorg. Chem.*, **1998**, *37*, 3620. (e) Z. Xu, L. K. Thompson, C. J. Matthews, D. O. Miller, A. E. Goeta, C. Wilson, J. A. K. Howard, M. Ohba, H. Okawa, *J. Chem. Soc.*, *Dalton Trans.*, **2000**, 69. (f) G. Dong, D. C. Ying, F. C. Jie, M. Q. Jin, *J. Chem. Soc.*, *Dalton Trans.* **2002**, 834. (g) J. Hamblin, A. Jackson, N. W. Alcock, M. J. Hannon, *J. Chem. Soc.*, *Dalton Trans.* **2002**, 1635. (h) G. Dong, P. Ke-liang, D. C. ying, H. Cheng, M. Q. jin, *Inorg. Chem.*, **2002**, *41*, 5978. (i) P. V. Bernhardt, P. Chin, D. R. Richardson, *J. Chem. Soc.*, *Dalton Trans.*, **2004**, 3342.

(7) G. Arcovito, M. Bonamico, A. Domenicano, A. Vaciago, *J. Chem. Soc., B.* **1969**, 733.

(8) S. Gopinathan, S. A. Pardhy, C. Gopinathan, V. G. Puranik, S. S. Tavale, T. N. G. Row, *Inorg. Chim. Acta.*, **1986**, *111*, 133.

(9) M. Mikuriya, M. Fukuya, *Chem. Lett.*, **1998**, 421.

(10) S. N. Pal, S. Pal, *Inorg. Chem.* **2001**, *40*, 4807.

(11) J. Saroja, V. Manivannan, P. Chakraborty, S. Pal, *Inorg. Chem.*, **1995**, *34*, 3099.

(12) (a) M. Hong, G. Dong, D. C. ying, L. Y. ting, M. Q. jin, *J. Chem. Soc.*, *Dalton Trans.*, **2002**, 3422. (b) M. Hong, F. C. jie, D. C. ying, L. Y. ting, M. Q. jin, *J. Chem. Soc.*, *Dalton Trans.*, **2003**, 1229.

(13) (a) F. Umland, E. Hohaus, K. Brodtke, *Chem. Ber.* **1973**, *106*, 2427. (b) E. *Z.* Hohaus, *Anorg. Allg. Chem.* **1983**, *506*, 185. (c) H. Höpfl, N. Farfán, *Can. J. Chem.* **1998**, *76*, 1853.

(14) W. E. Hatfield, In *Theory and Applications of Molecular Paramagnetism:* E. A. Boudreaux, L. N. Mulay, Eds., Wiley: New York, 1976; p. 491.

(15) *SMART* V5.630 and *SAINT-plus* V6.45, Bruker-Nonius Analytical X-ray Systems Inc.: Madison, WI, USA, 2003.

(16) G. M. Sheldrick, *SADABS*, Empirical Absorption Correction Program, University of Göttingen, Göttingen, Germany, **1997**.

(17) A. C. T. North, D. C. Philips, F. S. Mathews, *Acta Crystallogr. Sect. A,* **1968**, *24*, 351.

(18) L. J. Farrugia, *J. Appl. Crystallogr.*, **1999**, *32*, 837.

(19) G. M. Sheldrick, *SHELX-97*, Structure Determination Software, University of Göttingen, Göttingen, Germany, **1997**.

(20) P. *J.* McArdle, *Appl. Crystallogr.,* **1995**, *28,* 65.

(21) A. L. Spek, *PLATON*, A Multipurpose Crystallographic Tool, Utrecht University, Utrecht, The Netherlands, **2002**.

(22) B. R. Serr, K. A. Andersen, C. M. Elliott, O. P. Anderson, *Inorg. Chem.* **1988**, *27*, 4499.

(23) C. J. O'Connor, *Prog. Inorg. Chem.*, **1982**, *29*, 203.

(24) G. V. R. Chandramouli, C. Balagopalakrishna, M. V. Rajasekharan, P. T. Manoharan, *Comput. Chem.,* **1996**, *20*, 353.

(25) (a) J. M. Ready, E. N. Jacobson, *J. Am. Chem. Soc.,* **1999**, *121*, 6086. (b) R. D. Reos, G. Nardin, L. Randacciu, G. Tayzher, V. Vrdoijak, *Inorg. Chim. Acta.,* **2003**, *349*, 249.

(26) G. R. Desiraju; T. Steiner, In *The Weak Hydrogen Bond in Structural Chemistry and Biology*; Oxford University Press, Oxford, **1999**.

(27) (a) P. K. Thallapally, A. Nangia, *CrystEngCommun,* **2001**, *3*, 114. (b) S. Basavoju, S. Aitipamula and G. R. Desiraju, *CrystEngCommun,* **2004**, *6,* 120.

Chapter 4

Co (II) and Co (III) Complexes with Aroylhydrazones: Spin–Crossover in the Co (II) Complexes[§]

4.1. Abstract

Complexes of cobalt(II) and cobalt(III) with tridentate N-(aroyl)-N'-(picolinylidene)hydrazines (HL, H stands for the dissociable amide proton) are described. The Schiff bases (HL) have been prepared by condensation of 2-pyridinecarboxaldehyde with benzhydrazide or 4-substituted benzhydrazides. The reactions of $Co(O_2CCH_3)_2{\cdot}4H_2O$ and HL at room temperature under aerobic condition afford the complexes with general formulae $[Co^{II}L_2]$ (-Cl and $-NO_2$ as substituents) and $[Co^{III}L_2]^+$ (-H, $-CH_3$, $-OCH_3$ and $-N(CH_3)_2$ as substituents). The cationic complexes have been isolated as PF_6^- salts. Analytical, spectroscopic, magnetic and electrochemical techniques were used for the characterization of these complexes. X-ray structure of $[Co(pamh)_2]PF_6$ has been determined. In each complex, the metal centre is in N_4O_2 coordination sphere constituted by the meridionally spanning pyridine–N, imine–N and deprotonated amide–O donor ligands. Infrared spectra are consistent with the enolate form of the amide functionalities in both ligands. Cobalt(III) complexes, $[CoL_2]PF_6$, are diamagnetic, NMR active and behave as 1:1 electrolyte in acetonitrle solutions. Electronic spectra of the complexes display charge transfer bands in the range 453 to 221 nm. All the complexes are redox active and display the Co(III)-Co(II) couple in the potential range –0.23 to +0.09 V (vs. Ag/AgCl). The trend in these

[§] This work has been published in *Indian J. Chem*., *Sect. A*, **2003**, *42*, 2352-2358.

potential values reflects the effect of the electronic nature of the substituents on the aroyl moiety of the ligands. Cobalt(II) complexes, [CoL_2], are paramagnetic and electrically nonconducting in solutions. Variable temperature magnetic susceptibility measurements and EPR spectra reveal S = 3/2 ↔ S = 1/2 spin-crossover in both cobalt(II) complexes.

4.2. Introduction

In the previous two chapters, the complexation behaviours of diazine based ligands N,N′-bis(picolinylidene)hydrazine and N,N′-bis(salicylidene)hydrazine and its substituted derivatives have been described. The present chapter deals with the results obtained in our efforts to explore the coordination chemistry of the cobalt with another diazine containing ligand system, deprotonated aroylhydrazones of the 2-pyridinecorbaxaldehyde (HL) (Figure 4.1).

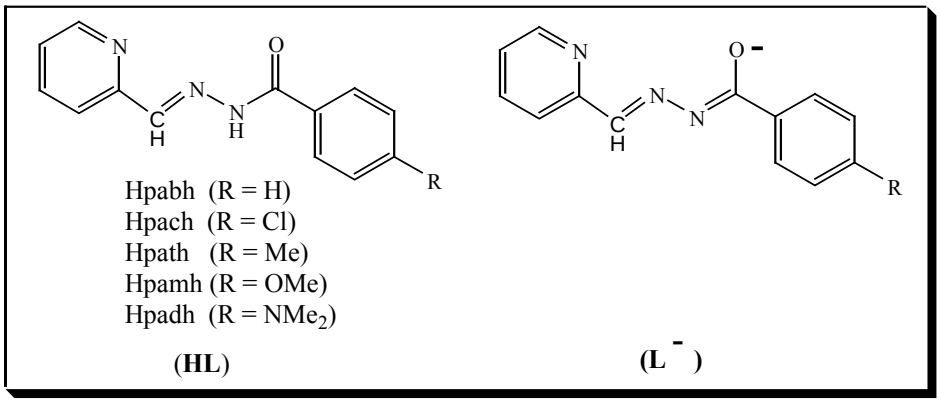

Figure 4.1

Aroylhydrazones and their metal complexes have been the subject of extensive investigations due to their wide applications in the field of pharmacology.[1] Such complexes are known as potent inhibitors of DNA synthesis, cell growth, antibacterial, antifungal and antineoplastic activities.[2-9] Apart from the biological applications, these amide containing tridentate aryolhydrazones (Figure 4.1) are of considerable interest in the areas of peroxidase catalysis,[10] and molecular electronics.[11-16]

Recently some bivalent transition metal ion complexes, $[ML_2]$ (M = Mn, Ni, Cu, Ru)[17] with HL (Figure 4.2) have been reported from our laboratory. These complexes contain the $M^{II}N_4O_2$ coordination sphere assembled via the pyridine-N, the imine-N and the deprotonated amide-O donor ligand (L^-). With this ligand system we have been able to demonstrate the following: +3 oxidation state of nickel can be accessed, subtle variation of the hexacoordinated copper(II) coordination geometry can be realised by changing the polar effect of the substituent (R), the energy separation between the metal-dπ and ligand-π* level remains constant in ruthenium(II) complexes despite the variation in the substituent polar effect.

In this chapter we describe the synthesis, structure, redox and magnetic properties of a group of cobalt(II) and cobalt(III) complexes of general formula $[CoL_2]^{0/+}$ with N-(aroyl)-N'-(picolinylidene)hydrazines (HL) ligands. Molecular structure of a representative complex has been determined by X-ray crystallography. The cobalt(II) complexes exhibit thermally induced quartet ↔ doublet spin transition.

4.3. Experimental section

4.3.1. Materials

The Schiff bases (HL) were prepared in 80-90% yield by condensation of one mole equivalent of 2-pyridinecarboxaldehyde with one mole equivalent of the corresponding aroylhydrazine in methanol.[17] All other chemicals and solvents used in this work were of reagent grade, available commercially, and were used without further purification.

4.3.2. Physical measurements

Elemental (C, H, N) analysis data were obtained with a Perkin-Elmer Model 240C elemental analyzer. Acetonitrile solutions of the cobalt(III) complexes and dichloromethane solutions of the cobalt(II) complexes were used to record the electronic spectra on a Shimadzu 3101-PC UV/vis/NIR spectrophotometer. Infrared spectra were collected by using the KBr pellets on a Jasco-5300 FT-IR spectrophotometer. Proton NMR spectra of $[Co(pabh)_2]PF_6$ and $[Co(path)_2]PF_6$ in $CDCl_3$ solutions and that of $[Co(pamh)_2]PF_6$ and $[Co(padh)_2]PF_6$ in CD_3CN solutions were recorded on a Bruker 200 MHz spectrometer using $Si(CH_3)_4$ as an internal standard. The variable temperature (10-300 K) magnetic susceptibility measurements were performed using the Faraday technique with a set-up comprising a George Associates Lewis coil force magnetometer, a CAHN microbalance and an Air Products cryostat. $Hg[Co(NCS)_4]$ was used as the standard. Diamagnetic corrections calculated from Pascal's constants,[18] were used to calculate the molar paramagnetic susceptibilities. EPR spectra were recorded on a Jeol JES-FA200 spectrometer.

Solution electrical conductivities were measured with a Digisun DI-909 conductivity meter. A CH-Instruments model 620A electrochemical analyzer was used for cyclic voltammetric experiments with dichloromethane-acetonitrile (1:1) solutions of the cobalt(III) complexes and dimethylformamide-acetonitrile (1:4) solutions of the cobalt(II) complexes containing tetrabutylammonium perchlorate (TBAP) as supporting electrolyte. The three electrode measurements were carried out at 298 K under a dinitrogen atmosphere with a glassy carbon working electrode, a platinum wire auxiliary electrode and an Ag/AgCl reference electrode. The potentials reported in this work are uncorrected for junction contributions.

4.3.3. Synthesis of complexes

$[Co(pabh)_2]PF_6$

To a methanol solution (20 cm^3) of Hpabh (200 mg, 0.88 mmol), a methanol solution (20 cm^3) of $Co(O_2CCH_3)_2{\cdot}4H_2O$ (110 mg, 0.44 mmol) was added. The mixture was stirred at room temperature in air for 4 h. The colour of the reaction mixture became dark brown. To this clear solution an aqueous solution (30 cm^3) of NH_4PF_6 (300 mg) was added with stirring. The reddish brown solid precipitated was collected by filtration, washed with water and dried under vacuum over anhydrous $CaCl_2$. The yield was 216 mg (75%).

Selected IR bands[19] (cm^{-1}) for the above complex 1605(m), 1485(s), 1460(s), 1414(s), 1379(vs), 1343(m), 1296(m), 1265(w), 1215(w), 1146(s), 1078(s), 841(vs), 737(s), 708(s), 608(w), 557(s), 517(w).

$[Co(path)_2]PF_6$, $[Co(pamh)_2]PF_6$ and $[Co(padh)_2]PF_6$ were synthesized in comparable yields by using procedures similar to the above.

Selected IR bands[19] (cm^{-1}) for these complexes are as follows:

$[Co(path)_2]PF_6$: 1609(s), 1483(s), 1431(s), 1383(vs), 1292(s), 1215(m), 1179(s), 1146(s), 1078(s), 1018(w), 837(vs), 766(m), 741(s), 679(w), 608(w), 557(s), 515(w), 484(w).

$[Co(pamh)_2]PF_6$: 1607(s), 1483(s), 1441(s), 1377(vs), 1292(w), 1258(s), 1221(m), 1169(s), 1084(s), 1026(s), 924(w), 905(m), 833(vs), 754(m), 683(w), 662(w), 602(w), 557(s), 511(m), 476(w).

$[Co(padh)_2]PF_6$: 1607(s), 1561(m), 1481(s), 1443(m), 1366(vs), 1289(m), 1223(m), 1190(s), 1153(m), 1086(s), 949(m), 895(w), 839(vs), 764(s), 694(w), 629(w), 604(w), 556(s), 503(m).

$[Co(panh)_2]$

A methanol solution (10 cm^3) of $Co(O_2CCH_3)_2{\cdot}4H_2O$ (92 mg, 0.37 mmol) was added to another methanol solution (10 cm^3) of Hpanh (200 mg, 0.74 mmol). A brown precipitate was formed immediately after mixing the two solutions. The mixture was allowed to stir for 1/2 h and the solid was collected by filtration, washed with methanol and dried in air. Yield was 184 mg (84%).

Selected IR band[19] (cm^{-1}): 1603(s), 1557(s), 1520(s), 1491(m), 1460(s), 1398(m), 1339(vs), 1163(w), 1142(s), 1105(s), 1071(s), 1011(w), 918(s), 870(m), 849(s), 777(s), 748(m), 718(s), 673(m), 638(w), 548(w), 519(s).

$[Co(pach)_2]$ was prepared similarly using Hpach instead of Hpanh. Selected IR bands[19] (cm^{-1}): 1593(s), 1555(m), 1489(s), 1454(s), 1350(vs), 1287(m), 1161(s),

1140(s), 1072(s), 1013(m), 920(m), 891(w), 851(w), 756(s), 671(w), 544(w), 484(w).

4.3.4. X-ray crystallography

Single crystals of $[Co(pamh)_2]PF_6$ were grown by diffusion of a dichloromethane solution of the complex into an overlying layer of hexane. The data were collected on an Enraf-Nonius Mach-3 single crystal diffractometer using graphite monochromated Mo Kα radiation (λ = 0.71073 Å) by ω-scan method at 298 K. Unit cell parameters were determined by the least-squares fit of 25 reflections having θ values in the range 5-11°. Intensities of 3 check reflections were measured after every 1.5 h during the data collection to monitor the crystal stability. No decay was observed in 67 h of exposure to X-ray. The ψ-scans of 2 reflections were used for an empirical absorption correction.[20] The structure was solved by direct methods and refined on F^2 by full-matrix least-squares procedures. The asymmetric unit contains a molecule of $[Co(pamh)_2]PF_6$. All non-hydrogen atoms were refined using anisotropic thermal parameters. Hydrogen atoms were placed geometrically by using a riding model and included in the structure factor calculation, but not refined. Calculations were done using the programs of WinGX[21] for data reduction and absorption correction, and SHELX-97 programs[22] for structure solution and refinement. Ortex6a[23] and Platon packages[23] were used for molecular graphics. Significant crystal data are summarized in Table 4.1. Atomic coordinates and equivalent isotropic displacement parameters are listed in the table 4.2.

Table 4.1. Crystallographic data table for $[Co(pamh)_2]PF_6$

Complex	**$[Co(pamh)_2]PF_6$**
Chemical formula	$C_{28}H_{24}N_6O_4F_6PCo$
Crystal size, mm	0.48 x 0.17 x 0.16
Formula weight	712.43
Space group	Orthorhombic, *Pnna*
a, Å	15.719(5)
b, Å	25.429(7)
c, Å	14.967(5)
α, deg.	90
β, deg.	90
γ, deg.	90
V, Å^3	5983(3)
Z	8
ρ_{calcd}, g cm^{-3}	1.582
μ mm^{-1}	0.710
Reflections collected/unique	5851/5191
Reflections $I > 2\sigma(I)$/parameters	1059
$R1$,[a] w$R2$[b] [$(I > 2\sigma(I)$]	0.0835 and 0.0904
$R1$,[a] w$R2$[b] (all data)	0.4039, 0.1658
Goodness-of-fit[c]	0.919
Largest peak, hole [e Å^{-3}]	0.711, -0.328

[a] $R1 = \sum||F_o| - |F_c||/\sum|F_o|$. [b] $wR2 = \{\sum[(F_o^2 - F_c^2)^2]/\sum[w(F_o^2)^2]\}^{1/2}$.

[c] GOF = $\{\sum[w(F_o^2 - F_c^2)^2]/(n - p)\}^{1/2}$ where 'n' is the number of reflections and 'p' is the number of parameters refined.

Table 4.2. Atomic coordinates (x 10^4) and equivalent isotropic displacement parameters ($Å^2$ x 10^3) for $[Co(pamh)_2]PF_6$

Atom	x	y	z	U(eq)
Co	3970(2)	1237(1)	1255(2)	39(1)
O(1)	4032(8)	1123(5)	-9(9)	39(4)
O(2)	734(12)	4(8)	-3771(14)	99(6)
O(3)	173(7)	1388(5)	1302(10)	40(4)
O(4)	8599(12)	2767(7	1224(14)	93(6)
N(1)	3994(11)	1150(7)	2511(11)	43(5)
N(2)	4033(10)	508(5)	1270(13)	39(4)
N(3)	3998(12)	258(7)	438(12)	49(5)
N(4)	2752(10)	1288(7)	1136(11)	45(5)
N(5)	3902(11)	1959(6)	1227(13)	47(4)
N(6)	4662(10)	2243(6)	1276(13)	46(5)
P	1392(5)	3670(3)	1359(5)	69(2)
F(1)	978(13)	3265(8)	728(14)	152(8)
F(2)	2025(12	3258(7)	1792(13)	134(7)
F(3)	696(11)	3521(7)	2088(12)	123(6)
F(4)	2093(11)	3817(7)	651(12)	123(6)
F(5)	772(11)	4101(7)	975(13)	128(7)
F(6)	1797(15)	4084(9)	2033(16)	173(9)
C(1)	4076(13)	1495(9)	3161(15)	51(6)
C(2)	4160(16)	1390(10	4072(18)	77(9)
C(3)	4154(15)	864(10)	4316(18)	66(8)
C(4)	4119(13)	490(9)	3688(17)	58(6)
C(5)	4017(15)	623(9)	2783(16)	57(7)
C(6)	4042(14)	277(9)	2032(15)	55(7)
C(7)	4009(15)	622(9)	-16+2(15)	49(6)
C(8)	3953(14	439(8)	-1124(15)	48(6)
C(9)	4112(13)	785(9)	-1778(15)	52(6)
C(10)	4052(15	624(10)	-2678(17)	63(7)
C(11)	3817(17)	-245(11)	-2217(18)	74(8)
C(13)	3754(14)	-75(9)	-1329(18)	67(7)
C(14)	2171(12)	909(8)	996(12)	38(5)
C(15)	1324(13)	995(8)	811(13)	43(6)
C(16)	1034(16)	1517(9)	827(15)	59(7)

C(17)	1621(13)	1916(9)	960(13)	50(6)
C(18)	2487(12)	1791(7)	1089(13	33(5)
C(19)	3160(13)	2176(8)	1152(15)	50(6)
C(20)	5276(13)	1896(8)	1287(17)	46(6)
C(21)	6152(12)	2100(7)	1294(15)	40(5)
C(22)	6873(13)	1797(9)	1339(16)	54(6)
C(23)	7691(15)	1982(9)	1302(17)	62(7)
C(24)	7800(14)	2523(9)	1253(18)	62(6)
C(25)	7111(16)	2859(11)	1226(19)	81(8)
C(26)	6299(15)	2656(9)	1220(18)	65(7)
C(27)	9313(17)	2427(11)	1250(20)	98(10)
C(28)	3430(20)	-526(12)	-3980(20)	133(13)

4.4. Results and discussion

4.4.1. Synthesis and some properties

The N-(aroyl)-N'-(picolinylidene)hydrazines (HL, Figure 4.2) were prepared from aroylhydrazines and 2-pyridinecarboxaldehyde. Each of them has one dissociable proton at the amide functionality. The reddish brown and dark brown complexes were synthesized under aerobic condition by reacting one mole equivalent of $Co(O_2CCH_3)_2{\cdot}4H_2O$ and two mole equivalents of HL in methanol. For Hpach and Hpanh the divalent metal complexes, $[Co(pach)_2]$ and $[Co(panh)_2]$, were precipitated from the reaction mixture due to their poor solubility. However, $[Co(pabh)_2]$, $[Co(path)_2]$, $[Co(pamh)_2]$ and $[Co(padh)_2]$ remained soluble in the reaction mixture and the trivalent metal complexes of general formula $[CoL_2]^+$ were formed. These complexes were isolated as their PF_6^- salts. For these four complexes the oxygen in air is the most likely oxidant for the oxidation of the metal ions from +2 to +3 state. Although the cobalt(III)/cobalt(II) potentials are low for all the complexes, $[Co(pach)_2]$ and $[Co(panh)_2]$ are not oxidized to the

corresponding cobalt(III) species during synthesis due to their immediate precipitation as solid from the reaction mixture.

Elemental analysis data are (Table 4.3) satisfactory with the general formulae $[Co^{II}L_2]$ (L^- = $pach^-$ and $panh^-$) and $[Co^{III}L_2]PF_6$ (L^- = $pabh^-$, $path^-$, $pamh^-$ and $padh^-$). The cobalt(III) complexes are NMR active and diamagnetic suggesting a low-spin d^6 configuration. In acetonitrile solutions, they are electrically conducting. The molar conductivity values (Table 4.3) are consistent with the 1:1 electrolytic behaviour.[24] $[Co(pach)_2]$ and $[Co(panh)_2]$ are paramagnetic and effective magnetic moments at 300 K are 4.75 and 4.49 μ_B, respectively. These values are in accordance with high-spin d^7 cobalt(II) complexes. As expected, both complexes are non-conducting in dimethylformamide solutions.

Table 4.3. Elemental analysis[a] and molar conductivity[b,c] data

Complex	%C	%H	%N	Λ_M (Ω^{-1} cm^2mol^{-1})
$[Co(panh)_2]$[b]	52.13(52.27)	2.98(3.04)	18.65(18.76))	7
$[Co(panh)_2]$[b]	53.97(54.19)	3.02(3.15)	14.43(14.58)	5
$[Co(pabh)_2]PF_6$[c]	47.51(47.87)	2.98(3.09)	12.67(12.88)	152
$[Co(path)_2]PF_6$[c]	49.15(49.43)	3.42(3.55)	12.19(12.35)	149
$[Co(pamh)_2]PF_6$[c]	47.06(47.21)	3.42(3.39)	11.64(11.80)	134
$[Co(padh)_2]PF_6$[c]	48.68(48.79)	4.15(4.09)	14.98(15.17)	145

[a] Calculated values are in parentheses, [b] in $(CH_3)_2NCHO$ and [c] in CH_3CN.

4.4.2. Infrared spectral properties

Infrared spectra of the complexes do not display the N–H and C=O stretches[25] observed for the free Schiff bases (Figure 4.2). A medium to strong band observed in the range 1593-1609 cm^{-1} is possibly due to the conjugate C=N–N=C fragment of the ligands.[17,26] Thus in each complex, the ligands are in the enolate form (L^-, Figure 4.1). The monoanionic meridionally spanning ligand can coordinate a metal ion through the pyridine-N, the imine-N, and the deprotonated amide-O atoms forming two five-membered chelate rings. This type of metal coordination by these ligands have been observed earlier for Mn(II), Ni(II), Cu(II) and Ru(II)[17] complexes. X-ray structure of $[Co(pamh)_2]PF_6$ confirms this mode of coordination by L^- in the present series of complexes. The $[CoL_2]PF_6$ complexes display a very strong peak ascribable to the PF_6^- anion in the range 833-841 cm^{-1}.

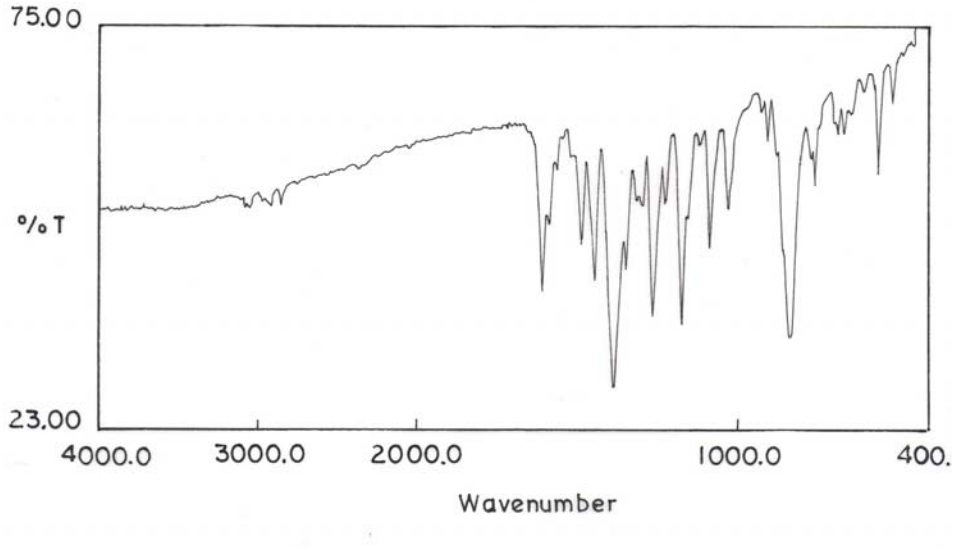

Figure 4.2. Infrared spectrum of $[Co(pamh)_2]PF_6$ in KBR disk

4.4.3. NMR spectral properties

The proton NMR spectra of the cobalt(III) complexes clearly suggest that, both ligands in each complex are magnetically equivalent in solution. Significant data are summarized in Table 4.4. The spectrum of $[Co(pabh)_2]PF_6$ in $CDCl_3$ is shown in Figure 4.3. The aromatic protons are observed in the range 6.76-8.14 δ. The azomethine proton is observed as singlet within 9.06-9.20 δ. The methyl protons of $[Co(path)_2]PF_6$, $[Co(pamh)_2]PF_6$ and $[Co(padh)_2]PF_6$ appear as singlet at 2.36, 3.80 and 3.15 δ, respectively.

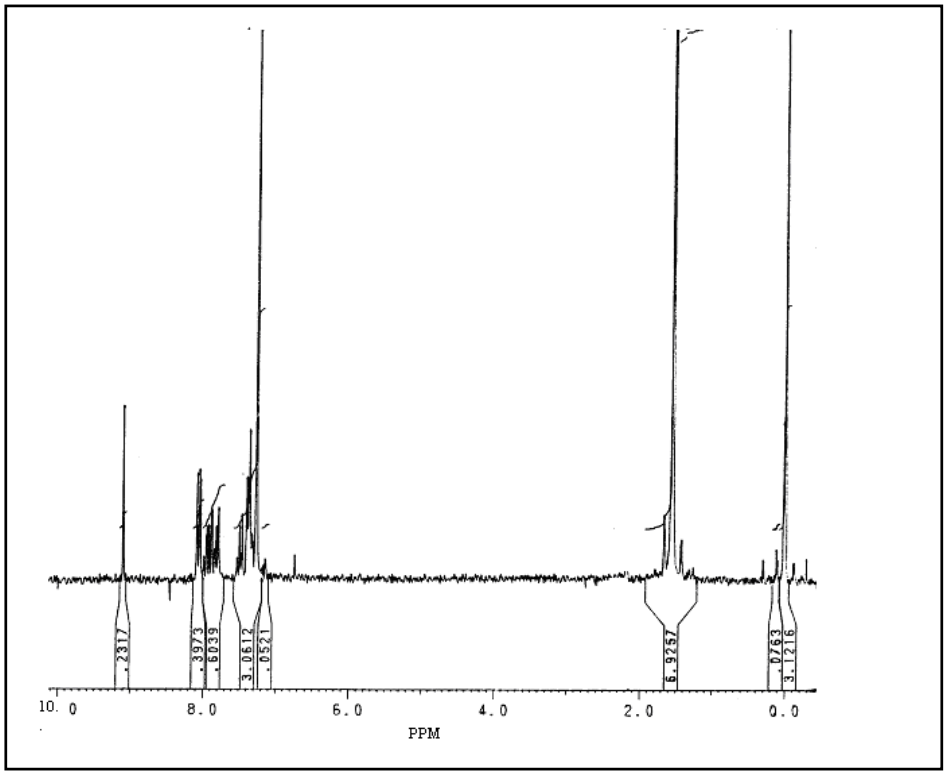

Figure 4.3. ^1H NMR spectrum of $[Co(pabh)_2]PF_6$ in $CDCl_3$.

Table 4.4. ^{1}H NMR spectral data (δ) in $CDCl_3$

Complex	Aromatic protons, δ	HC=N, δ	CH_3 Protons,δ
$[Co(pabh)_2]PF_6$	7.2-8.7 (m)	9.12(s)	–
$[Co(path)_2]PF_6$	7.2-8.6 (m)	9.06(s)	2.36
$[Co(pamh)_2]PF_6$	6.9-8.7 (m)	9.15(s)	3.80
$[Co(padh)_2]PF_6$	7.1-8.6 (m)	9.20(s)	3.15

s = singlet; m= multiplet.

4.4.4. Electronic spectral properties

The electronic spectral data of all the complexes are listed in Table 4.5. The spectral profiles of $[Co(pach)_2]$ and $[Co(panh)_2]$ are very similar. Two strong absorptions are observed near 380 and 270 nm (Figure 4.4). The spectral profiles of the cobalt(III) complexes are also similar but different when compared to that of cobalt(II) complexes (Figure 4.4). The cobalt(III) complexes display several strong peaks and shoulders in the range 453-221 nm. These absorptions are most likely due to ligand-to-metal charge transfer and intraligand transitions. In general, there is a red shift of band positions as the substituents on the aroyl fragment of the ligands become better electron releasing. Such a low energy shift effected by the electron releasing substituents on the ligands has been observed before for some Mn(IV)/(II), Fe(III), Ni(II) and Cu(II) complexes.[17,27]

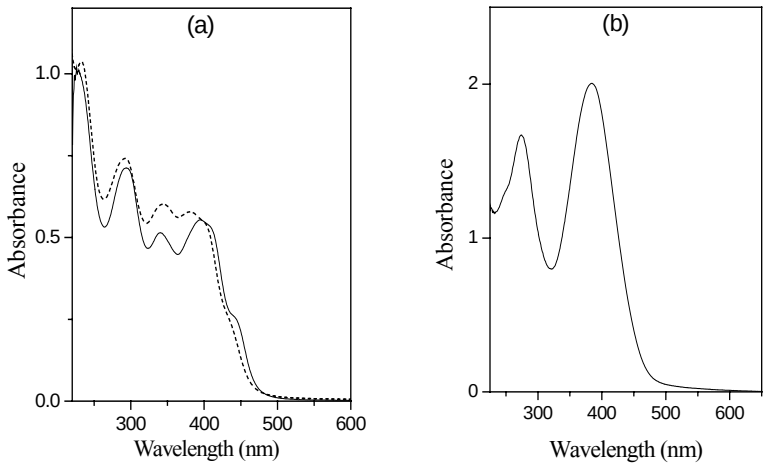

Figure 4.4. Electronic spectra of (a) $[Co(pabh)_2]PF_6$ (–) and $[Co(pamh)_2]PF_6$ (·····) in CH_2Cl_2 and (b) $[Co(panh)_2]$ in N,N′dimethylformamide.

Table 4.5. Electronic spectral and molar conductivity data

Complex	λ_{max} (nm) (ε ($M^{-1}cm^{-1}$))	$E_{1/2}$,V (ΔE_p), mV
$[Co(panh)_2]$	385(40200), 273(33491)	0.09 (70)
$[Co(pach)_2]$	376(37700), 271(22600), 247(22200)	0.03 (70)
$[Co(pabh)_2]PF_6$	436 ^{sh} (3900), 401^{sh}(18700),383(19700), 332(17500), 282(27800), 270 ^{sh} (39900)	-0.10 (70)
$[Co(path)_2]PF_6$	437 (9200), 403 ^{sh} (21600),381(23200), 343(24300), 293(29400), 233(42300)	-0.15 (70)
$[Co(pamh)_2]PF_6$	438^{b}(14100), 417 ^{sh}(31900),378(34252), 299(25100), 241(41400)	-0.17 (60)
$[Co(padh)_2]PF_6$	453(84600), 302(27200), 250 ^{sh} (21900), 221(34500)	-0.23 (70)

$Co[L_2]$ in dimethylformamide, $Co[L_2]PF_6$ in acetonitrile and ^{Sh}Shoulder.

4.4.5. Electrochemical properties

The redox properties of the complexes have been investigated using cyclic voltammetry. The relevant data are listed in Table 4.5 and a representative cyclic voltammogramms are shown in Figure 4.5. Each complex displays a well-defined one electron nearly reversible response. The one electron stoichiometry of these responses was validated by comparing the current heights with known one electron redox processes under identical conditions.[28] For the cobalt(III) complexes, $[CoL]PF_6$, this response is found to be a reduction response. On the other hand, for the cobalt(II) complexes, $[CoL_2]$, the observed response is due to

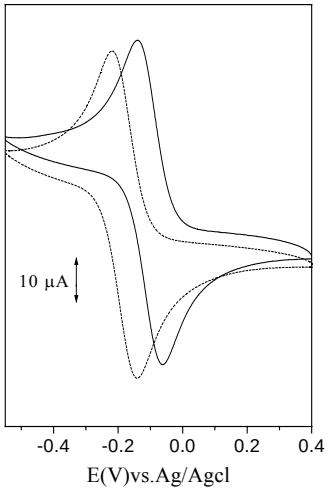

Figure 4.5. Cyclic voltammograms (scan rate 100 mVs^{-1}) of ~10^{-3} M solutions of $[Co(pabh)_2]PF_6$ (–) and $[Co(pamh)_2]PF_6$ (·····) in CH_2Cl_2-CH_3CN (1:1) mixture (0.1 M TBAP) at a glassy carbon electrode (298 K).

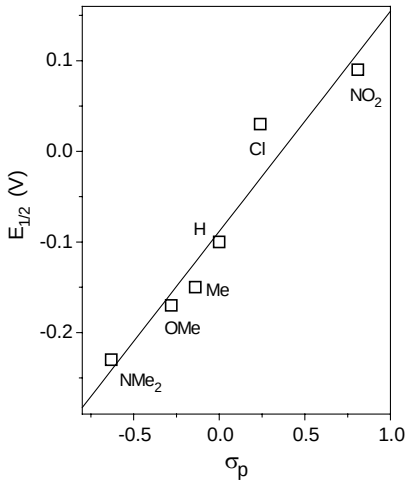

Figure 4.6. Correlation between the $E_{1/2}$ values for Co(III)/Co(II) couple and the Hammett substituent constants. The straight line represents a linear least-squares fit.

an oxidation process. These responses are assigned to the cobalt(III)-cobalt(II) couple ($[Co^{III}L_2]^+ + e^- \rightleftharpoons [Co^{II}L_2]$). The $E_{1/2}$ values for this couple are sensitive to the substituents at the *para* position of the aroyl fragment of the ligands. These values show an anodic shift with the increase of electron withdrawing ability of the substituents (Table 4.5). A satisfactory linear correlation has been observed (Figure 4.6), when the $E_{1/2}$ values are plotted against the Hammett substituent constants (σ_p).[29]

4.4.6. Magnetic properties of the cobalt(II) complexes

The magnetic susceptibility measurements with powdered samples of the cobalt(II) complexes were performed in the temperature range 15–300 K at a constant magnetic field of 5 kG. The effective magnetic moments at 300 K of

$[Co(pach)_2]$ and $[Co(panh)_2]$ are 4.75 and 4.49 μ_B, respectively (Figure 4.7). The moment of $[Co(panh)_2]$ decreases slowly to 4.24 μ_B at 101 K. Below 101 K the moment decreases more markedly and reaches a value of 3.95 μ_B at 15 K. This gradual decrease of the magnetic moment values for $[Co(panh)_2]$ with the lowering of temperature (Figure 4.7) can be accounted for by either of the following two possibilities : continuous high-spin (S = 3/2) to low-spin (S = 1/2) conversion or spin-orbit coupling.[30] The EPR results corroborate the former possibility. On the other hand, the moment of $[Co(pach)_2]$ decreases gradually to a value of 4.34 μ_B at 140 K. Below 140 K the decrease in the moment is more rapid and becomes 3.91 μ_B at 100 K. After 100 K there is again a gradual and continuous drop of the moment (Figure 4.7). At 15 K the magnetic moment is 3.29 μ_B. This magnetic behaviour of $[Co(pach)_2]$ is indicative of an incomplete thermally induced spin transition from S = 3/2 to S =1/2.[31]

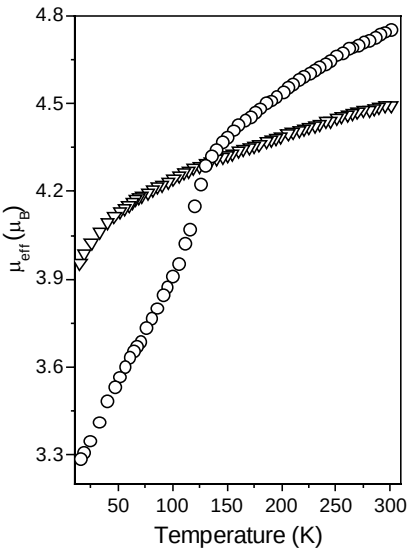

Figure 4.7. Effective magnetic moments as a function of temperature For $[Co(pach)_2]$ (O) and $[Co(panh)_2]$ (∇).

4.4.7. EPR spectral properties of the cobalt(II) complexes

The X-band EPR spectral characteristics of $[Co(pach)_2]$ and $[Co(panh)_2]$ provide clear evidence for the spin-crossover in both complexes (Figure 4.8). At room temperature (298 K) none of the complexes, in powder phase displays any signal in the EPR spectra. However, each of the two complexes displays a broad asymmetrical signal ($g = 2.07$ for $[Co(panh)_2]$ and $g = 2.06$ for $[Co(pach)_2]$) at low temperature (103 K). The spectral profiles are very similar except that the very weak absorption at $g \sim 2.4$ is relatively more prominent for $[Co(pach)_2]$ (Figure 4.8). From the magnetic susceptibility data it is very clear that for both complexes at 103 K the fraction of the high-spin form is very high compared to that of the low-spin form. However, none of the EPR spectra display any signal in the low-field region normally associated with the high-spin cobalt(II) complexes.[31b-d] Generally high-spin cobalt(II) complexes are EPR active only at very low temperature due to fast spin-lattice relaxation. Thus the observed powder spectral features of both complexes at 103 K are most likely associated with the low-spin cobalt(II) species. The EPR spectra of the complexes in frozen (103 K) solutions prove conclusively the existence of low-spin cobalt(II) species. In each case, an axial spectrum is observed (Figure 4.8). The $g_{\|}$ and $g_{\perp}$ values are: 2.25 and 2.02 for $[Co(pach)_2]$ and 2.26 and 2.01 for $[Co(panh)_2]$. In both spectra, the $g_{\|}$ signal shows the ^{57}Co hyperfine structure. In each case, the average hyperfine splitting constant ($A_{\|}$) obtained is 106 G. This type of axial spectrum is typical for tetragonally compressed octahedral low-spin d^7 species.[31b,32] Such tetragonal compression is not unusual in bis complexes with rigid tridentate meridionally spanning ligands.[17, 33]

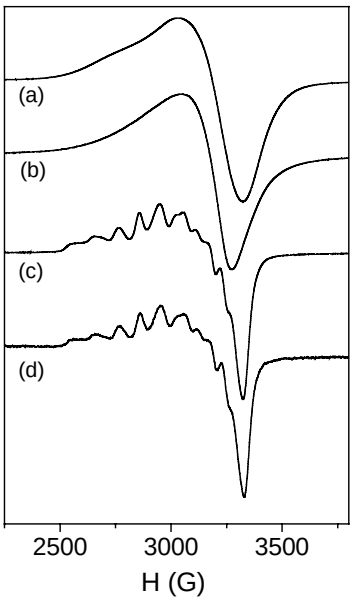

Figure 4.8. X-band EPR spectra at 103 K of (a) polycrystalline $[Co(pach)_2]$, (b) polycrystalline $[Co(panh)_2]$, (c) frozen dimethylformamide-toluene (1:1) solution of $[Co(pach)_2]$ and (d) frozen dimethylformamide solution of $[Co(panh)_2]$.

Although EPR spectra clearly indicate the presence of the low-spin form of both complexes at 103 K, the solid state moment versus temperature curves (Figure 4.7) suggest that the high-spin character of $[Co(panh)_2]$ is more than that of $[Co(pach)_2]$ over the temperature range 15–300 K. This is most likely the consequence of the less ligand field strength of $panh^-$ compared to that of $pach^-$. The difference in the polar effects of the nitro and chloro substituents is possibly the major reason for the variation in the ligand field strengths of $panh^-$ and $pach^-$.

4.4.8. Molecular structure of $[Co(pamh)_2]PF_6$

The crystal structure of one of the cobalt(III) complexes has been illustrated in Figure 4.9. The selected bond parameters associated with the metal ion are listed in Table 4.6. The structure of $[Co(pamh)_2]PF_6$ consists of discrete $[Co(pamh)_2]^+$ cations and PF_6^- anions The cobalt(III) center is in a distorted octahedral N_4O_2 coordination sphere assembled via the tridentate meridionally spanning pyridine-N, imine-N and deprotonated amide-O donor ligands. The average N–N, N–C and C–O distances in the =N–N=C(O^-)- fragments of the ligands are 1.397, 1.325 and 1.294 Å, respectively. These distances are consistent with the enolate form of the amide functionalities in both ligands.[17] The chelate bite angles of all the five-membered rings are very similar and in the range 81.7(5)-83.2(6)^o. The bond angle (179.7(6)^o) at the metal center involving the imine-N atoms which are mutually *trans* to each other is very close to the ideal value of 180^o. The large deviations of the other two *trans* bond angles (163.3(4) and 164.6(4)^o) from the ideal value reflect the rigidity of the tridentate ligand. The Co–$N_{pyridine}$, the Co–N_{imine} and the Co–O_{amide} bond lengths are comparable with the corresponding bond lengths reported for a cobalt(III) complex having the similar coordinating atoms.[34] The Co(III)–$N_{pyridine}$ bond lengths are significantly longer than the Co(III)–N_{imine} bond lengths. The rigidity of the tridentate ligand and better π-backbonding in the Co(III)–N_{imine} bond than that in the Co(III)–$N_{pyridine}$ bond are possibly responsible for this difference.[17,33]

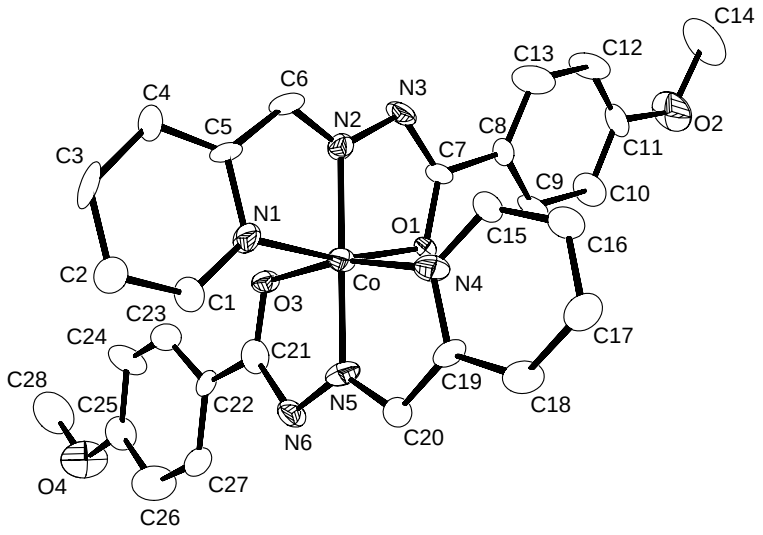

Figure 4.9. The structure of $[Co(pamh)_2]^+$ with the atom-labeling scheme. Hydrogen atoms are omitted for clarity.

Table 4.6. Selected bond distances (Å) and angles (°) for $[Co(pamh)_2]PF_6$

Co-O(1)	1.927(9)	Co-O(3)	1.908(7)
Co-N(1)	1.930(11)	Co-N(2)	1.854(9)
Co-N(4)	1.940(10)	Co-N(5)	1.851(10)
O(1)-Co-O(3)	90.7(4)	O(1)-Co-N(1)	163.3(4)
O(1)-Co-N(2)	81.8(5)	O(1)-Co-N(4)	88.4(5)
O(1)-Co-N(5)	98.3(5)	O(3)-Co-N(1)	89.7(5)
O(3)-Co-N(2)	98.6(4)	O(3)-Co-N(4)	164.6(4)
O(3)-Co-N(5)	81.7(5)	N(1)-Co-N(2)	81.7(5)
N(1)-Co-N(4)	95.5(6)	N(1)-Co-N(5)	98.3(6)
N(2)-Co-N(4)	96.4(5)	N(2)-Co-N(5)	179.7(6)
N(4)-Co-N(5)	83.2(6)		

4.4.9. One-dimensional helical self-assembly of $[Co(pamh)_2]^+$

In the crystal lattice, self-assembly of the complex cations *via* C–H···N interactions leads to a one-dimensional helical superstructure (Figure 4.10). In this one-dimensional arrangement, each cation participates in four C–H···N interactions involving the *ortho* C–H (C1–H1) and the *meta* C–H (C16–H16) groups of the two metal coordinated pyridine rings and the two deprotonated and uncoordinated amide N-atoms (N3 and N6). It is connected to one adjacent neighbor by a pair of reciprocal C1–H1···N6 bridges and with the other adjacent neighbor by another pair of reciprocal C16–H16···N3 bridges. The C1···N6 and C16···N3 distances are 3.41 3.28 Å, respectively. The C1–H1···N6 and C16–H16···N3 angles are 134 and 142°, respectively. These values are comparable with the values reported in literature for C–H···N interactions.[35] The helices thus formed are parallel to each other and propagate along the crystallographic *b*-axis. The counter anions (PF_6^-) are not involved in any non-covalent interactions. In the crystal lattice, they are placed in the space between the parallel helices.

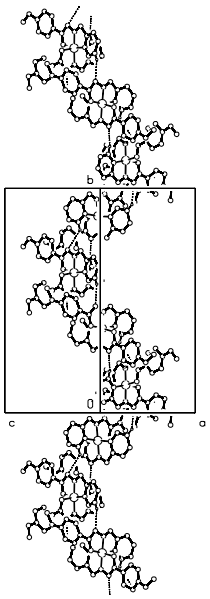

(a)

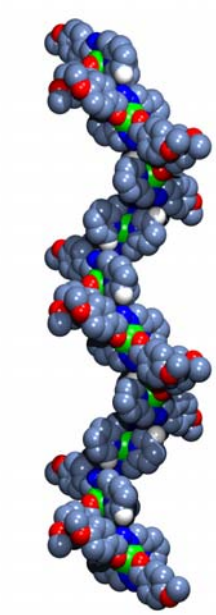

(b)

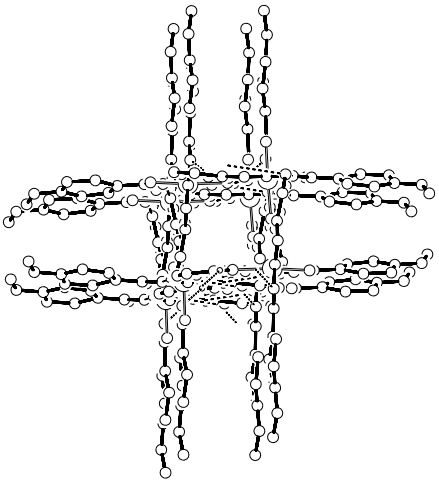

(c)

Figure 4.10. One-dimensional helical arrangement of $[Co(pamh)_2]^+$. (a) Ball and stick model and (b) space-filling model viewed perpendicular to the *b*-axis. (c) The channel through the helix viewed parallel to the *b*-axis.

4.5. Conclusion

In this chapter, a series of new mononuclear Co(II) and Co(III) complexes ($[CoL_2]^{0/+}$) with N,N,O-donor N-(aroyl)-N'-(picolinylidene)hydrazines (HL) has been described. The complexes were characterized with the help of analytical, magnetic, spectroscopic, electrochemical and X-ray crystallographic techniques. In solutions, electronic spectral features and redox properties of the complexes are strongly influenced by the polar effects of the substituents on the ligands. X-ray structure of one of the complexes reveals that the metal ion is in distorted octahedral N_4O_2 coordination sphere, consisted by the two meridionally spanning pyridine-N, imine-N and deprotonated amide-O donor ligands. Cryomagnetic and EPR spectral studies indicate the S = 3/2 $\leftrightarrow$ S = 1/2 spin-crossover in the Co(II) complexes.

4.6. References

1. J. R. Merchant, D. S. Clothia, *J. Med. Chem.*, **1970,** *13,* 335. (b) D. Richardson, E. Baker, P. Ponka, P. Wilairat, M. L. Vitolo, J. Webb, *Thalassemia: Pathohysiology and management*, *Part B*, eds. S. Fucharoen, P. T. Rowley, N. W. Paul, *R. Alan. Liss, New York*, **1988**, 81.
2. (a) J. C. Craliz, J. C. Rub, D. Willis, J. Edger, *Nature*, **1955,** *34,* 176. (b) L. Pickart, W. H. Goodwin, W. Burgua, T. B. Murphy, D. K. Johnson, *Biochem. Pharmacol.*, **1983**, *32*, 3868.
3. (a) N. Nawar, M. A. Khattab, N. M. Hosny, *Synth. React. Inorg. Met. Org. Chem*., **1999**, *28,* (8), 1365. (b) R. C. Sharma, J. Ambwani, V. K. Varshney, *J. Indian Chem. Soc*., **1992**, *69*, 770.
4. Z. H. Chohan, *Synth. React. Inorg. Met. Org. Chem*., **2001,** *31,* 1, 116.
5. A. Gürsoy, N. Terzioglu G. J. Otuk, *Med. Chem*., **1997**, *32*, 753.

6. D. B. Levejoy, D. R. Richardson, *Expert Opin. Investig. Drugs,* **2000**, *9*, 6, 1257.
7. D. Van Reyk, S. Sarel, N. Hunt, *Biochem. Pharmacol*., **2000,** *60,* 4, 581.
8. (a) D. Negoiu, M. Calinescu, A. Emandi, E. Badau, Russ. *J. Coord. Chem*., **1999**, *25*, 1, 36. (b) N. K. Singh, N. Agrawal, R. C. Aggarwal, *Indian. J. Chem.,* **1984**, *23A,* 1011.
9. (a) D. R. Richardson, C. Mouralian, P. Ponka, E. R. Richardson, *J. Lab. Clin. Med.,* **1999**, *134*, 510. (c) D. R. Richardson, E. Becker, P. V Bernhardt, *Acta Crystallogr., Sect. C,* **1999**, *55*, 2102. (d) E. Becker, D. R. Richardson, *The International Journal of Biochemistry & Cell Biology*, **2001**, *33,* 1. (e) P. V. Bernhardt, P. Chin, D. R. Richardson, *J Bio. Inorg. Chem.,* **2001**, *6,* 801.
10. R. Malhottra, S. Kumar, Jyoti, H. R. Singal, K. S. Dhindsa, *Indian Journal of Chemistry*, Sec., *A,* **2000**, *39,* 421.
11. J. Hou, L. Chen, X. Tang, W. H. Sun,. *Gaofenzi Xuebao.,* **2004**, *5*, 754.
12. (a) O. Kahn, J. C. Martinez, *Science,* **1998**, *279*, 44. (b) M. Irie, *Chem. Re*V*.,* **2000**, *100*, 1685. (c) M. E. Itkis, X. Chi, A. W. Cordes, R. C. Haddon, *Science,* **200**2, *29*6, 1443. (d) M. Irie, T. Fukaminato, T. Sasaki, N. Tamai, T. Kawai, *Nature,* 2002, *42*0, 759. (e) J. S. Miller, *Angew. Chem., Int. Ed.,* **2003**, *42,* 27.
13. (a) P. Gutlich, *Struct. Bonding,* **1981**, *15,* 181. (b) E. Konig, *Struct. Bonding,* **1991**, *7*6, 51. (c) O. Kahn, *Molecular Magnetism*, *VCH Publishers: New York*, **1993**. (d) P. Gutlich, A. Hauser, *Coord. Chem. Rev*., **1990**, 97,1.
14. (a) P. Gütlich, A. Hauser, H. Spiering, *Angew. Chem., Int. Ed. Engl*., **1994,** *33,* 2024. (c) E. König, *Prog*. *Inorg. Chem.,* **1987**, *5,* 527. (b) H. Toftlund, *Coord. Chem. Rev*., 1989, *67*, 108. (c) J. F. Létard, P. Guinneau, L. Rabardel, J. A. K. Howard, A. E. Goeta, D. Chasseau, O. Kahn, *Inorg. Chem*., **1998,** *37*, 4432. (d) C. Roux, J. Zarembowitch, B. Gallois, T.

Granier, R. Claude, *Inorg. Chem*., **1994,** *33,* 2273. (e) M. L. Boillot, C. Roux, J. P. Audiére, A. Dausse, J. Zarembowitch, *Inorg. Chem*., **1996**, *35,* 3975. (f) M. L. Boillot, S. Chantraine, J. Zarembowitch, J. Y. Lalle-mand, J. Prunet, *New J. Chem*., **1999**, *21,* 79. (g) M.L. Boillot, H. Soyer, *New J. Chem*., 1997, *21,* 889. (h) A. Sour, M. L. Boillot, E. Riviére, P. Lesot, *Eur. J. Inorg. Chem.,* **1999**, 2117. (i) M. D. Timken, A. M. Abdel-Mawgoud, D. N. Hendrickson, *Inorg. Chem*., **1986**, *25,* 160.

15. (a) J. Zarembowitch, *New J. Chem.,* **1992**, *16,* 255. (b) B. J. Kennedy, G. D. Fallon, B. M. K. C. Gatehouse, K. S. Murray, *Inorg. Chem.,* **1984**, *23,* 580. (c) K. S. Murray, R.M. Sheahan, *J. Chem. Soc., Dalton Trans.,* **1976**, 999. (d) A. L. Nivorozhkin, H. Toflund, M. Nielsen, *J. Chem. Soc., Dalton Trans.,* **1994** 361. (e) J. Faus, M. Julve, F. Lloret, J. A. Real, J. Sletten, *Inorg. Chem.*, **1994,** *33,* 5535.
16. (a) X. Xiaoming, M. Haga, T. M. Inoue, Y. Ru, A. W. Addison, *J. Chem. Soc., Dalton Trans*. **1993**, 2477. (b) D. J. Hathcock, K. Stone, J. Madden, S. J. Slattery, *Inorg. Chim. Acta.,* **1998**, *282,* 131. (c). S. J. Slattery, N. Gokaldas, T. Mick, K. A. Goldsby, *Inog. Chem.,* **1994**, *33,* 3621. (e) M. Haga, T. M. Ionue, K. Shimizu, G. P. Sato, *J. Chem. Soc., Dalton Trans*., **1989**, 371. (f) P. Gutlich, A. Hauser, H. Hartmut, *Angew. Chem., Int. Ed. Engl*., **1994,** *33*, 2024.
17. (a) A. Choudhury, B. Geetha, N. R. Sangeetha, V. Kavitha, V. Susila, S. Pal, *J. Coord. Chem.*, **1999**, *48,* 87. (b) G V. Karunakar, N. R. Sangeetha, V. Susila, S. Pal, *J. Coord. Chem.*, **2000**, *50,* 51. (c) S. N. Pal, J. Pushparaju, N. R. Sangeetha, S.Pal, *Trans. Met. Chem.*, **2000**, *25*, 529. (d) S. N. Pal, S. Pal, *J. Chem. Soc.*, *Dalton Trans*., **2002,** 2102.
18. W E. Hatfield, *Theory and applications of molecular paramagnetism*, eds. E. A. Boudreaux, L. N. Mulay, *John Wiley and Sons, New York*, **1976,** 491.
19. Symbols: vs, very strong; s, strong; m, medium; w, weak.

20. A. C. T. North, D. C. Philips, F. S. Mathews, *Acta Crystallogr., Sect A*, **1968**, *24,* 351.
21. L. J. Farrugia, *J. Appl. Crystallogr.*, **1999**, *32,* 837.
22. G. M. Sheldrick, *SHELX-97 Structure Determination Software*, University of Göttingen, Göttingen, Germany, **1997**.
23. (a) P. McArdle, *J. Appl. Crystallogr.*, **1995**, *28,* 65. (b) A. L. Spek, *PLATON*, A Multipurpose Crystallographic Tool, Utrecht University, Utrecht, The Netherlands, **2002**.
24. W. J. Geary, *Coord. Chem. Rev.*, **1971**, 7, 81.
25. (a) W. Kemp, Organic spectroscopy, Macmillan, Hampshire, **1987**, pp. 62. (b) K. Nakamoto, *Infrared and Raman spectra of inorganic and coordination compounds,* John Wiley and Sons, New York, **1986,** pp. 241-244.
26. L. El-Sayed, M. F. Iskander, *J. Inorg. Nucl. Chem.*, **1971**, *33,* 435.
27. (a) A. V. Lakshmi, N. R. Sangeetha, S. Pal, *Indian. J. Chem.*, **1997**, *36A,* 844. (b) N. R. Sangeetha, S. Pal, *J. Coord. Chem.*, **1997**, *42,* 157. (c) R. N. Mukherjee, O. A. Rajan, A. Chakravorty, *Inorg. Chem.*, **1982**, *21,* 785.
28. S. Pal, D. Bandyopadhyay, D. Datta, A. Chakravorty, *J. Chem. Soc.*, *Dalton Trans.*, **1985**, 159.
29. J. March, *Advanced Organic Chemistry*, John Wiley and Sons, New York, 4th ed., **1992**, p. 280.
30. L. Banci, A. Bencini, C. Benelli, D. Gatteschi, C. Zanchini, *Struct. Bonding, Berlin*, **1982**, *52,* 37.
31. (a) M. G. Simmons, L. J. Wilson, *Inorg. Chem.*, **1977**, *16,* 126. (b) S. Kremer,W. Henke, D. Reinen, *Inorg. Chem.*, **1982**, *21,* 3013. (c) J. Zarembowitch, O. Kahn, *Inorg. Chem.*, **1984**, *23,* 589. (d) P. Thuéry, J. Zarembowitch, *Inorg. Chem.*, **1986**, *25*, 2001. (e) A. B. Gaspar, M. C. Muñoz, V. Niel, J. A. Real, *Inorg. Chem.*, **2001**, *40,* 9.

32. (a) A. Bencini, L. Fabbrizzi, A. Poggi, *Inorg. Chem.*, **1981**, *20*, 2544. (b) S. Mukhopadhyay, D. Ray, *J. Chem. Soc.*, *Dalton Trans.*, **1995**, 265.
33. G. D. Storrier, S. B. Colbran, D. C. Craig, *J. Chem. Soc.*, *Dalton Trans.*, **1997**, 3011.
34. L. P. Battaglia, P. G. Berzollo, A. B. Corradi, C. Pelizzi, *J. Crystallogr. Spectrosc. Res.*, **1993**, *23,* 973.
35. G. R. Desiraju; T. Steiner, In *The Weak Hydrogen Bond in Structural Chemistry and Biology*; Oxford University Press, Oxford, **1999**.

Chapter 5

Novel Carboxylate-Free Trinuclear μ_3-oxo-centered M(III) {M = Mn, Fe} Complexes Containing Distorted Pentagonal–Bipyramidal Metal Centers[§]

5.1. Abstract

The reactions of metal perchlorates, $Mn(ClO_4)_2 \cdot 6H_2O$ and $Fe(ClO_4)_3 \cdot 6H_2O$ and 1,2-bis(biacetylmonoximeimino)ethane (H_2bamen) in the presence of triethylamine (1:1:2 mole ratio) in methanol afford the trinuclear complexes having the general formula $[M(\mu_3\text{-}O)(\mu_3\text{-bamen})_3]ClO_4 \cdot 2H_2O$, [M = Mn, Fe]. The structure of each of the two complexes shows a symmetric planar central $\{M_3(\mu_3\text{-}O)\}^{7+}$ unit, coordinated to three N_4O_2 donor bridging (*via* oximate groups) ligands ($bamen^{2-}$). The N_4O_3 coordination sphere around each metal center is very close to pentagonal-bipyramidal. Four N-atoms of one $bamen^{2-}$ and the oxo group satisfy five coordination sites and form a pentagonal plane around the metal ion. The axial sites are occupied by two oximato O-atoms from the other two $bamen^{2-}$. Thus in addition to the μ_3-oxo group, two oximate groups provide two additional bridges between each pair of metal centers. In the crystal lattice of both complexes, the water molecules exist as hydrogen bonded dimers and these water dimers and the perchlorate ions form a hydrogen bond supported helix. The complex cations form a chain *via* C–H···O interactions involving a methyl group and a metal coordinated oximato O-atom. The helix of $\{(H_2O)_2ClO_4^-\}$ units and

[§] This work has been published in *Inorg. Chem.*, **2002**, *41*, 4843–4845 and *Eur. J. Inorg. Chem.*, **2004**, 4718-4723.

the chain of $[M_3O(bamen)_3]^+$ are connected by O–H···O interactions that involve a water molecule and a second oximato O-atom. In cyclic voltammetry, the complexes display the metal centered redox responses. Variable temperature magnetic susceptibility measurements reveal the presence of a ferromagnetic interaction (J = 22.3(1) cm^{-1}) between the manganese(III) in $[Mn_3O(bamen)_3]ClO_4{\cdot}2H_2O$ centers and an antiferromagnetic interaction (J = –41.0(2) cm^{-1}) between the iron(III) metal centers in $[Fe_3O(bamen)_3]ClO_4{\cdot}2H_2O$.

5.2. Introduction

In the previous chapters we have described the coordination chemistry of Mn, Fe and Co with diazine ligands N,N′-bis(picolinylidene)hydrazine, N,N′-bis(salicylidene)hydrazine and one of its substituted analogue and deprotonated N-(aroyl)-N'-(picolinylidene)hydrazines. In this chapter, we have used a dioxime Schiff base (H_2bamen, two H represent the dissociable oxime protons) derived from one mole equivalent of ethylenediamine and two mole equivalents of biacetylmonoxime, to explore the chemistry of Mn and Fe. The oxime containing ligands are known to stabilize the higher oxidation states of metal ions through the strong L $\rightarrow$ M σ- donation.[1] Such ligands also have the capability to produce complexes containing more than one metal ion which are bridged by the oximate function.[2] We have been able to isolate trinuclear complexes of formula $[M_3(\mu_3\text{-}O)(\mu_3\text{-}bamen)_3]ClO_4{\cdot}2H_2O$ (M = Mn and Fe) using H_2bamen (Figure 5.1).

The trinuclear μ_3-oxo-bridged transition metal ion complexes have been of considerable interest for their molecular structures, magnetic properties and

intramolecular electron transfer features of the mixed-valent variety. Such complexes are also useful precursors for the synthesis of higher nuclearity metal clusters. A number of complexes containing this $\{M_3(\mu_3\text{-}O)\}$ unit have been reported.[3-13] Essentially in all of them the triangular metal ion core with the central oxo bridge is stabilized by six carboxylates (RCO_2^-) and three monodentate ligands (L). In these complexes of general formula $[M_3(\mu_3\text{-}O)(\mu_2\text{-}O_2CR)_6L_3]^{0/+}$, each metal ion is in a distorted octahedral coordination sphere. The O-atoms of the bridging carboxylates constitute an O_4 square plane and the μ_3-O and the monodentate ligand L occupy the remaining two *trans* sites. The central $\{M_3(\mu_3\text{-}O)\}$ core is usually planar and close to 3-fold symmetry. Complexes of $\{M_3(\mu_3\text{-}O)\}$ without carboxylate ligands are scarce. A few mixed-ligand complexes of this type are known.[14,15] However, in these complexes the $\{M_3(\mu_3\text{-}O)\}$ unit is asymmetric and pyramidal.

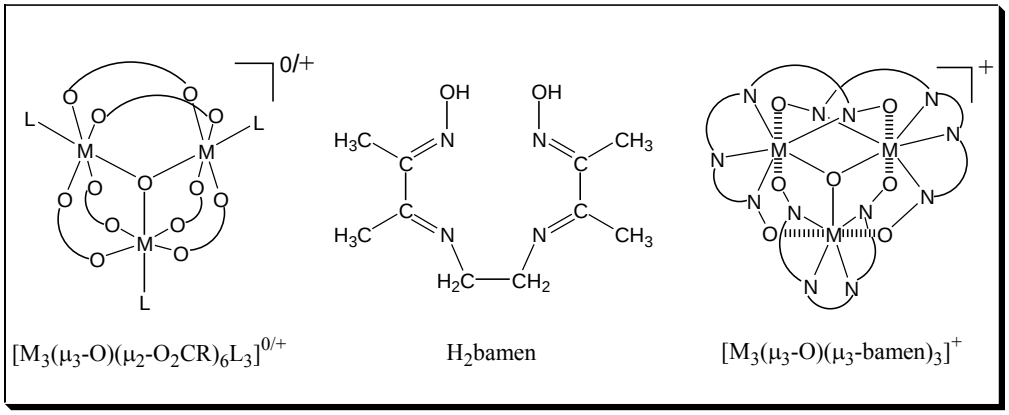

$[M_3(\mu_3\text{-}O)(\mu_2\text{-}O_2CR)_6L_3]^{0/+}$ H_2bamen $[M_3(\mu_3\text{-}O)(\mu_3\text{-bamen})_3]^+$

Figure 5.1

The complex cations, $[M_3(\mu_3\text{-}O)(\mu_3\text{-}bamen)_3]^+$ (M = Mn and Fe) described in this chapter are very original with respect to the known complexes containing the $\{M_3(\mu_3\text{-}O)\}$ core. Here the trianglular ensemble of the metal ions with the central oxo-bridge is stabilized without any carboxylate and each of the three metal ions is in distorted pentagonal-bipyramidal N_4O_3 coordinated sphere (Figure 5.1). In the following account, we have described the synthesis, characterization, X-ray crystal structures, electrochemical and magnetic properties of these two novel complexes.

5.3. Experimental section

5.3.1. Materials

The Schiff base H_2bamen was obtained in 90% yield by reacting two mole equivalents of biacetylmonoxime and one mole equivalent of ethylenediamine in methanol followed by recrystallization from the same solvent as reported procedure.[16] All other chemicals and solvents used in this work were of analytical grade available commercially and were used without further purification.

5.3.2. Physical measurements

Microanalytical (C, H, N) data were obtained with a Perkin-Elmer Model 240C elemental analyzer. A Shimadzu 3101-PC UV/vis/NIR spectrophotometer was used to record the electronic spectra. Infrared spectra were collected by using

KBr pellets on a Jasco-5300 FT-IR spectrophotometer. The variable temperature (18–300 K) magnetic susceptibility measurements were performed using the Faraday technique with a set-up comprising a George Associates Lewis coil force magnetometer, a CAHN microbalance and an Air Products closed-cycle helium cryostat. $Hg[Co(NCS)_4]$ was used as the standard. Diamagnetic corrections (-411×10^{-6} and -468×10^{-6} emu mol^{-1} for $[Mn_3O(bamen)_3]ClO_4 \cdot 2H_2O$ and $[Fe_3O(bamen)_3]ClO_4 \cdot 2H_2O$ respectively), calculated from Pascal's constants[17] were used to obtain the molar paramagnetic susceptibilities. Solution electrical conductivities were measured with a Digisun DI-909 conductivity meter. A CH-Instruments model 620A electrochemical analyzer was used for cyclic voltammetric experiments with acetonitrile solutions of the complexes containing tetrabutylammonium perchlorate (TBAP) as supporting electrolyte. The three electrode measurements were carried out at 298 K under a dinitrogen atmosphere with a glassy carbon or platinum working electrode, a platinum wire auxiliary electrode and a saturated calomel reference electrode (SCE). The potentials reported in this work are uncorrected for junction contributions.

5.3.3. Synthesis of complexes

$[Mn_3O(bamen)_3]ClO_4 \cdot 2H_2O$ (1)

A methanol solution (20 ml) of $Mn(ClO_4)_2 \cdot 6H_2O$ (800 mg, 2.2 mmol) was added to a suspension of H_2bamen (500 mg, 2.2 mmol) in methanol (20 ml).

Immediately the colour of the reaction mixture became brown. After addition of triethylamine (450 mg, 4.45 mmol), the reaction mixture was stirred in air at room temperature (298 K) for 5 h. The green solid precipitated was collected by filtration, washed with ice-cold methanol and finally dried in air. Recrystallisation was performed by dissolving the complex in methanol-xylene mixture (2:1). Yield obtained was 400 mg (55%).

Selected IR bands[18] (cm^{-1}): 3470(br), 1640(s), 1545(s), 1427(m), 1379(m), 1317(m), 1182(w), 1074(vs), 729(w), 698(s), 623(m), 577(m), 532(s), 503(m), 414(s).

$[Fe_3O(bamen)_3]ClO_4 \cdot 2H_2O$ (2)

This complex was prepared by following the same procedure as described for **1** using $Fe(ClO_4)_3 \cdot 6H_2O$ instead of $Mn(ClO_4)_2 \cdot 6H_2O$. The complex was isolated as brown solid in 63% yield.

Selected IR bands[18] (cm^{-1}), for $[Fe_3O(bamen)_3]ClO_4 \cdot 2H_2O$.(**2**)

3500(br), 1641(s), 1533(s), 1431(m), 1379(m), 1323(m), 1188(m), 1090(vs), 692(s), 621(m), 592(m), 505(s), 411(s).

5.3.4. X-ray crystallography

Single crystals of $[M_3O(bamen)_3]ClO_4 \cdot 2H_2O$ {M = Mn (**1**) and Fe (**2**)} were grown by slow evaporation of methanol-xylene (2:1) solutions of the complexes. The data were collected on an Enraf-Nonius Mach-3 single crystal

diffractometer using graphite monochromated Mo $K\alpha$ radiation (λ = 0.71073 Å) by ω-scan method at 298 K. Unit cell parameters were determined by least-squares fit of 25 reflections having θ values in the range 11-14^o for **1** and 9–11^o for **2**. In each case, intensities of 3 check reflections were measured after every 1.5 h during the data collection to monitor the crystal stability. No decay was observed in either case. The ψ-scans[19] of selected reflections were used for an empirical absorption correction of each data set. The structures were solved by direct methods in the $P\bar{1}$ space group and refined on F^2 by full-matrix least-squares procedures. In each case, the asymmetric unit contains a molecule of $[M_3O(bamen)_3]ClO_4$ {M = Mn, Fe} and two water molecules. All non-hydrogen atoms were refined using anisotropic thermal parameters. The hydrogen atoms of the water molecules were located in a difference map and refined with geometric restraints and $U_{iso}(H) = 1.5U_{eq}(0)$. All other hydrogen atoms were included in the structure factor calculations at idealized positions, but not refined. The programs of the WinGX package[20] was used for data reduction and absorption correction. The structure solution and refinement were performed with the SHELX-97 programs.[21] The ORTEX6a[22] and the PLATON[23] packages were used for molecular graphics. Selected crystal and refinement data are summarized in Table 5.1. The atomic coordinates and equivalent isotropic displacement parameters for **1** and **2** are listed in Tables 5.2 and 5.3, respectively.

Table 5.1 Crystallographic data for $[Mn_3O(bamen)_3]ClO_4{\cdot}2H_2O$ (**1**) and $[Fe_3O(bamen)_3]ClO_4{\cdot}2H_2O$ (**2**)

Complex	**1**	**2**
Chemical formula	$Mn_3ClC_{30}H_{52}N_{12}O_{13}$	$Fe_3ClC_{30}H_{52}N_{12}O_{13}$
Crystal size, mm	0.49 x 0.45 x 0.42	0.48 x 0.40 x 0.24
Formula weight	989.11	991.84
Space group	Triclinic, $P\bar{1}$	Triclinic, $P\bar{1}$
a, Å	8.6591(7)	8.6821(9)
b, Å	14.8224(9)	14.7950(11)
c, Å	16.6760(14)	16.586(2)
α, deg.	84.512(8)	84.404(13)
β, deg.	81.976(9)	82.13(2)
γ, deg.	85.358(6)	85.970(8))
V, Å^3	2104.7(3)	1598.3(5)
Z	2	2
ρ_{calcd}, g cm^{-3}	1.561	1.571
μ mm^{-1}	1.024	1.162
Reflections collected/unique	7397/7397	7389/7389
Reflections $I > 2\sigma(I)$	6104	5346
Parameters	544	544
$R1$,[a] w$R2$[b] [$(I > 2\sigma(I)$]	0.0335, 0.0876	0.0381, 0.0889
$R1$,[a] w$R2$ (all data)	0.0490, 0.0945	0.0670, 0.1005
Goodness[c]-of-fit on F^2	1.031	1.014
Largest peak, hole [e Å^{-3}]	0.481, -0.466	0.479, -0.449

[a] $R1 = \sum||F_o| - |F_c||/\sum|F_o|$. [b] $wR2 = \{\sum[(F_o^2 - F_c^2)^2]/\sum[w(F_o^2)^2]\}^{1/2}$.
[c] GOF = $\{\sum[w(F_o^2 - F_c^2)^2]/(n - p)\}^{1/2}$ where 'n' is the number of reflections and 'p' is the number of parameters refined.

Table 5.2. Atomic coordinates (x 10^4) and equivalent isotropic displacement parameters ($Å^2$ x 10^3) for $[Mn_3O(bamen)_3]ClO_4 \cdot 2H_2O$

Atom	x	y	z	U(eq)
Mn(1)	4644(1)	2396(1)	1270(1)	27(1)
Mn(2)	3569(1)	817(1)	2728(1)	26(1)
Mn(3)	4843(1)	2723(1)	3179(1)	27(1)
Cl	1180(2)	2974(1)	7944(1)	84(1)
O(1)	732(2)	3788(1)	2699(1)	36(1)
O(2)	5053(2)	236(1)	1927(1)	32(1)
O(3)	2591(2)	2062(1)	1138(1)	35(1)
O(4)	6012(2)	1724(1)	3707(1)	35(1)
O(5)	2015(2)	1321(1)	3545(1)	34(1)
O(6)	6700(2)	2788(1)	1333(1)	35(1)
O(7)	4370(2)	1976(1)	2395(1)	27(1)
O(8)	1490(6)	3850(3)	7921(4)	81(3)
O(9)	2563(7)	2444(4)	7807(4)	195(3)
O(10)	109(8)	2857(4)	7456(4)	205(3)
O(11)	540(8)	2702(6)	8703(4)	251(4)
O(12)	7718(5)	3538(3)	6290(2)	119(1)
O(13)	4712(6)	4308(4)	6984(3)	148(2)
N(1)	3715(3)	3722(2)	1893(1)	34(1)
N(2)	4049(3)	3554(2)	364(1)	38(1)
N(3)	5718(3)	1997(2)	39(1)	35(1)
N(4)	5395(2)	823(2)	1267(1)	29(1)
N(5)	2143(2)	1368(2)	1677(1)	31(1)
N(6)	1629(3)	-64(2)	2637(1)	35(1)
N(7)	4064(3)	-500(2)	3462(1)	35(1)
N(8)	5424(3)	928(2)	3621(1)	31(1)
N(9)	2539(2)	2052(2)	3814(1)	30(1)
N(10)	3808(3)	3326(2)	4351(1)	33(1)
N(11)	6663(3)	3540(2)	3527(1)	36(1)
N(12)	6795(2)	3023(2)	2089(1)	32(1)
C(1)	3155(3)	4412(2)	1475(2)	35(1)
C(2)	3259(3)	4266(2)	598(2)	38(1)
C(3)	4257(4)	3321(2)	-475(2)	50(1)
C(4)	5751(4)	2724(2)	-617(2)	50(1)

C(5)	6447(3)	1224(2)	-53(2)	34(1)
C(6)	6232(3)	515(2)	637(2)	31(1)
C(7)	2479(4)	5271(2)	1825(2)	50(1)
C(8)	2431(4)	4945(2)	45(2)	58(1)
C(9)	7462(4)	977(2)	-816(2)	52(1)
C(10)	6878(3)-	444(2)	584(2)	40(1)
C(11)	853(3)	1018(2)	1618(2)	33(1)
C(12)	533(3)	227(2)	2220(2)	35(1)
C(13)	1521(4)	-860(2)	3227(2)	49(1)
C(14)	3158(4)	-1246(2)	3317(2)	48(1)
C(15)	5260(3)-	625(2)	3837(2)	37(1)
C(16)	6031(3)	200(2)	3965(2)	34(1)
C(17)	-177(3)	1329(2)	979(2)	48(1)
C(18)	-1011(4)	-179(3)	2285(2)	62(1)
C(19)	5914(5)	-1532(2)	4166(2)	59(1)
C(20)	7372(4)	181(2)	4449(2)	50(1)
C(21)	1667(3)	2438(2)	4388(2)	32(1)
C(22)	2411(3)	3201(2)	4667(2)	34(1)
C(23)	4692(4)	4022(2)	4599(2)	43(1)
C(24)	6419(4)	3762(2)	4373(2)	45(1)
C(25)	7925(3)	3679(2)	3050(2)	34(1)
C(26)	7993(3)	3428(2)	2202(2)	33(1)
C(27)	114(4)	2113(2)	4761(2)	49(1)
C(28)	1493(4)	3772(3)	5292(2)	64(1)
C(29)	9324(4)	4094(2)	3266(2)	51(1)
C(30)	9326(3)	3656(2)	1555(2)	47(1)

Table 5.3. Atomic coordinates (x 10^4) and equivalent isotropic displacement parameters ($Å^2$ x 10^3) for $[Fe_3O(bamen)_3]ClO_4 \cdot 2H_2O$

Atom	x	y	z	U(eq)
Fe(1)	4657(1)	2352(1)	1254(1)	27(1)
Fe(2)	3578(1)	781(1)	2737(1)	27(1)
Fe(3)	4850(1)	2705(1)	3172(1)	28(1)
Cl	1157(2)	3022(1)	7903(1)	86(1)
O(1)	3753(3)	3786(2)	2638(2)	38(1)
O(2)	5070(3)	205(2)	1892(1)	33(1)
O(3)	2552(3)	1984(2	1147(2)	36(1)
O(4)	5986(3)	1670(2)	3736(2)	37(1)
O(5)	2026(3)	1325(2)	3572(2)	35(1)
O(6)	6730(3)	2783(2)	1348(1)	6(1)
O(7)	4389(3)	1942(2)	2391(1)	27(1)
O(8)	1495(7)	3888(3)	7920(5)	178(3)
O(9)	2484(8)	2483(4)	7761(5)	201(3)
O(10)	78(10)	2924(5)	7424(5)	226(4)
O(11)	535(11)	2719(8)	8655(5)	262(5)
O(12)	7734(7)	3623(4)	6285(3)	123(2)
O(13)	4793(7)	4368(4)	7054(4)	147(2)
N(1)	3719(3)	3682(2)	1839(2)	33(1)
N(2)	4012(4)	3469(2)	321(2)	39(1)
N(3)	5795(4)	1982(2)	28(2)	35(1)
N(4)	5428(3)	804(2)	1246(2)	29(1)
N(5)	2126(3)	1304(2)	1708(2)	31(1)
N(6)	1603(4)-	98(2)	2700(2)	37(1)
N(7)	4096(4)	-548(2)	3437(2)	38(1)
N(8)	5419(3)	880(2)	3622(2)	32(1)
N(9)	2554(3)	2073(2)	3805(2)	30(1)
N(10)	3830(4)	3357(2)	4311(2)	35(1)
N(11)	6705(4)	3488(2)	3546(2)	38(1)
N(12)	6808(3)	3004(2)	2105(2)	33(1)
C(1)	3154(4)	4352(2)	1406(2)	35(1)
C(2)	3251(4)	4192(3)	536(2)	39(1)
C(3)	4268(5)	3231(3)	-513(2)	52(1)
C(4)	5820(5)	2708(3)	-630(2)	52(1)

C(5)	6516(4)	1213(3)	-65(2)	33(1)
C(6)	6277(4)	507(2)	617(2)	30(1)
C(7)	2482(5)	5210(3)	1742(3)	49(1)
C(8)	2484(6)	4873(3)	-39(3)	61(1)
C(9)	7529(5)	975(3)	-828(2)	51(1)
C(10)	6893(4)	-454(3)	569(2)	40(1)
C(11)	815(4)	963(3)	1680(2)	36(1)
C(12)	504(4)	175(3)	2283(2)	37(1)
C(13)	1525(5)	-908(3)	3275(3)	54(1)
C(14)	3166(6)	-1293(3)	3303(3)	54(1)
C(15)	5266(5)	-670(3)	3827(2)	38(1)
C(16)	6023(4)	155(3)	3963(2)	34(1)
C(17)	-235(5)	1276(3)	1049(3)	51(1)
C(18)	-1018(5)	-258(4)	2340(3)	60(1)
C(19)	5892(6)	-1582(3)	4168(3)	59(1)
C(20)	7343(5)	147(3)	4455(3)	50(1)
C(21)	1689(4)	2477(2)	4369(2)	32(1)
C(22)	2443(4)	3244(2)	4631(2)	35(1)
C(23)	4744(5)	4030(3)	4573(3)	47(1)
C(24)	6441(5)	3716(3)	4393(3)	50(1)
C(25)	7945(4)	3657(2)	3072(2)	36(1)
C(26)	8018(4)	3404(2)	2223(2)	35(1)
C(27)	144(5)	2151(3)	4743(3)	50(1)
C(28)	1557(5)	825(3)	5250(3)	63(1)
C(29)	9325(5)	4093(3)	3282(3)	51(1)
C(30)	9335(4)	3632(3)	1577(3)	49(1)

5.4. Results and discussion

5.4.1. Synthesis and some properties

Both complexes were synthesized by using a general method. Reactions of metal (Mn and Fe) perchlorates, H_2bamen and triethylamine in 1:1:2 mole ratios in methanolic media under aerobic conditions afford the complexes in good

yield. The cationic complexes were precipitated as their perchlorate salts from the reaction mixture. The elemental analysis (Table 5.4) data are satisfactory with the assigned general molecular formula $[M_3O(bamen)_3]ClO_4{\cdot}2H_2O$. In CH_3CN solution, the molar conductivity (Table 5.4) values of both the complexes are consistent with 1:1 electrolytic behavior.[24]

Table 5.4. Elemental analysis[a] and Molar conductivity data[b]

Complex	%C	%H	%N	Λ_M ($\Omega^{-1}cm^2mol^{-1}$)
1	36.23 (36.43)	5.12 (5.30)	16.75 (16.99)	180
2	36.12 (36.33)	5.48 (5.28)	17.13 (16.95)	152

[a] Calculated values are in parentheses, [b] in CH_3CN solution

5.4.2. Infrared spectral properties

The infrared spectra of **1** and **2** complexes do not display any band near 3000 cm^{-1}. Thus the oxime−OH groups of the ligand are deprotonated. A broad band centered at 3500 cm^{-1} is most likely due to the lattice water molecules. Presence of the perchlorate is indicated by the bands at 1090 and 621 cm^{-1}. Two strong bands are observed at 1641 and 1533 cm^{-1}. Comparable bands observed for complexes with dioxime ligands are attributed to the coupled C=N and C=C stretching modes.[25] There is a 1:1 correspondence in the infrared spectra (Figure 5.2) of $[Mn_3O(bamen)_3]ClO_4{\cdot}2H_2O$ and $[Fe_3O(bamen)_3]ClO_4{\cdot}2H_2O$. This

observation together with the elemental analysis and molar conductivity data suggest that the Mn^{III}_3 and Fe^{III}_3 complexes have similar structures (isomorphs).

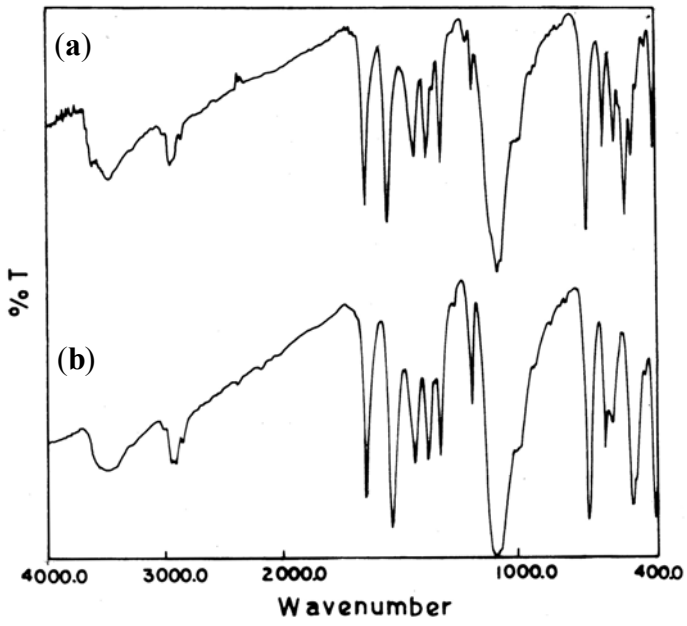

Figure 5.2. Infrared spectra of (a) **1** and (b) **2** in KBr disks.

5.4.3. Electronic spectral properties

Electronic spectral data of the complexes in CH_3CN solutions are listed in Table 5.5. Both the complexes show weak absorption bands in the range 840–620 nm followed by three strong absorptions in the range 383–243 nm (Figure 5.3). The origin of the weak absorptions is most likely d–d transitions. Such absorptions observed for $[Fe_3O(O_2CR)_6(H_2O)_3]^+$ in the range 980–625 nm

have been assigned to d-d transitions and the large extinction coefficients unusual for spin-forbidden transitions are attributed to the spin-exchange between the metal ions.[3] The remaining absorptions are most likely due to ligand-to-metal and intraligand charge transfer transitions.[25a]

Table 5.5. Electronic spectral data

Complex	λ_{max} (nm) (ε ($M^{-1}cm^{-1}$))
1	840 (1150), 631(1729), 318 (24,458), 276[sh] (29,791), 243 (35,625)
2	720 (115), 383 (11 900), 277[sh] (37,900), 248 (47,800)

[sh]Shoulder

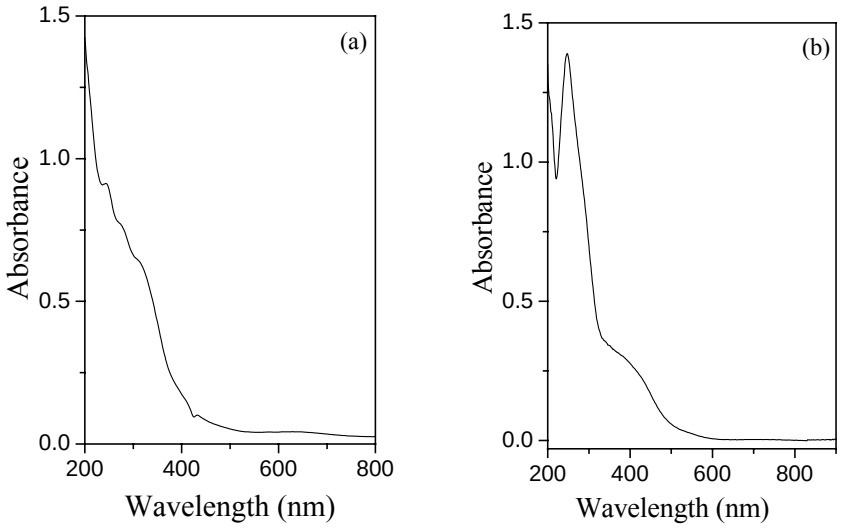

Figure 5.3. Electronic spectra of the (a) $[Mn_3O(bamen)_3]ClO_4$ (b) $[Fe_3O(bamen)_3]ClO_4$ in acetonitrile solutions.

5.4.4. Electrochemical properties

The electron transfer behaviors of the trimanganese(III) (**1**) and the triiron(III) (**2**) complexes in acetonitrile solutions have been studied by using cyclic voltammetry. The potential data are listed in Table 5.6. The cyclic voltammograms are illustrated in Figures 5.4 and 5.5. Each complex shows three oxidation responses on the anodic side of the reference electrode SCE (Table 5.6). Complex **1** does not display any response on the cathodic side of SCE. However, complex **2** shows two reduction responses on the cathodic side of SCE. Under the same experimental conditions the deprotonated ligand ($bamen^{2-}$) obtained by mixing H_2bamen and tetramethylammonium hydroxide in 1:2 mole ratio does not display any redox response in the potential range –2.1 to +2.1 V. Thus all the redox responses displayed by both complexes are metal centered.

Table 5.6. Cyclic voltammetric[a] data

Complex	**Metal centered oxidation**		**Metal centered reduction**	
	$E_{1/2}$ /V (ΔE_p/mV)	E_{pa}/V	$E_{1/2}$ /V (ΔE_p/mV)	E_{pc}/V
1	+0.87 (80) +1.45 (100)	+1.98	—	—
2	+1.05 (80)	+1.41 +1.75	–1.05(60)	–1.66

[a]E_{pa} = anodic peak potential, E_{pc} = cathodic peak potential, $E_{1/2} = (E_{pa} + E_{pc})/2$, $\Delta E_p = E_{pa} - E_{pc}$.

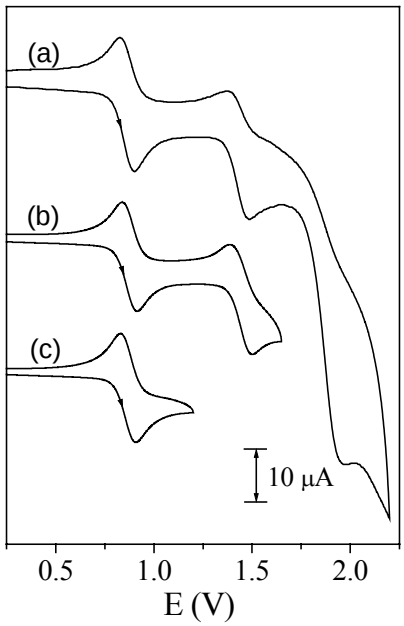

Figure 5.4. Cyclic voltammograms (scan rate 50 mVs^{-1}) of $[Mn_3O(bamen)_3]ClO_4 \cdot 2H_2O$ in acetonitrile solution (0.1 M TBAP) at a glassy-carbon electrode (298 K). (a) Successive oxidations of all three Mn(III) centers. (b) Oxidations of two Mn(III) centers. (c) Oxidation of the first Mn(III) center.

Three oxidation responses displayed by **1** are observed at $E_{1/2}$ = +0.87 V (ΔE_p = 80 mV), $E_{1/2}$ = +1.45 V (ΔE_p = 100 mV), and E_{pa} = 1.98 V (Figure 5.4). The first two responses are very close to reversible processes (Figure 5.4b,c). The current heights of these two responses are similar and comparable with known one-electron processes under identical conditions.[26] These two reversible oxidation responses are assigned to the $Mn^{III}_2Mn^{IV}/Mn^{III}_3$ and $Mn^{III}Mn^{IV}_2/Mn^{III}_2Mn^{IV}$ couples. The highest potential response is irreversible and the anodic peak current is ~2.5 times larger than that of the first two responses (Figure 5.4a). The potential (1.98 V) of this oxidation response is very close to the solvent cut-

off and hence solvent may contribute to the observed peak current. Considering that the free ligand does not display any response in this region, we tentatively assign this electrode process to the $Mn^{III}Mn^{IV}_2 \rightarrow Mn^{IV}_3$ oxidation.

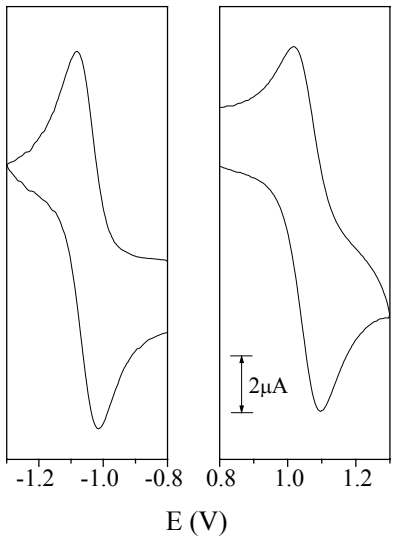

Figure 5.5. Cyclic voltammograms (scan rate 50 mVs^{-1}) of $[Fe_3O(bamen)_3]ClO_4 \cdot 2H_2O$ in acetonitrile solution (0.1M TBAP) at a platinum electrode (298 K).

The triiron(III) complex (**2**) displays a reversible oxidation response at $E_{1/2}$ = +1.05 V (ΔE_p = 80 mV) and another reversible reduction response at $E_{1/2}$ = −1.05 V (ΔE_p = 60 mV) (Figure 5.5). The peak currents observed for these two responses are comparable with the peak currents of known one-electron processes under identical conditions.[26] The oxidation response is assigned to the $Fe^{III}_2Fe^{IV}/Fe^{III}_3$ couple and the reduction response is assigned to the $Fe^{III}_3/Fe^{III}_2Fe^{II}$ couple. On the anodic side of SCE, in addition to the reversible oxidation

response two more irreversible oxidation responses (E_{pa} = 1.41 and 1.75 V) are observed. However, the peak current of the lower potential response is 1/3rd and that of the higher potential response is almost twice compared to the peak current of the reversible oxidation response. The free ligand (bamen^{2-}) is redox silent in this region and the trimanganese(III) analogue (**1**) displays two reversible and one irreversible metal centered oxidations. Thus these two irreversible oxidations observed for **2** may involve the metal centers. However, the irreversible nature and unequal peak currents clearly indicate that the corresponding oxidized species are unstable in the cyclic voltammetric time scale. Similarly on the cathodic side of SCE an irreversible reduction at −1.66 V having peak current comparable with that of the reversible reduction response is observed. This response may be due to the $Fe^{III}_2Fe^{II} \rightarrow Fe^{III}Fe^{II}_2$ process as the ligand is redox inactive at this potential. It is interesting to note that there is no report of metal centered oxidation displayed by $[M_3O(O_2CR)_6L_3]^+$ species containing first row metal ions. Normally for these species metal centered reductions are observed and very few of them display more than one reversible redox steps.[11]

5.4.5. Magnetic properties

Magnetic susceptibility measurements in the temperature range 18–310 K and at a constant magnetic field of 5 KG were performed with the powdered samples of $[Mn_3O(bamen)_3]ClO_4{\cdot}2H_2O$ and $[Fe_3O(bamen)_3]ClO_4{\cdot}2H_2O$. Diamagnetic corrections calculated from Pascal's constants[17] were applied to obtain the molar paramagnetic susceptibilities. The magnetic behavior of the complexes are not similar at this magnetic field and temperature range. For

$[Mn_3O(bamen)_3]^+$ the effective magnetic moment (12.04 μ_B) at 310 K is significantly larger than the spin-only value (8.48 μ_B) for a trinuclear complex containing three Mn(III) ions (S = 2). The moment gradually increases to 13.32 μ_B at 95 K. The change of moment below 95 K is much smaller and reaches the value of 13.40 μ_B at 18 K (Figure 5.6). This behavior clearly indicates the ferromagnetic nature of this complex. The data were fitted using an expression for χ_M *vs T* for a triangular trimanagnese(III) complex in which all the metal ions are equivalent and have the spin state S = 2.[5] The best least-squares fit[29] was obtained with J = 22.3(1) cm^{-1} and g = 2.06(1). It may be noted that very few Mn(III) complexes are known where ferromagnetic interaction is operative between the metal ions.[30] Antiferromagnetic interactions are reported for $[Mn_3O(O_2CR)_6(py)_3]^{0/1+}$ complexes.[5] In this type of species, the metal ions are in distorted octahedral coordination sphere and each pair of the Mn(III) centers are bridged by two corboxylates in addition to the μ_3-oxo bridge. The magnetic interaction in these complexes is considered to be propagated mainly via the μ_3-oxo bridge.[5] In contrast, the metal ions in $[Mn_3O(bamen)_3]^+$ are pentagonal–bipyramidal. Apart from the μ_3-oxo bridge, two oximate groups provide additional bridges between each pair of metal centers. Ferromagnetic interaction through such μ-oximate bridges are known.[31]

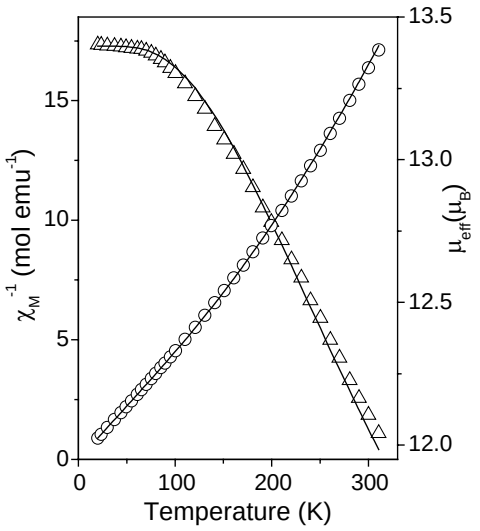

Figure 5.6. Inverse molar magnetic susceptibility (O) and effective magnetic moment (Δ) of $[Mn_3O(bamen)_3]ClO_4{\cdot}2H_2O$ as a function of temperature. The solid lines were generated from the best least-squares fit parameters given in the text.

The effective magnetic moment of $[Fe_3O(bamen)_3]ClO_4{\cdot}2H_2O$ at 300 K is 5.00 μ_B. The moment gradually decreases with the lowering of the temperature and reaches a value of 1.71 μ_B at 18 K. The nature of the curve obtained by plotting the moments against temperature (Figure 5.7) clearly indicates the antiferromagnetic character of the complex and the value of the moment at lowest temperature is consistent with the S = 1/2 ground state. The data were fitted using an expression for χ_M vs T obtained from the isotropic spin exchange Hamiltonian $H = -2J(S_1S_2 + S_2S_3 + S_3S_1)$ for a triangular triiron(III) complex in which all the metal ions are equivalent and have the same spin state $S_1 = S_2 = S_3 = 5/2$.[32] The best least-squares fit[29] was obtained with $J = -41.0(2)$ cm^{-1} and g = 1.984(4).

Complexes of formula $[Fe_3(\mu_3\text{-}O)(\mu_2\text{-}O_2CR)_6L_3]^+$ are known to be antiferromagnetic and the *J* values reported for such species span the range –15 to –33 cm^{-1}.[1,3,5-7,13]

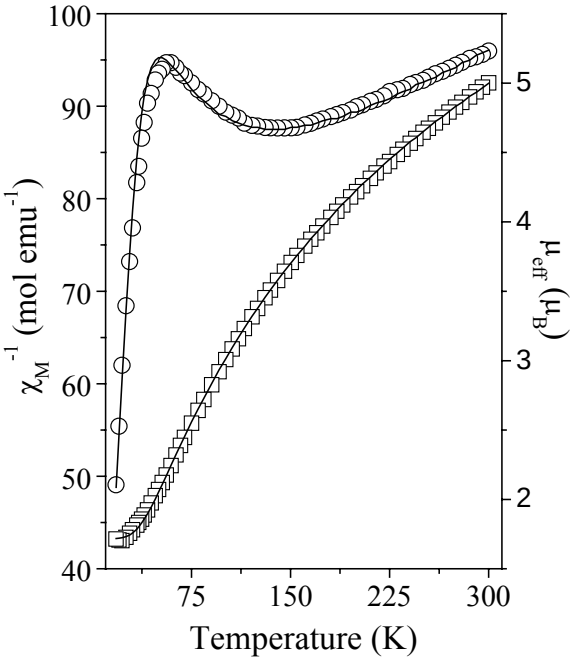

Figure 5.7. Temperature dependence of inverse molar magnetic susceptibilities (O) and effective magnetic moments (□) of $[Fe_3O(bamen)_3]ClO_4{\cdot}2H_2O$. The continuous lines were generated from the best least-squares fit parameters given in the text.

It has been noted that the antiferromagnetic interaction decreases as the metal ion is changed from Fe(III) to Mn(III) in the acetate complexes of $\{M_3(\mu_3\text{-}O)\}^{7+}$. In this type of species, the metal ions are in distorted octahedral coordination sphere. The unpaired electrons present in the σ-interacting e_g orbitals are involved in the antiferromagnetic exchange process. Thus the

decrease in the $-J$ value has been attributed to the decrease in the number of unpaired electrons in the e_g orbitals are involved in the antiferromagnetic exchange process. Thus the decrease in the $-J$ value has been attributed to the decrease in the number of unpaired electrons in the e_g orbitals as one goes from high-spin Fe(III) ($t_{2g}^3e_g^2$) to high-spin Mn(III) ($t_{2g}^3e_g^1$).[5] Interestingly, the antiferromagnetic interaction in $[Fe_3O(bamen)_3]^+$ is noticeably higher than that in the $[Fe_3O(O_2CR)_6L_3]^+$ complexes and a ferromagnetic interaction (J = 22.3(1) cm^{-1}) is operative in $[Mn_3O(bamen)_3]^+$ rather than a weaker antiferromagnetic interaction as observed in $[Mn_3O(O_2CR)_6L_3]^+$. It is very likely that the change in the coordination geometry around the metal ions from octahedral in $[M_3O(O_2CR)_6L_3]^+$ to pentagonal-bipyramidal in $[M_3O(bamen)_3]^+$ is primarily responsible for the differences in the magnetic properties of these two types of complexes containing the same $\{M_3(\mu_3\text{-}O)\}^{7+}$ core. It may be noted that in the pentagonal-bipyramidal coordination sphere the highest energy d_z^2 orbital in the high-spin Fe(III) species will have an unpaired electron but that in the high-spin Mn(III) species will be empty. Thus the alteration in the nature of the spin-coupling from ferromagnetic in $[Mn_3O(bamen)_3]^+$ to antiferromagnetic in $[Fe_3O(bamen)_3]^+$ is perhaps dictated by the absence or presence of electron in the d_z^2 orbital of the metal ion.

5.4.6. Description of molecular structures

In the solid state, structures of the two complexes $[Mn_3O(bamen)_3]ClO_4{\cdot}2H_2O$ and $[Fe_3O(bamen)_3]ClO_4{\cdot}2H_2O$ have been determined by X-ray crystallography. This study revealed that the two complexes are isomorphous. Both the species

crystallized in the same space group with very similar unit cell dimensions (Table 5.1). The structures of the cations are illustrated in Figures 5.8 and 5.9. Selected bond parameters are listed in Tables 5.7 and 5.8. Each of the two complex cations contains three bridging N_4O_2 donor bamen^{2-} ligands, one μ_3-oxo group and three metal centers. Presence of one ClO_4^- per complex cation indicates that the oxidation state of each metal center is +3. In both the complex cations, each hexadentate N_4O_2 donor ligand binds all the three metal centers. The four N-atoms are coordinated to one metal center forming three five-membered chelate rings and two oximato O-atoms are coordinated to the remaining two metal centers. Consequently each pair of metal centers are bridged by two oximate groups in a reciprocal manner with respect to the N- and the O-atom coordination (Figures 5.8 and 5.9). The μ_3-oxo atom satisfies the seventh coordination site of each of the three metal atoms. The C–N and N–O bond lengths in the oximate ($-(CH_3)C=N-O^-$) fragments are in the ranges 1.277(4)–1.290(3) Å and 1.337(4)–1.360(3) Å, respectively. These bond lengths are comparable with the corresponding bond lengths reported for deprotonated oxime functionalities.[25] The $C=N_{imine}$ bond lengths are significantly shorter than the $C= N_{oximate}$ bond lengths. The partial double bond character of the $N–O^-$ bond is likely to cause this difference. In each complex, $M–N_{imine}$ bond lengths are significantly shorter than the $M–N_{oximate}$ bond lengths (Table 5.7 and 5.8). Most probably the longer $M\text{-}N_{oximate}$ distances are mainly due to the bridging nature of the oximate ($=N–O^-$) groups. Among the four N-atoms of the bamen^{2-} unit that are coordinated to a

single metal center, two imine N-atoms are in the middle and two oximate N-atoms are terminal. Thus the rigidity of the N_4 fragment may also be partially responsible for this difference.[27] The central $\{M_3(\mu_3\text{-}O)\}^{7+}$ core is essentially planar. The μ_3-O atoms (O7) is marginally displaced by 0.024(2) Å **1** and 0.015(2) Å **2** from the M_3 plane. The M to the μ_3-O bond lengths and the M···M distances [3.2992(9)–3.3013(7) Å] are comparable with the corresponding values reported for complexes containing the $\{M_3(\mu_3\text{-}O)\}^{7+}$ (M = Mn and Fe) core.[8,11,31] The N_4O_3 coordination geometry around each metal center can be best described as distorted pentagonal-bipyramidal. The μ_3-oxo atom and the four N-atoms of

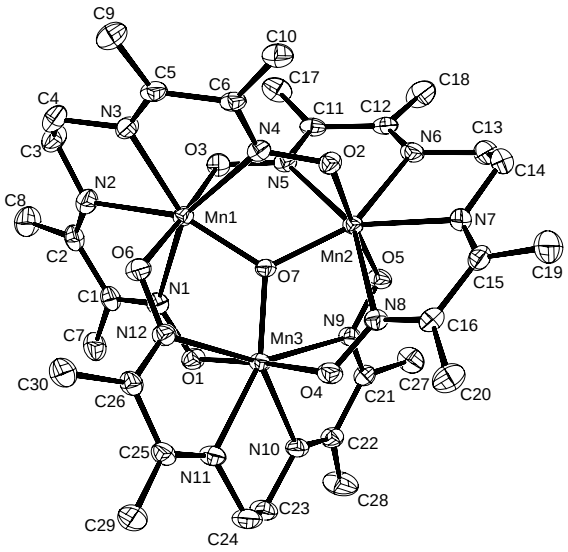

Figure 5.8. Structure of $[Mn_3(\mu_3\text{-}O)(\mu_3\text{-bamen})_3]^{3+}$. All atoms are represented by their 30% probability thermal ellipsoids. Hydrogen atoms are omitted for clarity.

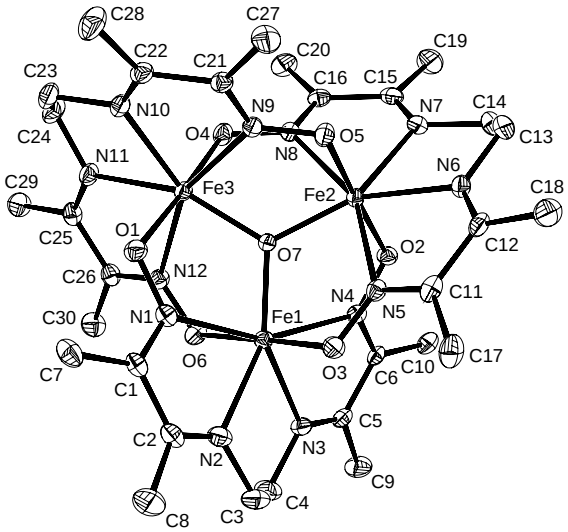

Figure 5.9. Structure of $[Fe_3(\mu_3\text{-}O)(\mu_3\text{-bamen})_3]^{3+}$. All atoms are represented by their 25% probability thermal ellipsoids. Hydrogen atoms are omitted for clarity.

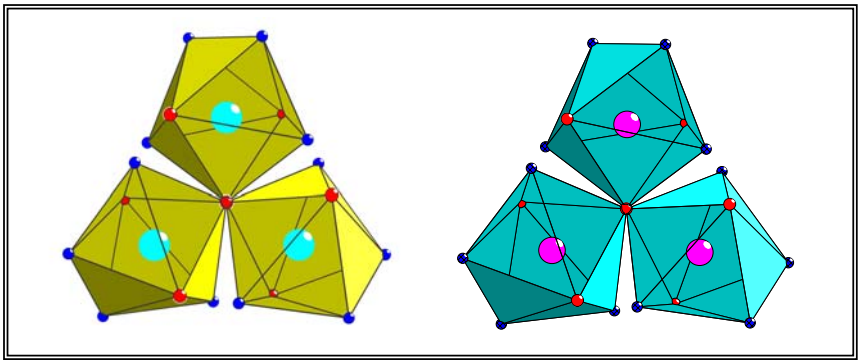

(a) **(b)**

Figure 5.10. Coordination polyhedra about the metal atoms in (a) $[Mn_3O(bamen)_3]^+$and (b) $[Fe_3O(bamen)_3]^+$.

one bamen^{2-} ligand constitute the pentagonal plane and the two oximate O-atoms of the other two ligands occupy the axial sites (Figure 5.10). Thus the three pentagonal–bipyramidal polyhedra have a common equatorial position and that is occupied by the μ_3-oxo atom. In each complex, the mean deviations from the pentagonal $N_4(\mu_3\text{-O})$ plane are in the range 0.16–0.17 Å in **1** and 0.21–0.22 Å respectively **2**. The $O_{oximate}$–M–$O_{oximate}$ angles are ≈ 176 °.

Table 5.7. Selected bond distances (Å) and angles (°) for $[Mn_3O(bamen)_3]ClO_4{\cdot}2H_2O$.

Mn(1)-N(1)	2.343(2)	Mn(1)-N(2)	2.253(2)
Mn(1)-N(3)	2.246(2)	Mn(1)-N(4)	2.370(2)
Mn(1)-O(3)	1.9304(18)	Mn(1)-O(6)	1.9359(18)
Mn(1)-O(7)	1.9081(17)	Mn(2)-N(5)	2.331(2)
Mn(2)-N(6)	2.238(2)	Mn(2)-N(7)	2.246(2)
Mn(2)-N(8)	2.362(2)	Mn(2)-O(2)	1.9340(18)
Mn(2)-O(5)	1.9352(18)	Mn(2)-O(7)	1.9088(17)
Mn(3)-N(9)	2.371(2)	Mn(3)-N(10)	2.267(2)
Mn(3)-N(11)	2.232(2)	Mn(3)-N(12)	2.338(2)
Mn(3)-O(1)	1.9445(19)	Mn(3)-O(4)	1.9362(19)
Mn(3)-O(7)	1.8978(16)		

N(2)-Mn(1)-N(1)	67.67(9)	O(2)-Mn(2)-N(8)	94.24(8)
N(3)-Mn(1)-N(2)	73.16(9)	O(7)-Mn(2)-O(2)	91.87(7)
N(3)-Mn(1)-N(4)	67.23(8)	O(5)-Mn(2)-N(5)	92.58(8)
O(7)-Mn(1)-N(1)	82.08(8)	O(5)-Mn(2)-N(7)	95.90(8)
O(3)-Mn(1)-N(1)	94.38(8)	O(5)-Mn(2)-N(8)	87.24(8)
O(3)-Mn(1)-N(3)	93.57(8)	O(7)-Mn(2)-O(5)	92.01(7)
O(3)-Mn(1)-N(4)	85.74(8)	N(10)-Mn(3)-N(9)	66.71(8)

O(7)-Mn(1)-O(3)	91.84(8)	N(11)-Mn(3)-N(10)	73.23(8)
O(6)-Mn(1)-N(1)	85.10(8)	N(11)-Mn(3)-N(12)	68.42(8)
O(6)-Mn(1)-N(2)	93.99(8)	O(7)-Mn(3)-N(12)	77.50(7)
O(6)-Mn(1)-N(3)	84.19(8)	O(7)-Mn(3)-N(9)	76.35(7)
O(6)-Mn(1)-N(4)	96.50(8)	O(1)-Mn(3)-N(9)	94.48(8)
O(7)-Mn(1)-O(6)	92.00(7)	O(1)-Mn(3)-N(10)	82.34(8)
N(6)-Mn(2)-N(5)	68.20(8)	O(1)-Mn(3)-N(11)	92.94(8)
N(6)-Mn(2)-N(7)	73.31(9)	O(1)-Mn(3)-N(12)	84.22(8)
N(7)-Mn(2)-N(8)	67.37(8)	O(7)-Mn(3)-O(1)	92.54(8)
O(7)-Mn(2)-N(8)	76.42(7)	O(4)-Mn(3)-N(9)	87.30(8)
O(5)-Mn(2)-N(5)	92.58(8)	O(4)-Mn(3)-N(10)	94.77(8)
O(2)-Mn(2)-N(5)	87.71(8)	O(4)-Mn(3)-N(11)	83.12(8)
O(2)-Mn(2)-N(6)	95.10(8)	O(4)-Mn(3)-N(12)	95.94(8)
O(2)-Mn(2)-N(7)	81.35(8)	O(7)-Mn(3)-O(4)	91.71(7)

Table 5.8. Selected bond distances (Å) and angles (°) for $[Fe_3O(bamen)_3]ClO_4 \cdot 2H_2O$.

Fe(1)-N(1)	2.326(3)	Fe(2)-N(5)	2.302(3)	Fe(3)-N(9)	2.334(3)
Fe(1)-N(2)	2.247(3)	Fe(2)-N(6)	2.235(3)	Fe(3)-N(10)	2.251(3)
Fe(1)-N(3)	2.236(3)	Fe(2)-N(7)	2.233(3)	Fe(3)-N(11)	2.236(3)
Fe(1)-N(4)	2.341(3)	Fe(2)-N(8)	2.334(3)	Fe(3)-N(12)	2.311(3)
Fe(1)-O(3)	1.979(2)	Fe(2)-O(2)	1.987(2)	Fe(3)-O(1)	1.997(2)

N(1)-Fe(1)-N(2)	67.57(11)	O(2)-Fe(2)-N(8)	94.72(10)
N(2)-Fe(1)-N(3)	72.31(12)	O(2)-Fe(2)-O(7)	90.85(10)
N(3)-Fe(1)-N(4)	67.28(11)	O(5)-Fe(2)-N(5)	91.75(10)
N(4)-Fe(1)-O(7)	77.48(10)	O(5)-Fe(2)-N(6)	80.73(10)
O(7)-Fe(1)-N(1)	78.43(10)	O(5)-Fe(2)-N(7)	98.73(11)

O(3)-Fe(1)-N(1)	93.53(10)	O(5)-Fe(2)-N(8)	87.04(10)
O(3)-Fe(1)-N(2)	81.43(11)	O(5)-Fe(2)-O(7)	90.92(10)
O(3)-Fe(1)-N(3)	96.64(11)	N(9)-Fe(3)-N(10)	67.00(10)
O(3)-Fe(1)-N(4)	86.04(10)	N(10)-Fe(3)-N(11)	72.47(11)
O(3)-Fe(1)-O(7)	90.74(10)	N(11)-Fe(3)-N(12)	68.15(11)
O(6)-Fe(1)-N(1)	84.22(10)	N(12)-Fe(3)-O(7)	78.17(10)
O(6)-Fe(1)-N(2)	96.12(11)	O(7)-Fe(3)-N(9)	77.28(10)
O(6)-Fe(1)-N(3)	83.88(10)	O(1)-Fe(3)-N(9)	94.17(10)
O(6)-Fe(1)-N(4)	96.71(10)	O(1)-Fe(3)-N(10)	82.03(11)
O(6)-Fe(1)-O(7)	90.48(10)	O(1)-Fe(3)-N(11)	95.20(11)
N(5)-Fe(2)-N(6)	68.24(11)	O(1)-Fe(3)-N(12)	83.45(10)
N(6)-Fe(2)-N(7)	72.52(12)	O(1)-Fe(3)-O(7)	92.02(10)
N(7)-Fe(2)-N(8)	67.48(11)	O(4)-Fe(3)-N(9)	87.01(10)
N(8)-Fe(2)-O(7)	77.21(10)	O(4)-Fe(3)-N(10)	96.08(11)
O(7)-Fe(2)-N(5)	77.99(10)	O(4)-Fe(3)-N(11)	82.20(11)
O(2)-Fe(2)-N(5)	87.24(10)	O(4)-Fe(3)-N(12)	96.56(11)
O(2)-Fe(2)-N(6)	97.02(11)	O(4)-Fe(3)-O(7)	90.75(10)
O(2)-Fe(2)-N(7)	80.69(10)		

5.4.7. Hydrogen bonding and crystal packing

In the crystal lattice of both the $[Mn_3O(bamen)_3]ClO_4{\cdot}2H_2O$ and $[Fe_3O(bamen)_3]ClO_4{\cdot}2H_2O$, the water molecules and the perchlorate ions exist in a helical fashion through hydrogen bonding interactions (Figure 5.11). The hydrogen bond lengths and angles in both the complexes are nearly same (Table 5.9). Two water molecules form a linear dimer (O···O distance, ~2.89 Å; O–H···O angle, ~153^o). The hydrogen bond acceptor molecule in this water dimer is again hydrogen bonded to one perchlorate oxygen atom (O···O distance, 3.099(8) –3.119(8) Å, O–H···O angle, ~140^o). The donor water molecule of the

dimer in the $\{(H_2O)_2ClO_4^-\}$ unit is hydrogen bonded with a perchlorate oxygen (O···O distance, ~3.04 Å; O–H···O angle, ~162°) of a symmetry related $\{(H_2O)_2ClO_4^-\}$ unit. These three hydrogen bonding interactions lead to the helical arrangement of the water molecules and the perchlorate ions (Figure 5.11).

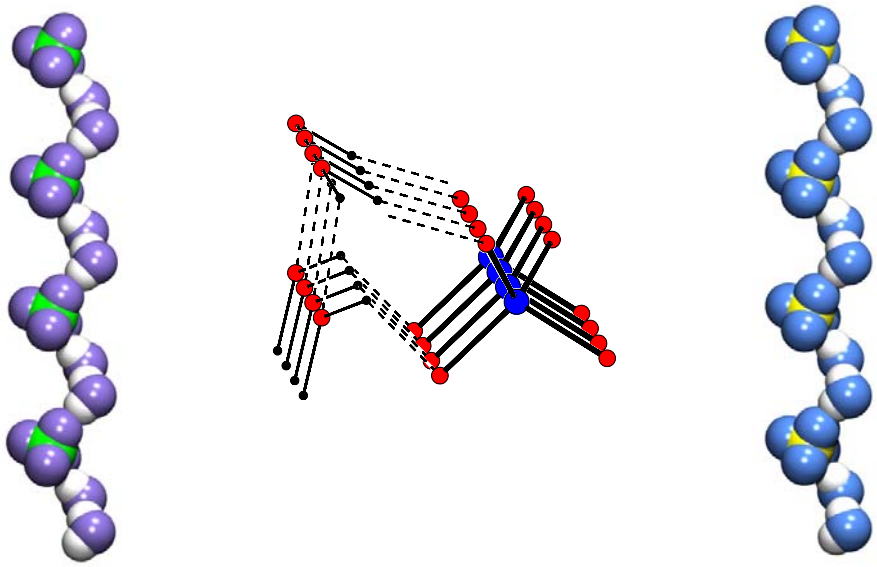

(a) **(b)** **(c)**

Figure 5.11. Helical arrangement of the $\{(H_2O)_2ClO_4^-\}$ units: Space-filling model of the helix in (a) **1** and (c) **2.** (b) Propagation of the helix through the hydrogen bonding interactions.

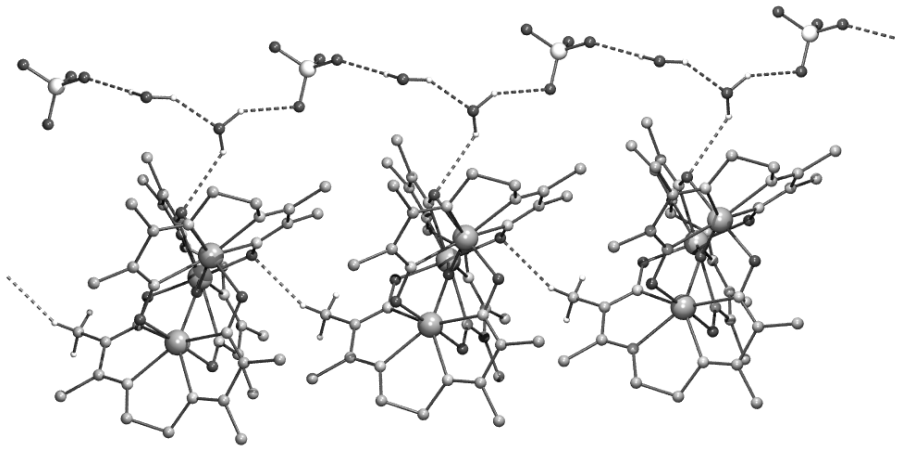

Figure 5.12. Ball-and-stick representation of the chain of complex cations and the helix of $\{(H_2O)_2ClO_4^-\}$ units connected by O–H···O interactions.

Interestingly the cations also exist in a chain like arrangement via inter-cation C–H···O interactions (C···O distance, 3.346(5) Å; C–H···O angle, 147.4°–151°) involving a methyl group (C17) and an oximato O-atom (O6).[33-35] Another metal coordinated oximato O-atom (O1) and the O-atom of the acceptor molecule in the water dimer present in $\{(H_2O)_2ClO_4^-\}$ unit are within hydrogen bonding distance (O···O distance, 3.201(7)-3.317(7) Å; O–H···O angle, ~129°). This is also reflected in the rather long M3–O1 bond length (1.9445(19) Å in **1** and 1.997(2) Å in **2** compared to the other $M–O_{oximate}$ bond lengths (for **1** 1.9081(17)–1.9362(19) and for **2** 1.979(2)–1.989(2) Å). Thus the chain of cations and the helix of $\{(H_2O)_2ClO_4^-\}$ units are bridged by O–H···O interactions (Figure

5.12) in the crystal lattices of the **1** and **2**. There is no other inter-chain or inter-helix non-covalent interaction.

Table 5.9. Hydrogen bonding parameters

Interaction	D···A (Å)	H···A (Å)	D–H···A (°)
1			
O12 – H12a···O13	2.897	1.970	156
O12 – H12b···O10	3.078	2.124	164
O13 – H13c···O8	3.099	2.512	139
O13 – H13d···O1	3.317	2.567	130
C17 – H17b···O6	3.346	2.360	151
2			
O12 – H12a···O13	2.890	2.016	150
O12 – H12b···O10	3.026	2.104	160
O13 – H13c···O8	3.119	2.303	142
O13 – H13d···O1	3.201	2.518	128
C17 – H17b···O6	3.346	2.497	147

5.5. Conclusion

In this chapter, we have synthesized and characterized, first carboxylate free cationic complexes $[M_3O(bamen)_3]^+$, (M = Mn and Fe) containing symmetric $\{M^{III}_3(\mu_3\text{-}O)\}$ unit. In both $[M_3O(bamen)_3]^+$ species, the metal ions are in pentagonal-bipyramidal N_4O_3 coordination sphere assembled by the bridging hexadentate N_4O_2 donor $bamen^{2-}$ and the μ_3-oxo group. Thus like carboxylates, three $bamen^{2-}$ ligands are fairly efficient in stabilizing the planar triangular ensemble of Mn(III) and Fe(III) with the central oxo bridge. Comparison of the

redox and magnetic properties of $[M_3O(O_2CR)_6L_3]^+$ where the metal ions are octahedral with that of $[M_3O(bamen)_3]^+$ (M = Mn(III) and Fe(III)) reveals some interesting differences. Both $[M_3O(bamen)_3]^+$ species exhibits several metal centered redox steps, uncommon for $[M_3O(O_2CR)_6L_3]^+$ complexes. The $[M_3O(O_2CR)_6L_3]^+$ species are antiferromagnetic. However, the antiferromagnetic exchange is weaker in the Mn(III) complex than in the Fe(III) complex. On the other hand, $[Mn_3O(bamen)_3]^+$ is ferromagnetic and the Fe(III) analogue is antiferromagnetic. The extent of antiferromagnetic coupling in $[Fe_3O(bamen)_3]^+$ is noticeably larger than that of the carboxylate complexes of $\{Fe_3(\mu_3\text{-}O)\}^{7+}$.

5.6. References

1. (a) A. Chakravorty, *Coord. Chem. Rev.,* **1974**, *13*, 1. (b) K. Nag, A. Chakravorty, *Coord. Chem. Rev*., **1980**, *33*, 87. (c) P. Chaudhuri, *Coord. Chem. Rev.*, **2003**, *243,* 143. (d) E .I. Baucom, R. S. Drago, *J. Am. Chem. Soc.*, **1972,** *11*, 2064. (e) G. sproul. G. D. Stucky. *Inorg. Chem.*, **1973**, *12*, 2898. (e) A. Hussein, Y. Sulfab, *Inorg. Chem.*, **1989**, *28,* 157.
2. (a) S. Pal, D. Bandyopadhyay, D. Datta, A. Chakravorty, *J. Chem. Soc., Dalton Trans.*, **1985**, 159. (b) S. Pal, T. Melton, R. N. Mukherjee, A. R. Chakravarty, M. Tomas, L. R. Falvello, A. Chakravorty, *Inorg. Chem.*, **1985**, *24*, 1250. (c) S. Pal, A. Chakravorty, *Inorg. Chem.*, **1987**, *26*, 4331. (d) P. Basu, S. Pal, A. Chakravorty, *J. Chem. Soc., Chem. Commun.*, **1989**, 977. (e) P. Basu, S. B. Choudhury, S. Pal, A. Chakravorty, *Inorg. Chem.*, **1989**, *28*, 2680. (f) P. Basu, S. Pal, A. Chakravorty, *J. Chem. Soc., Dalton Trans.*, **1990**, 9. (g) S. Chattopadhyay, P. Basu, D. Ray, S. Pal, A. Chakravorty, *Proc. Indian Acad. Sci., Chem. Sci.*, **1990**, *102*, 195. (h) S. Chattopadhyay,

P. Basu, S. Pal, A. Chakravorty, *J. Chem. Soc., Dalton Trans.*, **1990**, 3829. (i) P. Basu, S. Pal, A. Chakravorty, *J. Chem. Soc., Dalton Trans.*, **1991**, 3217. (j) D. Burdinski, E. Bill, F. Birkelbach, K. Wieghardt, P. Chaudhuri, *Inorg. Chem.,* **2001**, *40*, 1160.

3. G. J. Long, W. T. Robinson, W. P. Tappmeyer, D. L. Bridges, *J. Chem. Soc., Dalton Trans*., **1973,** 573.
4. D. N. Hendrickson, S. M. Oh, T. Y. Doug, T. Kambara, M. J. Cohn, M. F. Moore, Comments *Inorg. Chem*., **1985**, *4*, 329.
5. J. B. Vincent, H.-R Chang, K. Folting, J. C. Huffman, G. Christou, D. N. Hendrickson, *J. Am. Chem. Soc*., **1987**, *109*, 5703.
6. R. D. Cannon, U. A. Jayasooriya, R. Wu, S. K. Arapkoske, J. A. Stride, O. F. Nielsen, R. P. White, G. J. Kearly, D. Summerfield, *J. Am. Chem. Soc*., **1994**, *116*, 11869.
7. R. D. Cannon, R. P. White, *Prog. Inorg. Chem*., **1988**, *36*, 195.
8. (a) C. E. Anson, J. P. Bourke, R. D. Cannon, U. A. Jayasooriya, M. Molinier, A. K. Powell, *Inorg. Chem.* **1997**, *36*, 1265. (b) R. Wu, M. Poyraz, F. E. Sowrey, C. E. Anson, S. Wocadlo, A. K. Powell, U. A. Jayasooriya, R. D. Cannon, T. Nakamoto, M. Katada, H. Sano, *Inorg. Chem.* **1998**, *37*, 1913.
9. T. Fujihara, J. Aonahata, S. Kumakura, A. Nagasawa, K. Murakami, T. Ito, *Inorg. Chem,*. **1998**, *37*, 3779.
10. R. D. Cannon, U. A. Jayasooriya, F. E. Sowrey, C. Tilford, A. Little, J. P. Bourke, R. D. Rogers, J. B. Vincent, G. J. Kearley, *Inorg. Chem,*. **1998**, *37*, 5675.
11. A. M. Bond, R. J. H. Clark, D. G. Humphrey, P. Panayiotopoulos, B. W. Skelton, A. H. White, *J. Chem. Soc.*, *Dalton Trans.,* **1998**, 1845.
12. C. P. Raptopoulou, V. Tangoulis, V. Psycharis, *Inorg. Chem.*, **2000**, *39*, 4452.
13. S. Supriya, S. K. Das, *New J. Chem.,* **2003**, *27*, 1568.

14. E. Bill, C. Krebs, M. Winter, M. Gerdan, A. X. Trautwein, U. Flörke, H.-J. Haupt, P. Chaudhuri, *Chem. Eur. J.,* **1997**, *3*, 193.
15. P. Chaudhuri, M. Hess, T. Weyhermüller, E. Bill, H. J. Haupt, U. Flörke, *Inorg. Chem. Commun.,* **1998**, *1*, 39.
16. V. E. Uhlig, M. Friedrich, *Z. Anorg. Allg. Chem.* **1966**, *343*, 299.
17. W. E. Hatfield, *Theory and Applications of Molecular Paramagnetism*, Eds.: E. A. Boudreaux, L. N. Mulay, Wiley, New York, **1976**, p. 491.
18. Symbols: vs, very strong; s, strong; m, medium; w, weak.
19. A. C. T. North, D. C. Philips, F. S. Mathews, *Acta Crystallogr., Sect. A.* **1968**, *24*, 351.
20. L. J. Farrugia, *J. Appl. Crystallogr.,* **1999**, *32*, 837.
21. G. M. Sheldrick, *SHELX-97*, *Structure Determination Software*, University of Göttingen, Göttingen, Germany, **1997**.
22. P. McArdle, *J. Appl. Crystallogr.,* **1995**, *28*, 65.
23. A. L. Spek, *PLATON*, *A Multipurpose Crystallographic Tool*, Utrech University, Utrecht, The Netherlands, **2002**.
24. W. J. Geary, *Coord. Chem. Rev.,* **1971**, *7*, 81.
25. (a) J. G. Mohanty, R. P. Singh, A. Chakravorty, *Inorg. Chem.,* **1975**, *14*, 217 (b) F. Birkelbach, T. Weyhermüller, M. Lengen, M. Gerdan, A. X. Trautwein, K. Wieghardt, P. Chaudhuri, *J. Chem. Soc.*, *Dalton Trans.,* **1997**, 4529. (c) S. Pal, R. N. Mukherjee, M. Tomas, L. R. Falvello, A. Chakravorty, *Inorg. Chem.* **1986**, *25*, 200. (d) F. Birkelbach, T. Weyhermüller, M. Lengen, M. Gerdan, A. X. Trautwein, K. Weighardt, P. Chaudhuri, *J. Chem. Soc., Dalton Trans.***1997**, 4529.
26. S. N. Pal, S. Pal, *Inorg. Chem.* **2001**, *40*, 4807.
27. S. N. Pal, S. Pal, *J. Chem. Soc., Dalton Trans*. **2002**, 2102.
28. S. N. Pal, S. Pal, *Eur. J. Inorg. Chem.,* **2003**, 4244.

29. G. V. R. Chandramouli, C. Balagopalakrishna, M. V. Rajasekharan, P. T. Manoharan, *Computers Chem.* **1996**, *20*, 353.
30. (a) K. Wieghardt, U. Bossek, B. Nuber, J. Weiss, J. Bonvoisin, M. Corbella, S. E. Vitols, J. J. Girerd, *J. Am. Chem. Soc.,* **1988**, *110*, 7398. (b) H. Toftlund, A. Markiewicz, K. S. Murray, *Acta. Chem. Scand.,* **1990**, *44*, 443. (c) M. Mikuriya, Y. Yamato, T. Tokii, *Chem. Lett.* **1992**, 1571.
31. F. Birkelbach, T. Weyhermüller, M. Lengen, M. Gerdan, A. Trautwein, K. Wieghardt, P. Chaudhuri, *J. Chem. Soc.*, *Dalton Trans.,* **1997**, 4529.
32. K. Kambe, *J. Phys. Soc. Japan,* **1950**, *5,* 48.
33. G. R. Desiraju, *Angew. Chem. Int. Ed. Engl.,* **1995**, *34*, 2328.
34. M. G. Davidson, A. E. Goeta, J. A. K. Howard, S. Lamb, S. A. Mason, *New J. Chem.,* **2000**, *24*, 477.
35. S. N. Pal, K. R. Radhika, S. Pal, *Z. Anorg. Allg. Chem.,* **2001**, *627*, 1631.

List of Publications

1. A trigonal prismatic Mn(II) complex, $[MnL(H_2O)]^{2+}$, with *bis*(picolinylidenehydrazyl)(2-pyridyl) methane (L). Synthesis, structure and properties

   S Gupta Sreerama, S. N. Pal and S. Pal

   Inorg. Chem. Commun., **2001**, *4*, 656–660.

2. A Novel Carboxylate–Free Ferromagnetic Trinuclear μ_3–Oxo Manganese(III) Complex with Distorted Pentagonal–Bipyramidal Metal Centers

   S Gupta Sreerama and S. Pal

   Inorg. Chem., **2002**, *41*, 4843–4845.

3. Cobalt(II) and cobalt(III) complexes with N-(aroyl)-N'-(picolinylidene)hydrazines. Spin-crossover in the cobalt(II) complexes

   S Gupta Sreerama, D. Shyamraj, S. N. Pal and S. Pal

   Indian J. Chem., Sect. A, **2003**, *42*, 2352-2358.

4. A Triiron Complex Containing Carboxylate-free $\{Fe_3(\mu_3\text{-}O)\}^{7+}$ Core and Distorted Pentagonal-bipyramidal Metal Centers

   S Gupta Sreerama and S. Pal

   Eur. J. Inorg. Chem., **2004**, 4718-4723.

5. Dinuclear Triple Helicates with Diazine Ligands: X-ray Structural, Electrochemical and Magnetic Studies
   S Gupta Sreerama and S. Pal
   Inorg. Chem., **2005,** In press.

6. Iron(III) complexes of unsymmetrical hypodenate diazine ligands with facially coordinated metal center: Synthesis, structure and properties
   S Gupta Sreerama and S. Pal
   Manuscript under preparation.

7. Self Assembled Supramolecular Triple-Stranded Helical Structures $[M_2L_3]$ {M = Mn(III), Co(III) } Containing Dianionic Diaza Ligands
   S Gupta Sreerama and S. Pal
   Manuscript under preparation.

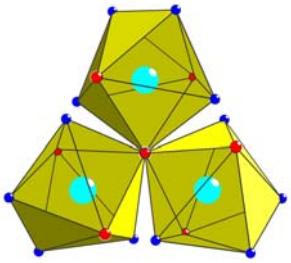

Trinuclear $[Mn_3O(bamen)_3]^+$

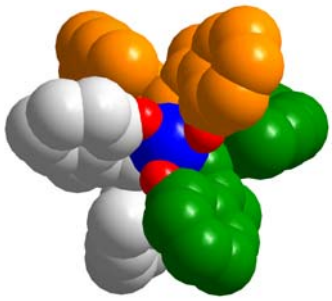

Triple Helicate $[Fe_2(mesalhn)_3]$

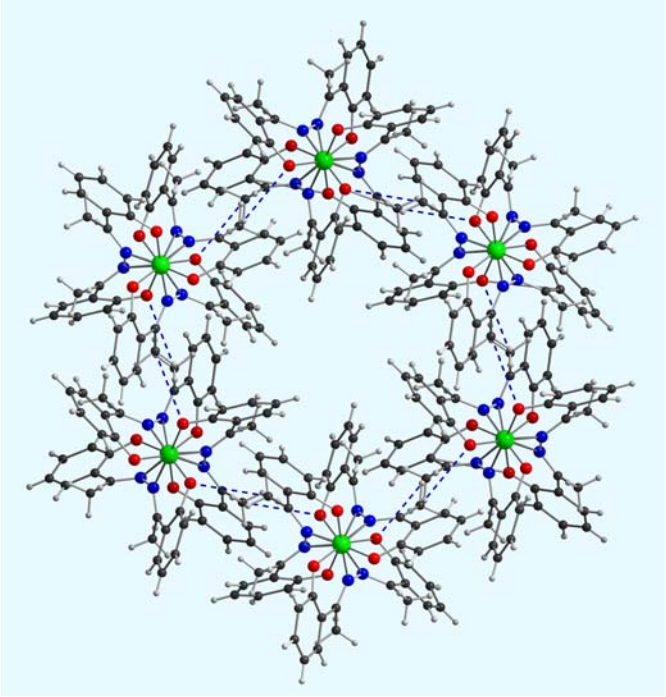

Hexagonal arrangement of the $[Co_2(mesalhn)_3]$